

AD-A148 889

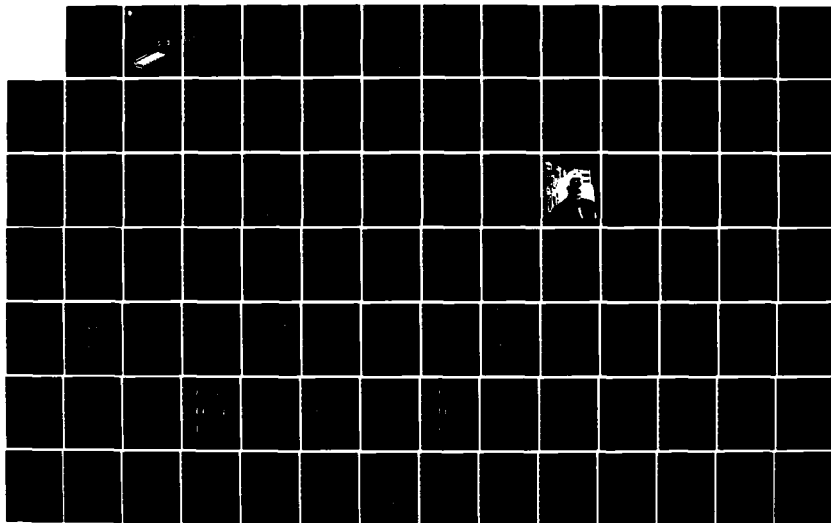
NEUROCOGNITIVE PATTERN ANALYSIS OF AN AUDITORY AND
VISUAL NUMERIC MOTOR C. (U) EEG SYSTEMS LAB SAN
FRANCISCO CA A S GEVINS ET AL. OCT 84 AFOSR-TR-84-1107
F49620-82-K-0006

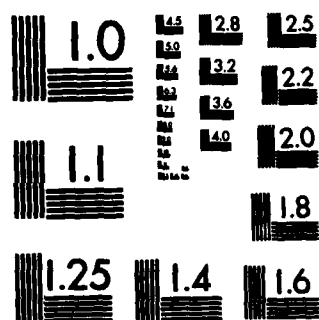
1/1

UNCLASSIFIED

F/G 5/10

NL





MICROCOPY RESOLUTION TEST CHART
NATIONAL BUREAU OF STANDARDS-1963-A

AFOSR-TR- 84 - 1107

13

EEG SYSTEMS LABORATORY

1855 FOLSOM ST., SUITE 610
SAN FRANCISCO, CA 94103
(415) 621-8343

OCTOBER 1984

NEUROCOGNITIVE PATTERN ANALYSIS
OF AN AUDITORY AND VISUAL NUMERIC MOTOR CONTROL TASK,
PART 1: DEVELOPMENT OF METHODS

FINAL REPORT AFOSR CONTRACT F49620-82-K-0006

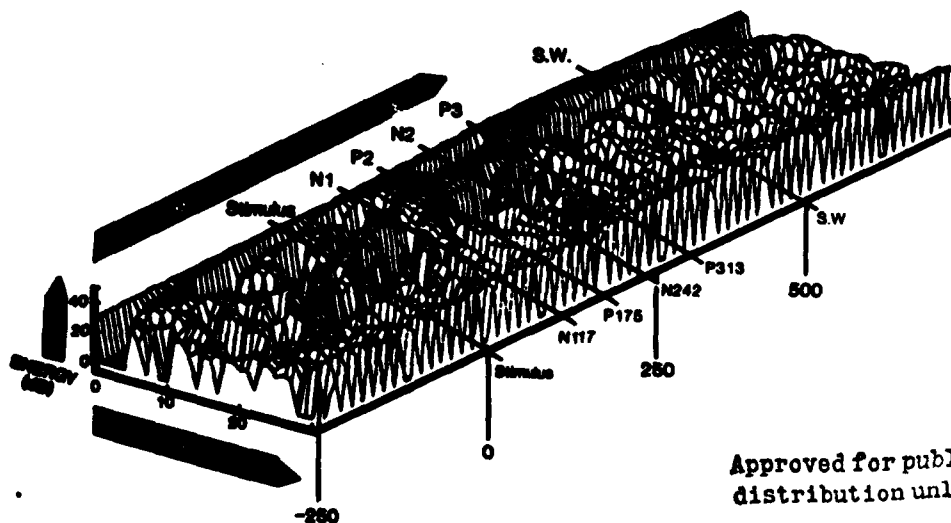
22 FEB 82 TO 30 SEPT 84

Dr. Alfred R. Fregly, Project Contract Officer
Directorate of Life Sciences
AFOSR
Bolling AFB, D.C. 20332

DTIC
ELECTE
DEC 14 1984
S B

Alan Gevins
A. Gevins, Director

DTIC FILE COPY



Approved for public release;
distribution unlimited.

84 12 05 010

A non-profit laboratory dedicated to research on the higher cognitive functions of the human brain

REPORT DOCUMENTATION PAGE

1a. REPORT SECURITY CLASSIFICATION UNCLASSIFIED		1b. RESTRICTIVE MARKINGS	
2a. SECURITY CLASSIFICATION AUTHORITY		3. DISTRIBUTION/AVAILABILITY OF REPORT APPROVED FOR PUBLIC RELEASE, DISTRIBUTION UNLIMITED.	
2b. DECLASSIFICATION/DOWNGRADING SCHEDULE			
4. PERFORMING ORGANIZATION REPORT NUMBER(S) AFOSR02		5. MONITORING ORGANIZATION REPORT NUMBER(S) AFOSR-TR- 84 - 1107	
6a. NAME OF PERFORMING ORGANIZATION EEG SYSTEMS LABORATORY	6b. OFFICE SYMBOL (If applicable)	7a. NAME OF MONITORING ORGANIZATION DIRECTORATE OF LIFE SCIENCES, AFOSR BOLLING AFB, D.C. 20332	
8a. ADDRESS (City, State and ZIP Code) 1855 FOLSOM STREET SAN FRANCISCO, CA 94103		7b. ADDRESS (City, State and ZIP Code)	
8a. NAME OF FUNDING/SPONSORING ORGANIZATION SQMC as # 7	8b. OFFICE SYMBOL (If applicable)	9. PROCUREMENT INSTRUMENT IDENTIFICATION NUMBER F49620-82-K-0006	
8c. ADDRESS (City, State and ZIP Code)		10. SOURCE OF FUNDING NOS.	
		PROGRAM ELEMENT NO.	PROJECT NO.
		61102F	2313
		TASK NO.	WORK UNIT NO.
		A4	-
11. TITLE (Include Security Classification) NEUROCOGNITIVE PATTERN ANALYSIS OF AN AUDITORY AND VISUAL NUMERIC MOTOR CONTROL TASK, PART I: DEVELOPMENT OF METHODS			
12. PERSONAL AUTHOR(S) GEVINS, ALAN S.; BRESSLER, STEVEN L.; CUTILLO, BRIAN A.; DOYLE, JOSEPH, C.; MORGAN, NELSON H.; ZEITLIN, GERALD M.			
13a. TYPE OF REPORT FINAL	13b. TIME COVERED FROM 82FEB22 TO 84SEP30	14. DATE OF REPORT (Yr., Mo., Day) 84OCT31	15. PAGE COUNT 90
16. SUPPLEMENTARY NOTATION			
17. COSATI CODES		18. SUBJECT TERMS (Continue on reverse if necessary and identify by block number)	
FIELD	GROUP	SUB. GR.	
0508			
0509			
		PLEASE SEE ATTACHED SHEET ENTITLED "SUPPLEMENT TO FORM DD 1473", SECTION 18: SUBJECT TERMS (1 page)	
19. ABSTRACT (Continue on reverse if necessary and identify by block number) PLEASE SEE ATTACHED SHEETS ENTITLED "ABSTRACT" (2 pages)			
20. DISTRIBUTION/AVAILABILITY OF ABSTRACT UNCLASSIFIED/UNLIMITED <input checked="" type="checkbox"/> SAME AS RPT. <input type="checkbox"/> DTIC USERS <input type="checkbox"/>		21. ABSTRACT SECURITY CLASSIFICATION UNCLASSIFIED	
22a. NAME OF RESPONSIBLE INDIVIDUAL ALFRED FREGLY		22b. TELEPHONE NUMBER (Include Area Code) (202) 767-5024	22c. OFFICE SYMBOL AFOSR/NL

SUPPLEMENT TO FORM NO 1473

SECURITY CLASSIFICATION: UNCLASSIFIED

SECTION 18: SUBJECT TERMS

functional neuroanatomy
higher brain functions
human performance
brain models
parallel processing

EEG
evoked potentials
digital signal processing
statistical pattern recognition

time-varying processes
spatial analysis
current source density
Wigner distribution
artifact rejection

AIR FORCE OFFICE OF SCIENTIFIC RESEARCH (AFSC)

NOTICE OF TRANSMISSION TO DTIC

This technical report is being submitted to DTIC
approved for

Distribution

MATTHEW J. KEMMER

Chief, Technical Information Division

November 12, 1984 (60)

EEG SYSTEMS LABORATORY, CONTRACT NO. F4962082-K-0007

AFOSR (FY82-84)

ABSTRACT

New advances in understanding human neurocognitive functions must come from new technologies for measuring split-second changes in event related electrical and magnetic fields which may soon complement the anatomical information produced by CT and NMR brain scans and the static metabolic images of PET scans.

As a contribution to this effort, the EEGSL is developing the method of Neurocognitive Pattern (NCP) Analysis to study both simple and complex cognitive tasks. A number of previous findings suggest that neither strictly localizationist ("single equivalent dipole") nor equipotentialist ("hologram") models of neurocognitive processing are realistic. Rather, a more appropriate model seems to be a distributed computational network in which there is continuous communication between many parallel, specialized processing elements. In order to better measure and model these complex processes, the initial thirty months of this project focused on developing experimental tasks and advanced recording and analysis technologies. The following milestones were achieved:

- 1) Development of a 6-second bimodal task which systematically manipulates functional relations between sensory, motor and association cortical areas by varying the expected and actual sensory modality of numeric stimuli requiring a precise isometric finger response and resulting in feedback about response accuracy. This extends the observation epoch beyond the 1-second interval most commonly used in event related potential (ERP) studies;
- 2) Implementation of a system for on-line recording and monitoring of up to 64 brain potential (BP) channels, for improved spatial sampling, as well as eye movement (EOG), muscle potential (EMG), heart rate and respiration signals;
- 3) Implementation of a current source density transform to convert scalp electric field distributions into measures of current flow into and out of the brain. The effect of the reference electrode is eliminated, and localization is improved;
- 4) Expansion of the ADIEEG Analysis system to a 64 channel capacity. Implementation of an analysis executive for automated execution of multi-stage analyses applied to 500 megabyte data sets. This makes detailed analysis of an unprecedented amount of data possible;

November 12, 1984 (60)

- 5) Development of improved spectral algorithms to remove contamination by eye-movement potentials from single-trial BP data;
- 6) Development of improved methods of averaged evoked time series analysis, including:
- a) A simple algorithm for ERP estimation which achieves a substantially higher signal-to-noise ratio without the imposition of a priori presumptions about the characteristics of event-related signal components;
 - b) The first application of Wigner (time/frequency domain) distributions to study split-second changes in the frequency composition of evoked time series. This promises to be a useful research tool which provides complementary information to that obtained from traditional time-domain measures;
- 7) Development of improved methods for single-trial pattern recognition analysis, including:
- a) A rapid single-channel scanning measure to select trials, intervals and channels with task-related signals for further analysis;
 - b) A statistical "baseline" estimation procedure which provides a nearly neutral reference data set against which to compare event-related patterns. This eliminates the necessity of using questionable "resting state" or prestimulus baselines;
- 8) Trial application of all of the above to a set of data consisting of about 500 trials of an auditory and visual perceptuomotor task recorded with 49 BP channels.

Note: Items 2-7 were also sponsored by the Office of Naval Research, the Air Force School of Aerospace Medicine, and the National Science Foundation.



Accession For	
NTIS GRA&I	<input checked="checked" type="checkbox"/>
DTIC TAB	<input type="checkbox"/>
Unannounced	<input type="checkbox"/>
Justification	
By	
Distribution/	
Availability Codes	
Dist	Avail and/or Special
A-1	

November 13, 1984 (56)

AFOSR FINAL REPORT FY82-FY84

I. OVERVIEW.....	4
A. Senior Personnel of the EEG Systems Laboratory.....	4
B. List of Publications, 1983-In Press.....	4
C. Major Presentations by A. Gevins, 1982-1984.....	5
D. Summary of Research Program and Results.....	5
1. Overview.....	5
2. Previous Experimental Findings.....	8
3. Similarities and Differences Between Our Experimental Designs and Analyses and Conventional ERP Techniques.....	9
4. Evoked Correlations Between Scalp Electrodes.....	10
5. Current Procedures Used in NCP Analysis.....	10
6. Major Obstacles to Progress.....	13
a. Biophysical and Engineering Obstacles.....	13
b. Basic Science Obstacles.....	14
c. Conceptual Obstacles.....	15
II. PILOTING OF AN AUDITORY-VISUAL PERCEPTUOMOTOR TASK.....	17
A. Design Considerations.....	17
1. Cognitive Considerations.....	17
2. Experimental Controls.....	17
3. Montage.....	18
B. Task Development and Pilot Recordings.....	18
1. Phase One (P's #1-8); (Respond to miscues).....	18
a. Rationale.....	18
b. Task.....	18
c. Recordings.....	19

November 13, 1984 (56)

d. Results and Discussion.....	19
2. Phase Two (P's #9-12): (No response to miscues).....	22
a. Rationale.....	22
b. Task.....	22
c. Recordings.....	23
d. Results and Discussion.....	23
3. Final Paradigm	23
III. PILOT ANALYSIS OF DATA FROM FINAL PARADIGM.....	24
A. Formation of Data Sets.....	24
B. Examination of Averaged Waveforms.....	24
1. Exogenous Peaks.....	25
2. Endogenous Peaks.....	25
3. Response Potentials.....	26
C. Initial Analysis.....	26
IV. THE ADIEEG III ANALYSIS SYSTEM.....	26
A. Overview of The New System.....	27
B. The ADISORT Program for Formation and Balancing of Data Sets.....	27
V. DEVELOPMENT AND TRIAL APPLICATION OF NEW ANALYSES.....	28
A. Analysis of Sets of Single Trials.....	28
1. Rapid Scanning Measure.....	28
2. Application of Scanning Measure to Within Task Analysis.....	29
a. Precue Interval Baseline.....	29
1) Stimulus Registered A/V Move Tasks...29	
2) Response Registered A/V Tasks.....	30
b. "Random Data" Baseline.....	30

November 13, 1984 (56)

1) Method.....	30
2) Application to Miscued (No-Move) A/V Data.....	31
3) Conclusion.....	31
B. Average Evoked Timeseries Analysis.....	33
1. "Purified" ERPs.....	33
2. Wigner (Time-Frequency) Distributions.....	33
C. Test of Principal Components Analysis for Defining Analysis Windows.....	35
D. Current Source Density Transform.....	35
1. Derivation of Current Source Densities from Potential Distributions.....	35
2. Determining Electrode Positions.....	37
E. Artifact Detection and Filtering.....	37
1. Eye-Movement Contaminants.....	37
2. Artifact Database.....	38
a. Overview.....	38
b. Criteria for Identification of Artifacts.....	39
VI. BIBLIOGRAPHY.....	41

The system and signal processing developments reported in Sections IV and V are also sponsored by the Office of Naval Research, the National Science Foundation and the Air Force School of Aerospace Medicine.

November 13, 1984 (56)

I. OVERVIEW

A. Senior Scientific Personnel of the EEG Systems Laboratory

Steven L. Bressler, Neurophysiologist
Brian A. Cutillo, Cognitive Scientist
Joseph C. Doyle, Biophysicist
Alan S. Gevins, Director
Nelson H. Morgan, Electrical Engineer
Ronald K. Stone, Neurologist and Psychiatrist
Gerald M. Zeitlin, Computer Systems Engineer

B. Publications: 1983 - In Press

1. Gevins, A.S., Schaffer, R.E., Doyle, J.C., Cutillo, B.A., Tannehill, R.L. and Bressler, S.L. Shadows of thoughts: Rapidly changing, asymmetric, brain potential patterns of a brief visuomotor task. Science, 1983, 220, 97-99.

2. Gevins, A.S. Brain potential evidence for lateralization of higher cognitive functions. In J.B. Hellige (Ed.), Cerebral Hemisphere Asymmetry: Method, Theory and Application. Praeger Press, 1983, 335-362.

3. Gersch, W., Gevins, A.S. and Kitagawa, G. Multivariate, time varying autoregressive modeling of nonstationary covariance time series. Proc. IEEE Conf. on Computers, Design and Control, 1983, New York, IEEE Press.

4. Gevins, A.S. Overview of the human brain as a distributed computing network. Proc. IEEE Conf. on Computer Design, 1983, New York, IEEE Press, pp. 13-15.

5. Gevins, A.S. and Morgan N.M. Ignorance-based systems. Proc. IEEE Conf. Acoustics, Speech and Signal Processing, 1984, New York, IEEE Press, pp. 39A.5.1-39A.5.4.

6. Gevins, A.S., Doyle, J.C., Cutillo, B.A., Schaffer, R.E., Tannehill, R.S. and Bressler, S.L. Neurocognitive pattern analysis of a visuospatial task: rapidly-shifting foci of evoked correlations between electrodes. Psychophysiology, 1984, In Press.

7. Gevins, A.S. Quantitative human neurophysiology. In, H.J. Hannay (Ed.), Experimental Techniques in Human Neuropsychology, Oxford Press, 1984, In Press.

8. Gevins, A.S. Rapidly shifting foci of single trial evoked correlations during a brief visuospatial task revealed by Neurocognitive Pattern Analysis. Proc. EPIC VII, 1983, and Electroenceph. Clin. Neurophysiol., In Press.

November 13, 1984 (56)

9. Gevins, A.S. Spatial electrical patterns of higher brain functions. Proc. Third European EEG Conference, 1983, and Electroenceph. Clin. Neurophysiol., In Press.

10. Gevins, A.S. Analysis of the electromagnetic signals of the human brain: milestones, obstacles and goals. IEEE Trans. on Biomedical Eng., 1984, In Press.

C. Major Presentations by A. Gevins: 1982-1984

1. Symposium Chairman, American Association for the Advancement of Science, Washington, D.C., 1982.

2. Symposium Chairman, Winter Conference on Brain Research, Steamboat Springs, 1982.

3. Special Invited Lecturer, Int. Conf. Neuropsychology, Pittsburg, 1982.

4. Invited Speaker, Society for Biological Psychiatry, New York, 1983.

5. Symposium Chairman, IEEE Int. Conf. on Computer Design, New York, 1983.

6. Invited Lecturer, Third European EEG Conference, Basle, 1983.

7. Plenary speaker, ONR Workshop on Analysis of Biomagnetic Signals, Los Angeles, 1984.

D. Summary of Research Program and Results

1. Overview

It is a great testimony to the inventive genius of the first generation of psychophysicists that so much has been learned from averaged evoked potentials with modest recording and analysis technologies. However, current pessimism expressed by many neuroscientists about future gains from this line of research seems justified. It does not seem likely that major advances in understanding mass neural action and human higher brain functions will result from continued application of essentially twenty-year-old experimental paradigms, and recording and analysis technologies. Amazingly, most psychophysicists are content to study variations in one or two averaged evoked potential peaks, and dismiss or even oppose the development of more advanced technologies. It is obvious that this attitude will soon lead to obscurity. Fortunately, there is a growing impetus for developing technologies to measure split-second

November 13, 1984 (56)

changes in functional neuroanatomy to complement the anatomical images generated by CT and NMR brain scans, and the static metabolic images of PET scans.

Neuroscientists who are accustomed to relating the activity of a few neurons to aspects of behavior should take pause to consider the future of their own line of research. Simultaneous recording of even a few dozen neurons will not reveal the emergent properties of functional neural masses. As clearly demonstrated in Walter Freeman's latest studies (see below), appropriate measurement and analysis of field potentials reveals information not otherwise obtainable, i.e. two-dimensional spatiotemporal electrical patterns which encode the specific properties of expected and perceived odors. This amounts to the demonstration of the existence of an "EEG code". While there are no fundamental obstacles to extending this line of research to the neocortex, such work requires use of advanced recording and analytic technologies, which unfortunately are foreign to most neuroscientists.

Basic studies using animal models, particularly primate models, are essential in studying mass neural action and basic perceptual, motor and cognitive processes. However, an animal model for complex human higher brain functions is not possible. If we are to study such functions, with the goal of extending the limits of human performance, it is necessary to advance the state of the art of methods for studying human neurocognitive functioning. This will require an interdisciplinary effort in which recording and analytic techniques with increased spatial resolution and source localization capability are applied to experimental paradigms more closely approximating normal cognitive functioning.

As a contribution to this effort, the EEG Systems Laboratory is developing the method of Neurocognitive Pattern (NCP) Analysis for quantifying mass neural processes related to perceptuomotor and cognitive activities. At the same time, we are designing experiments for measuring sequences of elementary cognitions while recording up to 64 brain potential (BP) channels and several other physiological signals. Generically speaking, NCP Analysis currently consists of the application of digital signal-processing techniques and statistical pattern classification analysis to extract small task-related signals from the obscuring background "noise" of the brain (Section 1.0.5). It is in a state of development at this time, but currently NCP Analysis is applied to sets of single-trial time series in about 25 brief analysis intervals, 125 to 250 msec wide, for up to 64 BP channels.

Several prior generations of NCP Analysis have been used to study both simple and complex tasks, and a number of findings have resulted. These results suggest that both strictly localizationist ("single equivalent dipole") and equipotentialist ("hologram") views of neurocognitive processes are unrealistic. Even simple tasks are associated with rapidly shifting, complex mosaics of regional BP patterns, and a more appropriate model of neurocognitive processing might be a distributed computational network involving continuous communication between many specialized parallel processing elements.

November 13, 1984 (56)

Our research goal is to develop experimental paradigms and analytic methods to measure and model these complex processes.

The initial thirty months of this project were directed toward advancing the technology of recording and analysis of multi-channel data obtained during perceptuomotor-cognitive tasks. The following milestones were achieved:

- 1) Development of a highly controlled 6 second bimodal task which manipulated functional relations between sensory, association and motor cortical areas by varying the expected and actual sensory modality of numeric stimuli requiring a precise isometric finger response and resulting in feedback about response accuracy (Section II);
- 2) Development of a system for on-line recording of up to 64 BP channels for much improved spatial sampling, as well as eye movements (EOG), muscle potentials (EMG), heart rate and respiration signals (Section IV.A);
- 3) Development of algorithms and software to perform a current source density (Laplacian) transform. This converts scalp electrical potential distributions into measures of current flow into and out of the brain at each electrode site. The effect of the reference electrode is eliminated, and in many instances localization is improved (Section V.D);
- 4) Expansion of the ADIEEG Analysis system to a 64-channel capacity. Automation of multi-stepped analyses of 500 megabyte data sets (Section IV);
- 5) Development of improved eye-movement-filtering algorithms to remove contamination by eye movement potentials from single-trial data based on differences in spectral signatures between eye movements and brain potentials (Section V.E.1). Compilation of a large data base of artifacts for development of a new generation of automated artifact rejection algorithms (Section V.E.2);
- 6) Development of improved methods of averaged evoked time series analysis, including:
 - a) A simple algorithm for improved averaged event-related potential (ERP) estimation which achieves a substantially higher signal-to-noise ratio on fewer trials without the imposition of a priori presumptions about the shape or exact time of event-related signal components (Section V.B.1);
 - b) Application of Wigner Distributions to study split-second changes in the frequency composition of evoked time series. This is the first application of this method to ERPs, and it may prove to be a useful research tool research, complementing the information provided by traditional time-domain amplitude analysis (Section V.B.2);

November 13, 1984 (56)

7) Development of improved methods for single-trial pattern recognition analysis, including;

a) A rapid single-channel scanning measure to select trials, intervals and channels with task-related signals for further analysis (Section V.A.1);

b) A statistical "baseline" estimation procedure which provides a nearly "neutral" comparison data set against which to compare event-related patterns (Section V.A.2.b). This eliminates the necessity of using questionable "resting state" or prestimulus "baselines";

8) Trial application of all of the above to a set of data consisting of about 500 trials of an auditory and visual perceptuomotor task recorded with 49 BP channels (Sections III & V).

2. Previous experimental findings which motivated the technical and experimental developments described above

NOTE: It must be understood that scalp-recorded potentials, even unaveraged time series, are not necessarily cortical in origin. Until the issue of source localization is better understood, conventional scalp designations for electrode positions, which refer to underlying cortical areas, should not be taken to imply measurement of the activity of those cortical areas. For convenience, we use the conventional scalp designations subject to this caveat.

a. Complex perceptuomotor and cognitive activities such as reading and writing produce unique, spatially differentiated scalp EEG spectral patterns. These patterns had sufficient specificity to identify the type of task (EEG Clin. Neurophysiol., 47:693-703, 1979). These results agree with previous reports of hemispheric lateralization of "spatial" and "linguistic" processing.

b. When tasks are controlled for stimulus, response and performance-related factors, complex cognitive activities such as arithmetic, letter substitution and mental rotation have identical, spatially diffuse EEG spectral scalp distributions. Compared with staring at a dot, such tasks had approximately 10% reductions in alpha and beta band spectral intensities (EEG Clin. Neurophysiol., 47:704-710, 1979; Science 203:665-668, 1979). This reduction may be an index of task workload. Since no patterns of hemispheric lateralization were found, this study suggests that previous and most current reports of EEG hemispheric lateralization may have confounded electrical activity related to limb and eye movements and arousal with those of mental activity per se (Science 207:1005-1008, 1980).

c. Split-second visuomotor tasks, controlled so that only the type of judgment varied, are associated with complex, rapidly shifting patterns of inter-electrode correlation of single-trial brain potential timeseries. Differences between spatial and numeric judgments were evident in the task-cued prestimulus interval. Complex and often lateralized patterns of task-related correlation changed

November 13, 1984 (56)

with split-second rapidity from stimulus onset to just prior to response, at which time there was no difference between tasks (Science 213:918-922, 1981). This suggests that once task-specific perceptual and cognitive processing were completed, a motor program common to both tasks was being executed.

d. Rapidly shifting, focal patterns of difference between tasks can be extracted with NCP Analysis. The move and no-move variants of a split-second visuospatial judgment task, which differed in expectation, in type of judgment, and in response (move or no-move), were associated with distinctly different patterns of single-trial evoked correlation between channels (Science 220:97-99, 1983; Psychophysiology, 1984, in press). These results concur with neuropsychological models of these tasks derived from functional deficits of patients with localized lesions. They suggest that although simple perceptuomotor tasks are associated with a complex, dynamic mosaic of BP patterns, it is possible to isolate foci of maximal differences between tasks. It is clear that without a split-second temporal resolution it is not possible to isolate rapidly shifting lateralizations which are presumably associated with stages of perceptual, cognitive, and efferent processing.

e. The focal patterns of evoked correlation derived by NCP Analysis significantly distinguished the single-trial data of 7 of the 9 people in the above study. This suggests that consistent neurocognitive processes were measured in the majority of right-handed male research participants (Psychophysiology, 1984, in Press).

3. Similarities and Differences Between Our New Experimental Paradigms and Analyses and Conventional ERP Techniques

Our experiments and analyses are grounded on the body of information gained from ERP research and have the same underlying goal: to resolve spatially and temporally overlapping, task-related neural processes. Our approach differs in several ways from the currently popular ERP paradigms which: a) require a differential judgment between task relevant and irrelevant (usually rare and frequent) stimuli; b) then extract a few features from averaged ERPs by peak picking or principal components analysis (PCA); and c) perform hypothesis testing on the features with ANOVA. First, because neurocognitive processes are complex, we are concerned with spatiotemporal task-related activity recorded by many (currently up to 64) electrodes in many (currently about 25) time intervals spanning a six-second period extending from before a cue, through stimulus and response, to presentation of feedback. By contrast, most ERP experiments are concerned with measurement of one to a few "components" associated with a single stimulus or response registration in a few channels in an epoch under one second. Additionally, NCP Analysis quantifies neurocognitive activity in terms of a variety of parameters, rather than just amplitude and latency of ERP peaks. This increased dimensionality of parametrization may facilitate the measurement of subtler aspects of neurocognitive processes. Second, the questionable assumption of a multivariate normal distribution of BP is not made in NCP Analysis.

November 13, 1984 (56)

Third, feature extraction and hypothesis testing are performed as a single process which determines the differences in signal properties between the conditions of an experiment, or their differences with respect to a "baseline". We think that this is more effective than feature extraction techniques such as PCA, which are based on possibly irrelevant criteria such as statistical independence of features regardless of discriminating power. Fourth, in NCP Analysis task-related patterns of consistency are extracted from sets of single-trial data. Significant results may be obtained as long as there is a pattern of consistent difference, even when the means of the two data sets are not significantly different.

These aspects of our experimental paradigm and NCP Analysis may enable us to resolve previously unseen neurocognitive signals from the overriding unrelated background activity of the brain, leading to a better understanding of mass neural processes of human goal-oriented behaviors. However, this approach is not without its cost. It currently takes 2-3 technicians to run an experiment with 64 channels. Manually editing this data for artifacts is time consuming but necessary. NCP Analysis requires orders of magnitude more computing than PCA and ANOVA. Because of the sensitivity of NCP Analysis, highly controlled experimental paradigms are required to assure that the results are truly related to the hypothesis and not to spurious factors. (The process of developing one such task is described in Section II.)

Performing these experiments and analyses requires a far greater allocation of effort and resources than conventional ERP experiments, and although we have obtained several promising results with previous generations of NCP Analysis, we must caution that "the jury is still out". If results in the next several years prove that this new approach is really worthwhile, it will be possible to optimize and standardize our methods and analysis for application by other laboratories, using current generation high-performance supermicrocomputer systems.

4. Evoked Correlations Between Scalp Electrodes

For the past few years we have concentrated on a measure of waveshape similarity (crosscorrelation) between time series from pairs of electrodes. The crosscorrelation approach is based on the hypothesis that when areas of the brain are functionally related there is a consistent pattern of waveshape similarity between their macropotentials. There are a number of considerations in interpreting correlation patterns of scalp recordings, such as volume conduction from subcortical sources and driving by distant generators. Some of the ambiguities may be mitigated by careful experimental design, but the neurophysiological interpretation of correlation patterns is an unsettled issue. We are engaged in collaborative studies using primate models and using MEG recordings to address this issue. The methods and results of these studies will be described in future reports.

5. Current Procedures Used in NCP Analysis

November 13, 1984 (56)

We use the generic term NCP Analysis to refer to the multi-stepped analysis we have been developing to extract task-related spatiotemporal patterns from the unrelated "noise" of the brain. There have been two prior generations of NCP Analysis. The first measured background EEG spectral intensities from 8 channels while people performed complex tasks, such as arithmetic problems, lasting up to a minute. The second measured crosscorrelations between 91 pairwise combinations of 15 electrodes recorded during performance of simple split-second perceptuomotor tasks. A third generation is currently nearing completion which operates on up to 64 channels recorded during a controlled sequence of stimuli in which a person prepares for and executes perceptual judgment and motor control tasks and receives performance feedback. Because of the large size of these single-trial data sets (up to 100 megabytes for each person), several passes through the data are required to complete the analysis. The first pass selects important channels, intervals and trials to reduce the amount of data prior to measuring interdependencies between channels (described in Section V.A along with an example of its application). The second pass, which is currently under development, will measure interdependencies and timing relations between channels on the reduced data set.

NCP Analysis essentially consists of the application of a layered-network, nonlinear mathematical pattern classification algorithm (also called a pattern recognition algorithm) to sets of single-trial brain potential features in order to extract task-related signals which distinguish two sets of data. The sets of data can be two different experimental tasks (between-task analysis), or they can be an experimental task and a reference "baseline" data set (within-task analysis). In order to extract the most spatiotemporal information, the pattern recognition algorithm is applied many times to separate groups of features organized according to their temporal relation to a stimulus or response and according to their anatomical position on the scalp. Diagrams are then drawn in a head outline format showing the times and areas with task-related information.

In the second generation of NCP Analysis, digital lowpass filtering was used for between-channel correlation measures due to the low signal-to-noise ratio (SNR) in single trials (Gevins, et al, 1981, 1983, 1984). This reduced the susceptibility of the correlation measure to noise but smeared temporal relationships. However, the measurement of precise time relationships of waveform components between channels is a prime objective in our current work. Therefore, a signal enhancement technique was required to improve SNR without the time-smearing effect of conventional filtering. This led to the development of a first-pass "scanning" method to select optimal subsets of signal-bearing trials, channels and intervals to improve the SNR for correlation-based measures. This method uses single-channel filtered amplitude as a feature for pattern-recognition. Trials without consistent task-related signals are rejected if the pattern recognition algorithm is unable to discriminate them from sets of data known to have a low event-related signal (see Section V.A.1). As of the date of this report, the second

November 13, 1984 (56)

pass of computing crosscorrelations between channels on trials selected in the first pass has not yet been evaluated. In both passes, separate analyses are performed on features computed from 125-250 msec data windows located at latencies determined for each person from the major peaks of their averaged ERPs, as well as from stimulus and response initiation times. However, the features themselves are always computed on single-trial data.

There are 17 major steps in NCP Analysis:

- 1) Record a sufficient amount of data using up to 64 electrodes. Compute current-source densities at each non-peripheral electrode location from the potential distribution (this method is currently under evaluation).

- 2) Create a single, artifact-free data set which will be compared with a reference "baseline" data set. Alternatively, create two data sets that differ according to a specified criterion, such as the type of expectation, but which are otherwise balanced for stimulus, response and performance-related factors. In either case, the two data sets represent conditions which are to be compared.

- 3) Compute average stimulus-registered (and response-registered when appropriate) time series for each person.

- 4) Use the latencies of peaks in each person's averaged time series (ERP) to determine the centerpoints of analysis windows for single-trial pattern recognition analysis. Adjust the window size to span the peak (usually 125 or 250 msec). Set other windows at stimulus and response times.

- 5) For the first scanning pass, low-pass filter the time series at 7 Hz, then decimate. Use 3-7 time series values as features.

- 6) Partition the data of the two conditions into three training and (non-overlapping) validation sets.

- 7) For each channel, apply a nonlinear, layered-network pattern recognition algorithm to generate equations which represent invariant differences in the current at the interval chosen. The overall performance is optimized to maximize the product of the performances.

- 8) Test the classification equations with the validation data to determine which electrodes differ significantly between conditions.

- 9) Repeat steps 7 and 8 for each training and validation data set and compute the mean validation set accuracy.

- 10) Set the level of significant classification well above that attained with the data randomly assigned to two pseudo-conditions.

November 13, 1984 (56)

11) Draw diagrams showing which electrodes contain task related information in each interval.

12) For each channel, compute average ERPS and Wigner Distributions of the average of those trials with task-related signals (i.e. trials correctly classified in the validation set). End of pass one.

13) Beginning of pass two. Select intervals and channels for measurement of spatial interdependencies and time delays by examination of the results of step 12.

14) Compute multilag cross covariance functions between chosen channels and many other channels for each trial in each selected analysis window on those trials with task-related signals. Use a measure of the center of gravity of the cross covariance function as a feature to characterize the lag time between channels.

15) Group center of gravity measures into anatomic constraint groups (also called "electrode groups"). These represent the time lag between a chosen principal electrode(s) and a number of secondary electrodes, (e.g. time lags between the left occipital electrode and many other electrodes).

16) Repeat steps 6-10 on each electrode group.

17) Tabulate equations of significant electrode groups. Diagram significantly differing principal electrodes and their most "prominent" time lags with other electrodes in each analysis interval. (The prominent time lags of a significant electrode group are determined by recursion over steps 7-10).

An eighteenth step is being tested which computes time-varying multivariate models of the spatio-temporal neurocognitive signals extracted in the first seventeen steps.

6. Major Obstacles to Progress

a. Biophysical and Engineering Obstacles

The development of precise electrophysiological methods for measuring brain function depends on technological advances in several areas. The fundamental problem in extracting meaningful information from brain electromagnetic signals is that only a subset of the brain's hundreds of simultaneously active major systems may be performing processing related to a particular perceptuomotor or cognitive function. Further, this subset seems to shift rapidly among widely distributed anatomical areas, and the diverse geometric orientations of neural generators in these dispersed systems results in complex potential and magnetic field distributions at the scalp. It is possible to determine the sources of these distributions only in special cases which meet a priori assumptions, such as an equivalent-single-dipole generator (Kavanaugh, et al., 1978; Sidman,

November 13, 1984 (56)

et al., 1978; Darcey, et al., 1980; Williamson and Kaufman, 1981a,b; Kaufman and Williamson, 1982; Romani 1982; Okada, 1983; Cohen and Cuffin, 1983; Barth 1984). These restrictions are unrealistic in the case of higher brain functions, which involve the integration of processing in a number of discrete systems (Luria 1970). In such cases, the "equivalent dipole" solution will not reflect the actual locations of several simultaneously-active sources.

Furthermore, the tissues which intervene between the cortex and the scalp greatly distort brain potentials (BPs) by acting as a spatial low-pass filter. Low temporal frequency BPs are spatially smeared and high temporal frequency BPs are attenuated because they have low spatial coherence at the cortex (Cooper, et al., 1965). Due to variations in tissue properties, the degree of distortion varies at different points on the scalp and is different for different people. This distortion can be corrected by two-dimensional spatial deconvolution (Nicholas and de Loeche, 1976; Doyle and Gevins, in Prep.), but measurements of the thickness and conductance of the intervening tissues at each electrode site are required to obtain accurate solutions (Ary, et al., 1981). Use of ultrasonic devices to measure skull thickness is problematic, but the availability of nuclear magnetic resonance (NMR) scanners should improve this situation.

The magnetic fields generated by the brain are not greatly distorted by intervening tissues, and improvements in superconducting quantum interference device (SQUID) sensor technology are eagerly awaited. Substantial progress in locating single equivalent current dipole sources has already been made with the cumbersome single-channel SQUIDS currently in use. The work of Williamson, Kaufman, Romani and Okada at N. Y. University with healthy people, and that of Barth, Beatty, Sutherling and Engel at U.C.L.A. with epileptic patients, have set the standard in this regard (Williamson and Kaufman, 1981ab; Kaufman and Williamson, 1982; Okada, 1983; Barth, et al, 1984; Richer, et al, 1983; MacIin, et al, 1983; Romani, et al, 1982).

Simultaneous recording of many electrical and magnetic channels is obviously desirable for improving source localization.

b. Basic Science Obstacles

There is a more fundamental impediment to progress, namely that the functional significance of mass brain signals is not known. The opinion of most neurophysiologists is that macropotential patterns are useful epiphenomena which can supplement the information gained from recording the all-or-nothing action potentials of individual neurons. According to this view, like the smoke from a factory, macropotentials may indicate when a brain region is processing, but cannot provide more specific information. However, this popular belief is challenged by the advanced studies of Freeman and his associates at U.C. Berkeley. These studies demonstrate unequivocally that stable macropotential patterns of the olfactory cortex of rabbits embody emergent properties not present in the firing of single neurons. The spatial amplitude patterns of these neural "search images" constitute

November 13, 1984 (56)

"templates" of specific expected odors and contain specific information about the odor actually perceived (Freeman, 1975, 1979abc, 1981, 1983). Of course, it is a large leap from the simpler paleocortex to the more complex structure of the neocortex (the source of most scalp-recorded activity -- Petsche, et al., 1984; Speckman, et al., 1984), but similar general principles of mass neural organization may well apply. The strict epiphenomenalist view is being challenged by other lines of advanced research. It has been suggested that low-intensity, low-frequency electromagnetic fields have the capability of influencing the metabolic activity of individual neurons (review in Adey, 1981). If so, such fields could play a significant role in mass neural information processing. There is some evidence for the existence of neural processes which are diffuse and widespread, rather than strictly localized as in traditional models. These processes are of relatively long duration compared to single-neuron firings, and their larger spatial extent enables them to exert facilitatory and inhibitory influence on vast numbers of neurons. These processes may operate by large-scale integration of classical synaptic mechanisms, or may involve less understood modes of communication, such as the serotonic fibers lining the walls of the cerebral ventricles. It has been proposed that these processes are responsible for the regulation of higher level behavioral states such as arousal, reinforcement, and memory formation (Dismukes, 1979). Macropotentials, rather than single-neuron firings, must be studied in order to determine the effects of these systems.

These technical obstacles and matters of basic science are currently being attacked by a number of interdisciplinary teams of physical, medical, biological and behavioral scientists, and considerable progress may be achieved in coming years. Advances in sensing, computing and digital signal-processing technologies, combined with carefully controlled experimental designs, are propelling this progress at an ever increasing pace. While earlier research was often characterized by technically naive "tinkering", or blind application of new analytic technologies without adequate attention to neurophysiology and experimental control, this current work reflects an integrated, interdisciplinary approach.

c. Conceptual Obstacles: Implicit Brain Models in EEG and ERP Studies

Current paradigms implicitly assume an overly simplistic model of brain activity. In exploring new directions for research, it would be useful to more carefully examine the assumptions upon which these models are based. In EEG studies, it is assumed that the brain essentially consists of the cerebral neocortex which is represented by regions corresponding in number to the scalp electrodes. The energy emitted by these regions in several frequency bands over periods from several seconds to minutes is thought to be related to the number of neurons engaged in "cooperative processes" (Elul, 1969, 1972ab). Specific higher brain functions are assumed to be associated with characteristic cooperative processes, which may be conceptualized as relatively stable macrostates with distinct spectral intensity

November 13, 1984 (56)

patterns; pathological conditions manifest as alterations of these patterns (Gevins and Schaffer, 1980).

A more dynamic model underlies ERP studies. In clinical paradigms which test the integrity of sensory pathways, there may be a direct conceptual association of the timing of successive peaks with ascending anatomical structures. But the situation is more complex in studies of the later stages of information processing. In these paradigms, many of which require performance of a task, it is assumed that once "programmed" with a set of task instructions, the brain operates on a stimulus in more-or-less sequential information processing stages resulting in a response deterministically related to the stimulus. The successive major peak complexes and low-frequency waves of the averaged time series, or principal components corresponding to them, are thought to correspond to these stages. Task-related changes in peak voltage or component amplitude are considered to represent changes in processing load, in direct analogy to reductions in background EEG alpha band spectral intensity during task performance. Differences in the scalp voltage distribution of an ERP peak or component are interpreted as reflecting the presence of distinct neural generators. Shifts in peak or component timing, particularly of the various N2 and P3 components, appear to correspond with changes in the timing of certain "endogenous" mental processes, but the contribution of trial-to-trial variability to these latency shifts is most often not explicitly measured, nor is the deconvolution of spatially overlapping processes explicitly attempted. While ERP experiments continue to generate interesting results, the fundamental problem is that the relations between ERP peaks and brain functions are not actually as direct or as simple as they are assumed to be (Gevins, 1983a, 1984a). Since the same ERP effects can be produced under a variety of circumstances, and since minor variations in experimental manipulations can result in different ERP effects, one must conclude that some of the effects have no intrinsic existence outside the context of a particular experimental paradigm.

Further improvements in event-related signal estimation can be expected when analytic models are used with greater neurophysiological fidelity. Classical models assume that physically distinct brain systems produce event-related signals and unrelated background EEG activity. In actuality, the activity pattern of a neural system seems to undergo a reorganization as some subset of the system's neurons becomes involved in event-related processing. The summated extracellular brain potentials may manifest this reorganization by changes of amplitude, frequency, morphology and timing characteristics of low frequency waveforms. A more realistic analytic model may thus be a hybrid of the "post-stimulus additive noise" and "pre- to post-stimulus transformation" approaches. In this case, the multichannel event-related signal would be modeled by a nonlinear, time-varying transformation of the pre-stimulus brain state plus an event-related process, plus random noise. The pre-stimulus brain state, a function of a person's expectations, would itself be modeled by a time-varying signal plus an additive noise process. A further complication is that, at least in the instance of higher cognitive functions, the brain does not necessarily behave deterministically.

November 13, 1984 (56)

Because of the hierarchical, parallel organization of the brain, and because of its adaptive learning capabilities, the same behavior can result from a variety of different processes involving different neural systems. In attempting to extract function-related signals, it would seem imperative to allow for this multiplicity of possible mechanisms.

While they continue to be fruitful, both currently popular approaches, EEG and ERP, are based on highly oversimplified models of the brain and information processing. The former has insufficient temporal resolution to resolve fraction-of-a-second processes, while the latter performs an excessive data reduction resulting in too few parameters to characterize complex processes. Although still exceedingly crude, a somewhat more realistic research model for the next generation of analytic studies may be to consider the brain as a local distributed computational network (Gevins, 1981, 1983b, 1984). A first step in empirically developing such a model will be to attempt to measure the input and output of each of a number of simultaneously active major processing nodes and the rapidly shifting temporal patterning of communication between them during simple tasks.

II. PILOTING OF AN AUDITORY-VISUAL PERCEPTUOMOTOR TASK

A. Design Considerations

A number of issues were considered in designing a bimodal paradigm sufficiently controlled to reveal NCPs which distinguish auditory and visual perceptuomotor tasks during the modality-cued prestimulus and post stimulus intervals.

1. Cognitive Considerations

Two hypotheses are being tested. First, NCPs should show neuroanatomically interpretable differences between the processing of auditory and visual numeric stimuli in post stimulus intervals when feature extraction is thought to occur in sensory and related cortical areas. There should be minimal differences after sense-specific processing is completed. Second, NCPs should differ in the modality-cued prestimulus interval as a function of the preparation to receive either visual or auditory stimuli. The second hypothesis requires complete equivalence of cue properties and performance-related factors between auditory and visual conditions, and also a strong inference that a modality-specific expectancy set exists in the cued prestimulus interval.

2. Experimental Controls

The first hypothesis (ie, post stimulus processing) requires control of stimulus, response and performance-related factors across conditions so that the major difference between conditions is stimulus modality. Visual and auditory modalities have fundamental differences. Input for the former is parallel (for brief foveally presented stimuli), while for the latter it is serial. Inherent

November 13, 1984 (56)

differences in auditory and visual processing latencies can be compensated for by centering several analysis windows on the average ERP peak latencies in each person for auditory and visual conditions separately. Differences in ERP amplitudes can be explicitly measured. With regard to the second hypothesis (ie. prestimulus attentional set), the modality-cued paradigm elicits a contingent negative variation (CNV) between cue and stimulus, with consequent resolution after stimulus presentation. NCP Analysis will be applied to measure pre- and post-stimulus modality differences. The results may shed some light on the interaction between preparatory activity and post-stimulus processes.

3. Montage

In the pilot recordings, a montage of 21 scalp electrodes positioned over auditory, visual, motor, parietal and dorsolateral prefrontal cortices was used. Four additional channels recorded vertical and horizontal EOG, EMG and the response. Formal recordings employed a 49 channel montage (Figure 3b) in order to achieve a resolution of approximately 10 square centimeters. A recent study of trimodal attentional set using the regional cerebral blood flow technique (Roland, 1982) revealed that the spatial patterns of focal neural activation related to attention and modality processing are complex and finely detailed, even with a 30 sec temporal resolution. For adequate sampling of brain potentials corresponding to these regions of focal activation, a dense coverage of lateral prefrontal, superior and inferior posterior parietal, and superior and posterior temporal areas is required.

B. Task Development and Pilot ERP Recordings

1. Phase One (P's #1-8): (Respond to miscues)

a. Rationale. The existence of a modality-specific prestimulus attentional set was investigated with the "miscueing" technique (Posner, 1978). In this method a randomly ordered 20% of the modality cues (a visually presented letter in both conditions) are incorrect. The lengthening of mean response time in these miscued trials is considered the "cost" incurred by the expectation of a stimulus in a specific modality, and is used to infer the existence of a modality-specific preparatory set.

b. Task. Stimulus presentation and response measurement were performed by the real time subsystem of the ADIEEG system, which also digitized the 25 channels of physiological signals (21 scalp) at 256 samples/sec. The participant (P) was instructed to fixate a point at the center of the CRT screen of an AED II graphics terminal and await a visually presented modality cue (V for visual; A for auditory; duration 375 msec). 1.5 sec later the stimulus was presented. Auditory stimuli consisted of the numbers 1 to 9 generated by a Votrax speech synthesizer and presented through two speakers about 70 cm above the participant's head. Duration varied from 245 to 420 msec (the number 7 was generated as "SEVN"). Visual stimuli were

November 13, 1984 (56)

single digit numbers presented on the CRT, subtending a visual angle of under one degree. Their duration was equated to that of their corresponding auditory numeric stimuli.

The participant was instructed to attend the modality cue and "focus his attention" on the speakers or screen as indicated by the cue, while maintaining his gaze on the screen. He was to respond to the stimulus without hesitation with a ballistic contraction of his right-hand index finger on a modified Grass force transducer, exerting a pressure corresponding to the stimulus number on a linear scale of 1 to 9. Feedback indicating the exact pressure applied was presented as a 2 digit number on the CRT screen (duration 375 msec) 1 second after completion of response as determined by the program.

If the response was sufficiently accurate, the feedback number was underlined, signifying a "win". The error tolerance for a "win" was continually adjusted throughout the session as a moving average of the accuracy of the preceding five correctly cued trials in visual and auditory modalities separately.

A random 18% of the trials were miscued (ie. the stimulus arrived in the wrong modality). The participant was to respond to these just like the correctly cued trials. Correctly cued and miscued auditory and visual trials were presented in randomly ordered blocks of 17 trials, self-initiated by the participant.

c. Recordings. Eight normal, right-handed adult male participants were recorded in pilot sessions consisting of about 350 to 700 trials each. The electrode montage was Fz, F7, F8, aF1, aF2, aCz, Cz, C3, C4, C5, C6, Pz, P3, P4, T3, T4, T5, T6, Oz, aO1 and aO2, referenced to linked mastoids (modified expanded 10-20 system nomenclature; see Fig. 3a). Vertical and horizontal eye movements, response muscle activity, and force transducer output were also recorded. All signals were amplified by a 64-channel Bioelectric Systems Model AS-64P amplifier with .10 to 100 Hz passband, continuously digitized to 11 bits at 256 samples/sec and stored on digital tape. Signals were also recorded on three 8-channel polygraphs to monitor the session and for off-line artifact editing. Average response times (RT) and error rate (proportion of "lose" trials) were computed for behavioral evidence of a "cost" due to a prestimulus attentional set in a total data set of 3735 trials.

d. Results and Discussion. For correctly cued trials, the mean response times were quicker for visual stimuli for all but two people. Average RT across P's was 675 msec for visual stimuli and 711 msec for auditory. The longer RT for auditory stimuli, which is opposite to the findings in simpler bimodal paradigms, may be due to the nature of the verbally presented number stimuli. All information needed for visual stimulus decoding appeared on the screen within 33 msec, while auditory information was not completed for up to several hundred msec. The longer RT for the auditory stimuli may also be due to the use of synthesized speech stimuli.

November 13, 1984 (56)

AFOSR

Table 1 - Average response time (in msec) and standard deviation for correctly cued and miscued auditory and visual trials for the 8 participants recorded in phase one of task development. (Miscues total 18% of trials; 9% of each type).

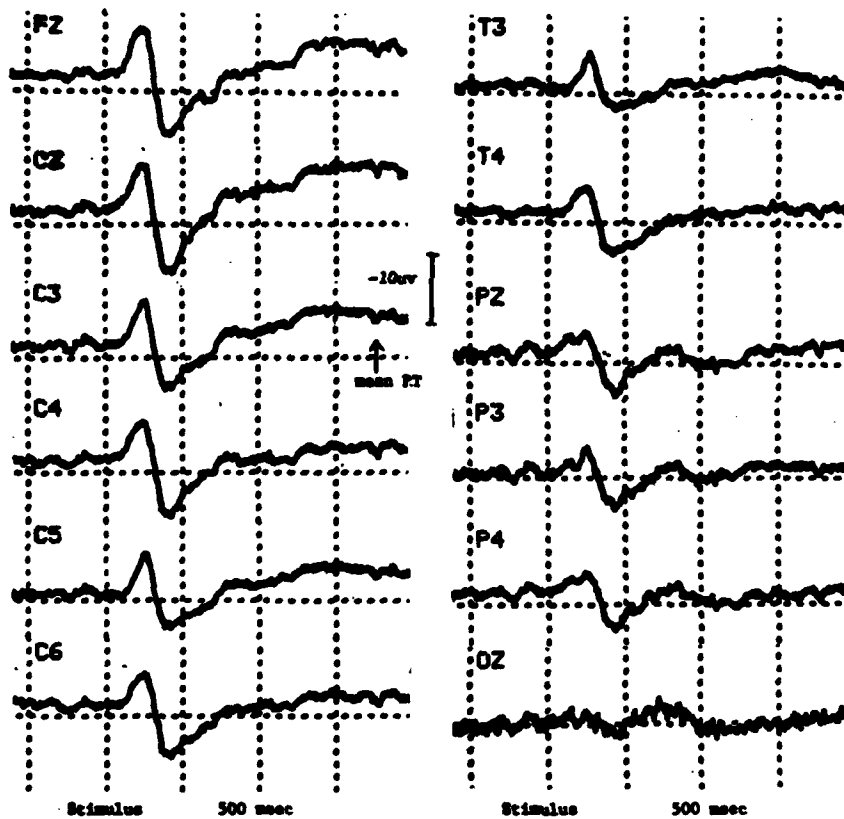
Pt	Trials	<u>Auditory</u>		<u>Visual</u>		<u>Increase</u>	<u>Increase</u>
		<u>correctly</u> <u>cued</u> <u>(S.D.)</u>	<u>mis-</u> <u>cued</u> <u>(S.D.)</u>	<u>Correctly</u> <u>cued</u> <u>(S.D.)</u>	<u>mis-</u> <u>cued</u> <u>(S.D.)</u>	<u>in R.T.</u> <u>miscued</u> <u>auditory</u>	<u>in R.T.</u> <u>miscued</u> <u>visual</u>
#1	318	830 (198)	803 (171)	710 (213)	757 (221)	-27 msec.	+47 msec
#2	368	702 (112)	803 (124)	648 (120)	796 (116)	+101	+148
#3	406	574 (81)	632 (89)	473 (93)	539 (93)	+58	+66
#4	609	687 (140)	718 (198)	578 (140)	652 (120)	+31	+74
#5	606	850 (136)	865 (124)	722 (140)	737 (116)	+15	+15
#6	668	528 (39)	625 (39)	603 (54)	664 (54)	+97	+61
#7	372	892 (43)	978 (58)	1052 (58)	1106 (19)	+86	+54
#8	388	626 (95)	636 (81)	609 (110)	667 (80)	+10	+58
<hr/>							
X (S.D. across persons)		711 (106)	758 (111)	675 (116)	740 (103)	+47 msec	+65 msec
<hr/>							
Total trials	3735	1560	302	1565	308		

November 13, 1984 (56)

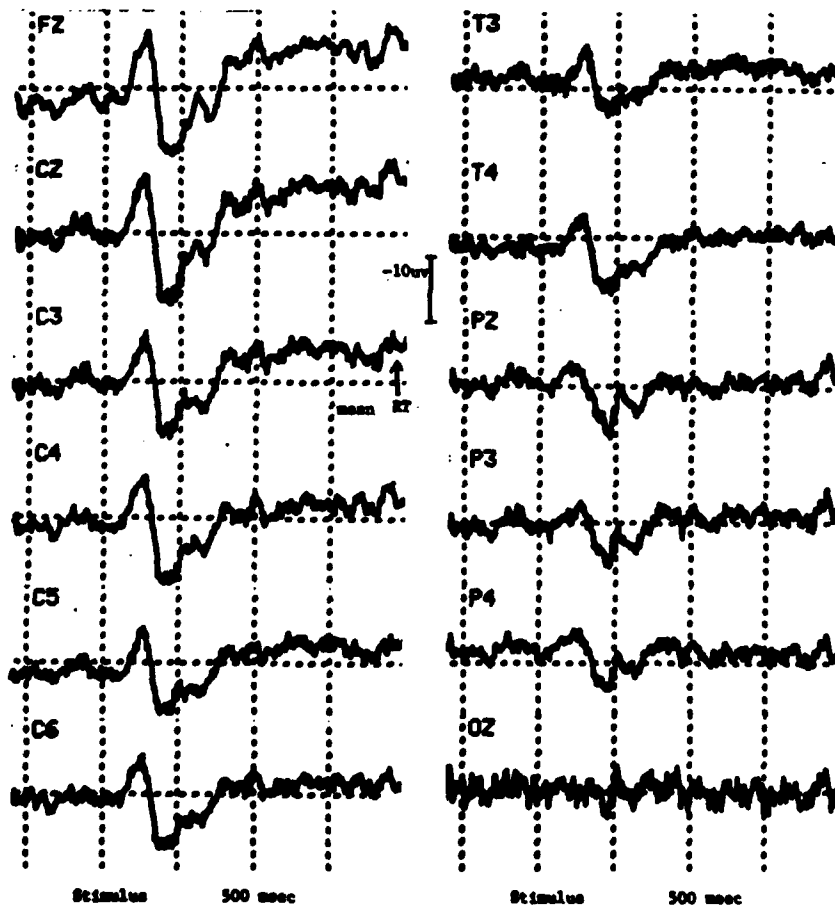
AFOSR

Table 2 - Error rate (% of "lose" trials) in correctly cued and miscued auditory and visual conditions in phase one of task development. (Miscued trials = 18%).

<u>P#</u>	<u>Trials</u>	<u>Auditory</u> <u>correct</u> <u>cued</u>	<u>Lose %</u> <u>mis-</u> <u>cued</u>	<u>Visual</u> <u>correct</u> <u>cued</u>	<u>Lose %</u> <u>miscued</u>	<u>Auditory</u> <u>increase</u> <u>in lose %</u> <u>%</u>	<u>Visual</u> <u>increase</u> <u>in lose %</u>
#1	318	57	53	45	80	-4	+35
#2	368	53	57	48	69	+4	+21
#3	406	50	63	55	53	+13	-2
#4	609	51	69	59	65	+18	+6
#5	606	52	61	54	58	+9	+4
#6	668	49	58	54	53	+9	-1
#7	372	47	66	49	59	+19	+10
#8	388	51	53	53	59	+2	+6
<hr/>							
X	3735 (Total)	51%	60%	52%	62%	+9	+10

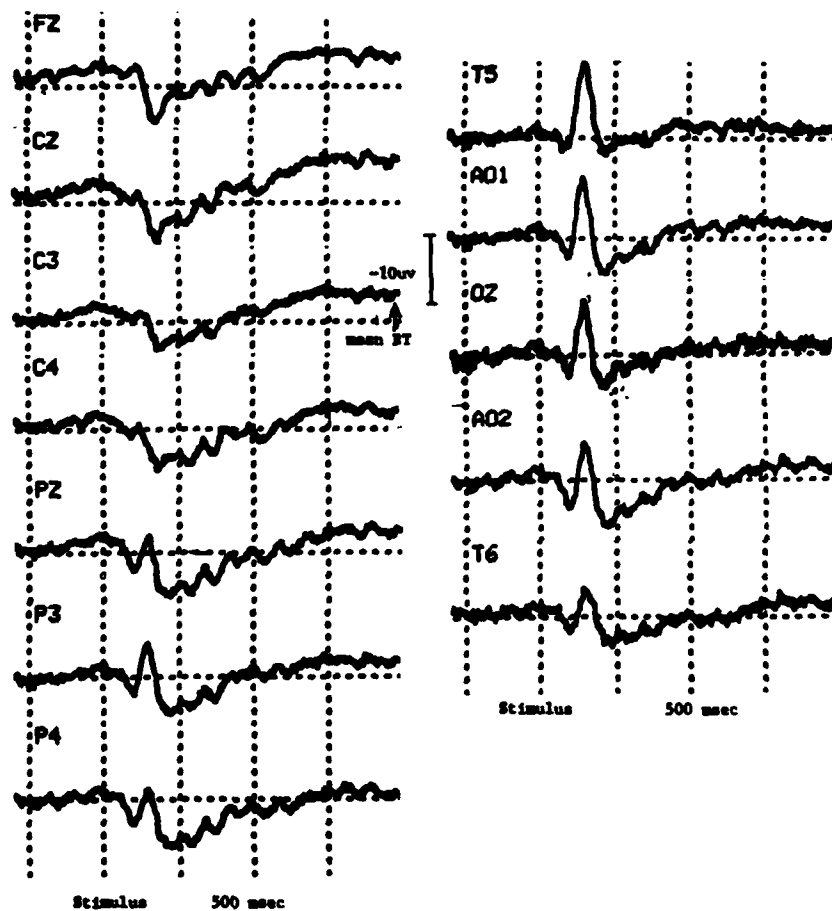


Auditory correctly cued condition, average event-related potentials for selected channels for p7. (91 trials, .1 to 100 Hz passband)

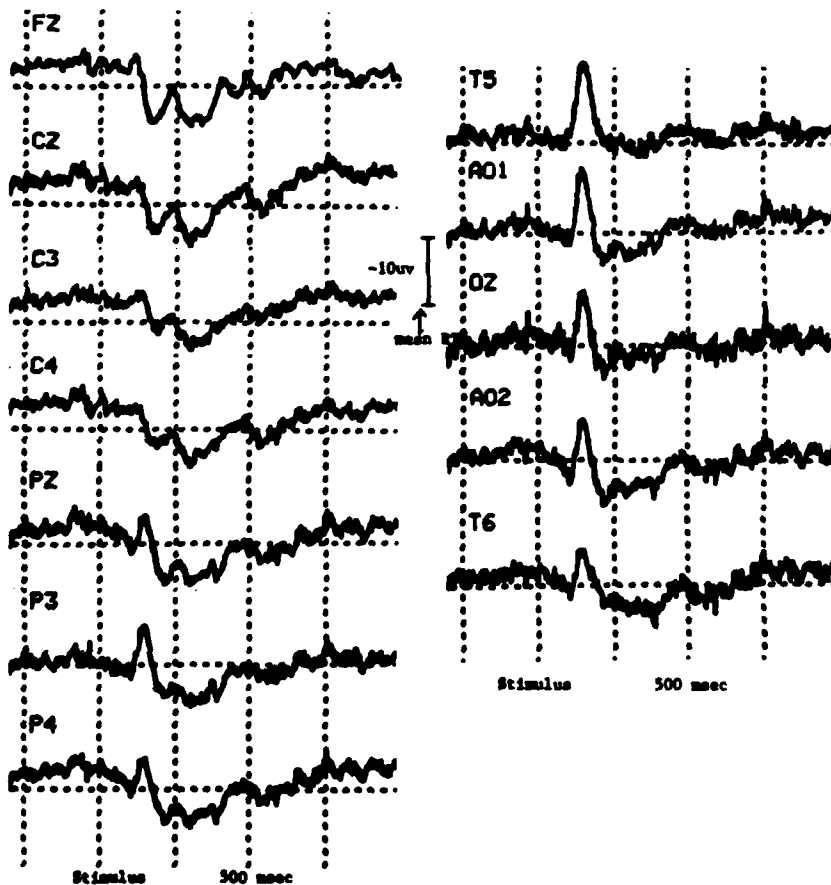


Auditory mislead condition with response (p7, 27 trials)

FIGURE 1a.



Visual correctly cued condition, selected channels (p77, 96 trials)



Visual uncued condition with response (p77, 31 trials)

FIGURE 1b.

November 13, 1984 (56)

In the miscued trials a lengthening of RT and increase in error rate was observed in almost every case (Tables 1 and 2). For miscued auditory stimuli the average increase in RT was 47 msec and the average increase in error rate (proportion of "lose" trials) was 9%. For miscued visual stimuli the "costs" of miscueing were slightly greater (increase in RT = 65 msec; increase in error rate = 10%). There was a small (18 msec) asymmetry in RT effect. That is, miscueing a visual stimulus caused a greater increase in RT than miscueing an auditory stimulus. This asymmetry and the magnitude of the RT lengthening in miscued trials is in agreement with previous studies using simpler tasks (Posner, 1978). Further, the standard deviations for all cued and miscued conditions were similar within persons, indicating that the RT "costs" due to miscueing were based on a consistent effect rather than greater variability in a smaller sample (about 4 to 1 ratio of correctly vs. incorrectly cued trials.) Thus it was verified that there was a "cost" in the miscued trials indicative of an attentional commitment to a particular modality in the prestimulus interval.

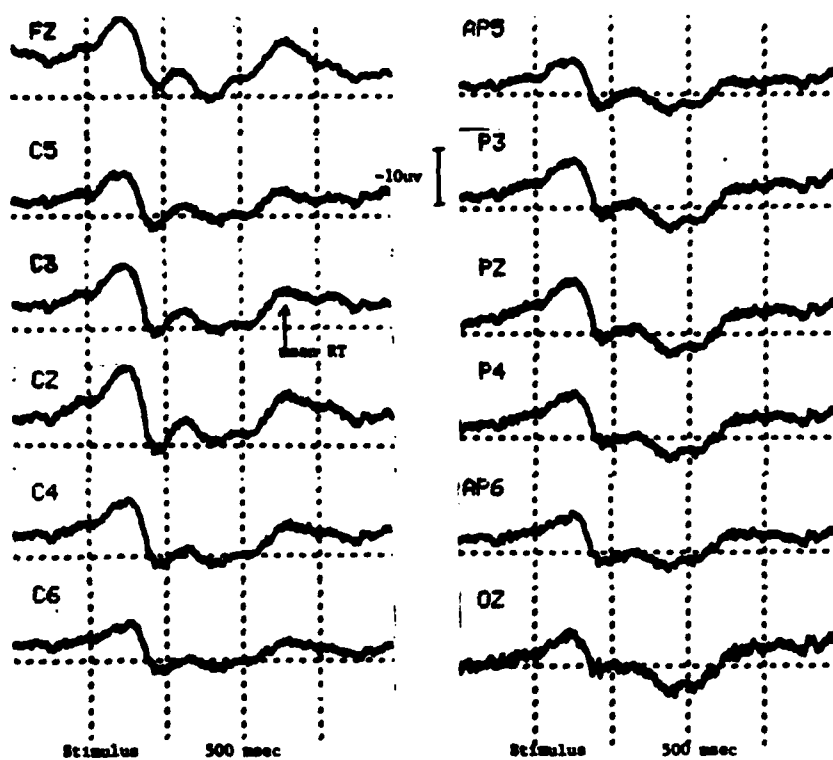
The ERPs for one person (P87) are shown in Figures 1a and 1b. The major difference between the correctly cued and miscued waveforms was in the P3 peak. In the auditory condition (Figure 1a), the miscued auditory stimuli produced an augmentation of the P3 peak at 314 msec. This P314 was maximal at the midline parietal electrode, and extended to midline fronto-central, lateral central and lateral parietal electrodes. In the visual condition (Figure 1b), the miscued stimuli elicited an augmentation of the P3 peak at 300 msec. The visual P300 was broader, and more anteriorly distributed than the auditory P314. A pre-stimulus CNV is evident as a fronto-central negativity. Its resolution could occur at different latencies after visual and verbal stimuli. Also, the information content of the verbal stimuli occurred at various latencies (as in "six" and "seven", or "four" and "five", as compared to the other numbers). What effect this may have upon the latencies of endogenous ERP components is not known. These issues will be addressed in the formal study.

2. Phase Two (P's 89-12): (No response to miscues)

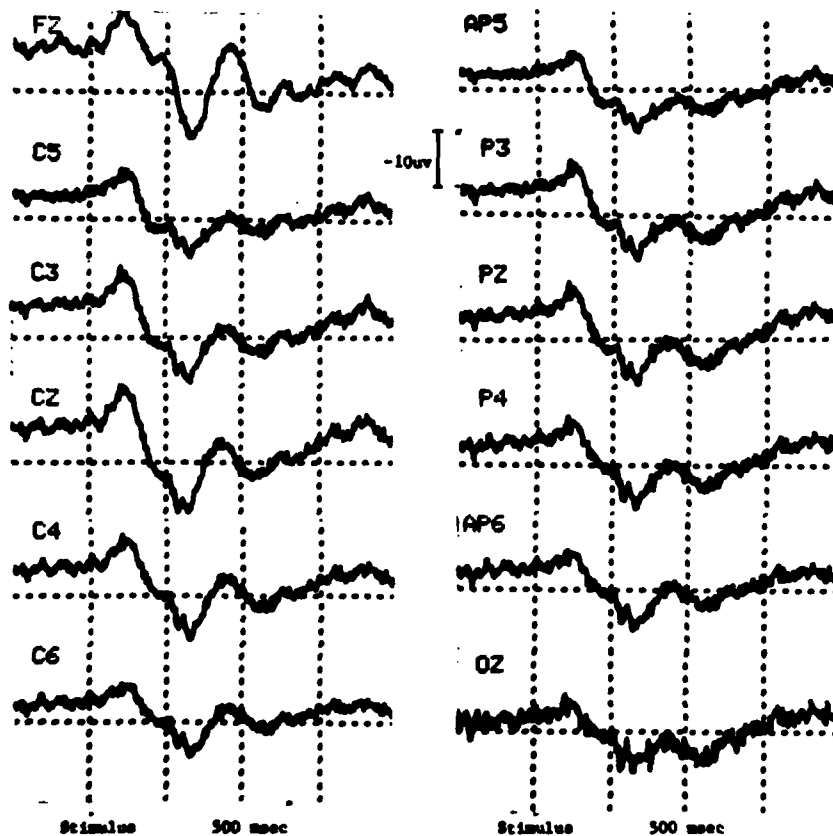
a. Rationale

The behavioral results of phase one confirmed the existence of a prestimulus attentional set. In phase two a move/no-move design was employed; the "response" to a miscued stimulus was to make no movement. This was done so that there would be confirmation of attention to the cue in each trial.

b. Task. The task was the same as before, except that the participant was instructed to make no response on miscued trials (random 20%). A monetary incentive was added by rewarding "win" trials according to the accuracy of response (about 5 cents for each win). The accrued monetary reward was displayed at the end of each block of 17 trials, along with the average error tolerances (performance index) for auditory and visual trials. The cue-to-stimulus interval was 2.5 sec for P's 89-11, and 1 sec for P812. For P812 a separate run was recorded with a 2.5 sec prestimulus interval for the visual modality only.

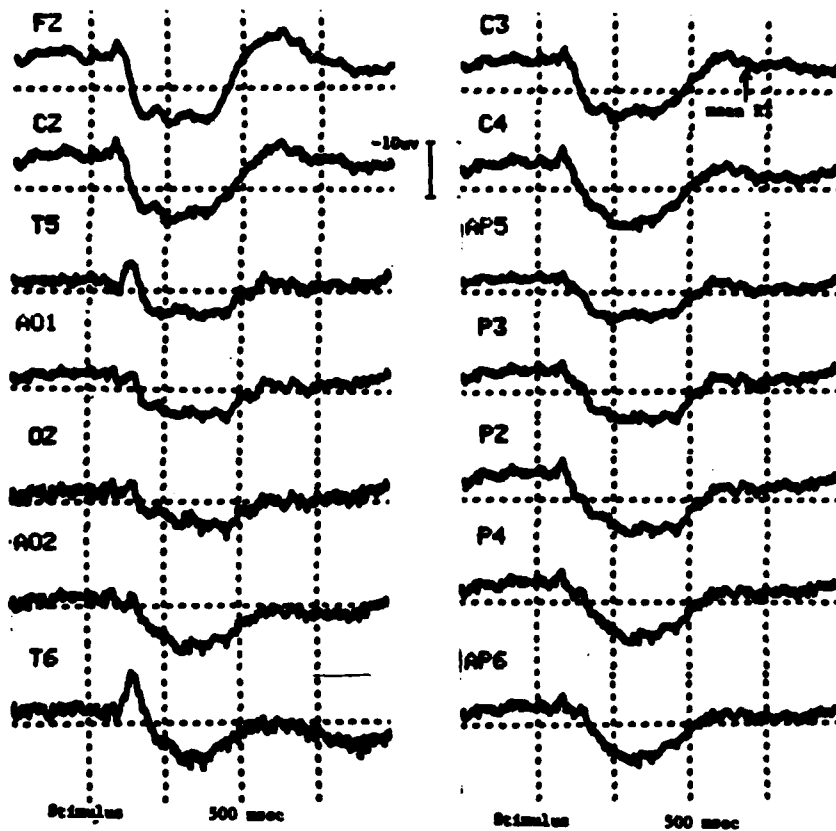


Auditory correctly cued (move) condition. Average event-related potentials from selected channels from p012 (103 trials, .1 to 100 Hz passband).

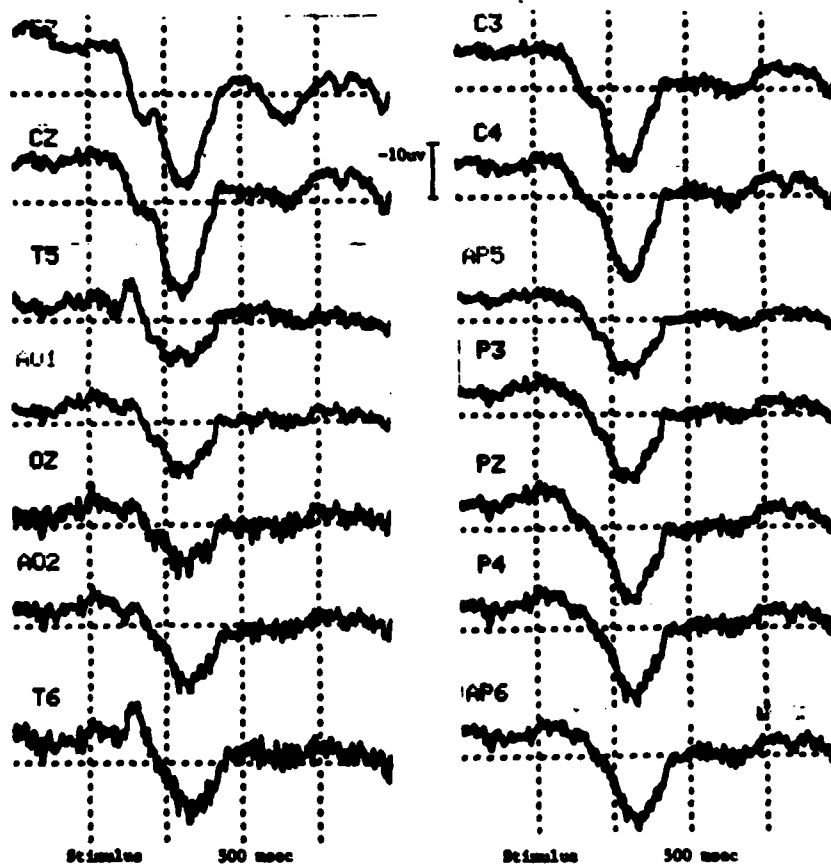


Auditory miscued (no-move) condition. (p012, 36 trials).

FIGURE 2a.



Visual correctly cued (move) condition. (p#12, 98 trials).



Visual mis-cued (no-move) conditions. (p#12, 33 trials).

FIGURE 2b.

November 13, 1984 (56)

c. Recordings. Four normal, right-handed adult males participated in sessions consisting of about 100 practice and 400 test trials. The 21 channel montage consisted of Fz, F7, F8, aF1, aF2, aCz, Cz, C3, C4, C5, C6, Pz, P3, P4, aP5, aP6, T5, T6, Oz, aO1 and aO2, referenced to linked mastoids. Tin scalp electrodes were attached using a stretchable nylon cap (Electrocap International). Vertical and horizontal eye movements and response muscle potentials were also recorded. Other aspects of the recording procedure and ERP computation were the same as phase one. Cue-registered averages were also computed for P812 for the cue-to-stimulus interval.

d. Results and Discussion. At the 2.5 sec cue-to-stimulus interval (P's 89-11), there was a high rate of data attrition (about 25%) in the no-move (miscued) trials due to mistaken overt responses. At the 1 sec interval (P812) there were no mistaken responses to no-move (miscued) stimuli. The high rate of incorrect responses to no-move stimuli at the 2.5 sec interval may have been due to decay of the attentional set. Therefore, the 1 second interval seems more desirable for the study of prestimulus expectancy.

The stimulus-registered ERPs for the move trials (Fig. 2a and 2b) were similar to the correctly cued trials of Phase one. In P's 89, 10 and 12 the no-move (miscued) trials elicited an augmentation of the P3 peak. The P3 peak amplitude in both move and no-move averages was maximal at midline fronto-central sites. A similar anterior distribution of P300 peak amplitude to no-go stimuli was reported in a go/no-go paradigm with equiprobable stimuli (Simpson, et al, 1977).

A pre-stimulus CNV was seen in all participants. In a cued paradigm such as this, a CNV may well be concomitant with the expectancy set we wish to study (reviewed by Tecce, 1972). CNV negativity was largest at midline fronto-central electrodes. Although its topography did not seem to differ with expected stimulus modality, NCP Analysis of the cue-to-stimulus interval in the formal study may shed more light on the important issue of the existence of a modality-specific effect on the anatomical distribution of CNV-related activity, an issue which has not been thoroughly examined (Ritter, et al, 1980).

3. Final Paradigm

A screening program was used to select and train candidate participants. During screening sessions EEGs were recorded from Fz, Cz, Pz, aO1 and aO2, and from T1 and T2 to assess EMG activity potentials from temporalis muscles. Vertical and horizontal eye movements were also recorded. Behavioral records were examined to assess the quality of task performance, polygraphs were inspected to determine the amount of data attrition due to artifact, and average ERPs were computed to verify the presence of expected ERP peaks. About one-third of the candidates screened were selected for the formal study.

As of 1 JUN 84, four full recordings have been made with the 49 electrode montage (Fig. 3b). (The 64 channel recording cap shown in Fig. 3c is now operational.) Approximately 800 trials were recorded from each

EXPANDED 10-20 SYSTEM

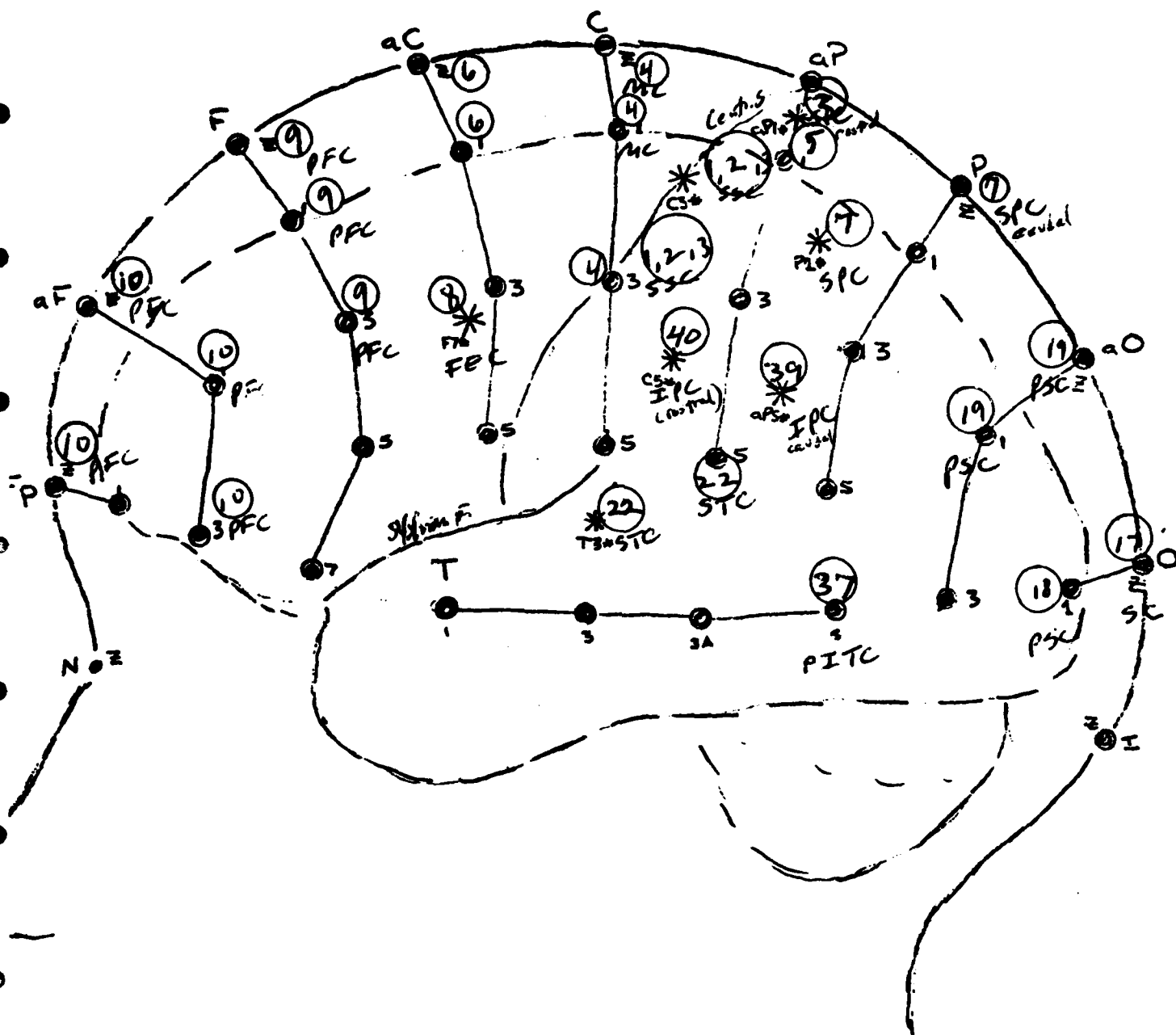


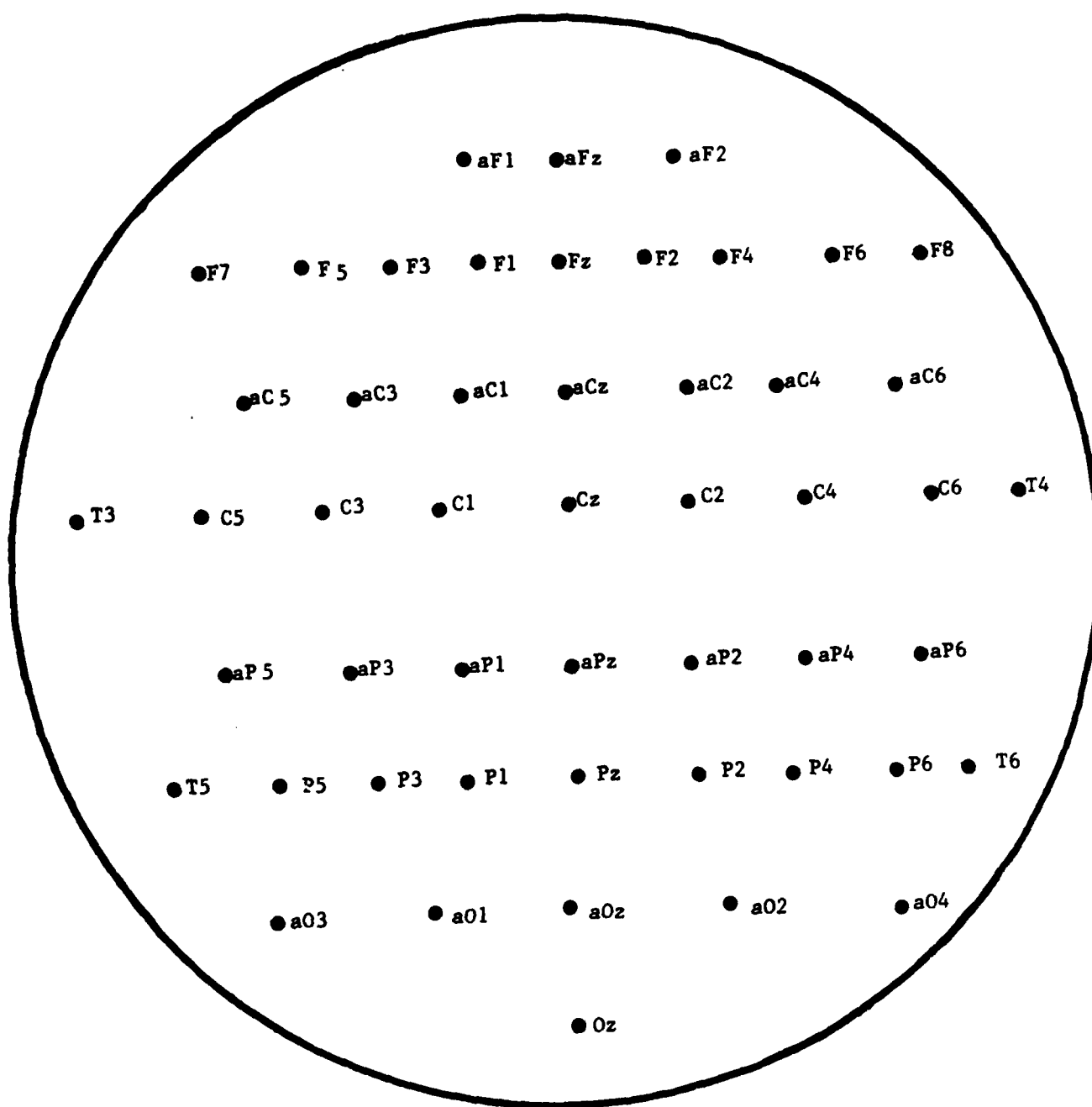
FIGURE 3a. Expanded 10-20 system as detailed by Picton et al. (1978). The nomenclature for coronal plane sites has been modified for consistency. Asterisks indicate special placements. Circled numbers are approximate location of Brodmann areas.

Figure 3a: Approximate cortical areas underlying scalp electrodes*

Area	Broadman #	Scalp Electrodes†
striate cortex (SC)	17	OZ
peristriate cortex (PSC)	18	O1, aO3
peristriate cortex (PSC)	19	aOz, aO1, aO3, T5, P5
post. inferotemporal cortex (ITC)	37	T5
prefrontal cortex (PFC)	9	Fz, F1, F3, aF1, aFz
prefrontal cortex (PFC)	10	Fpz, Fp1, aFz, aF1, aF3
sup. temporal cortex (STC)	22	T3, aP5 (caudal end)
inferoparietal cortex (IPC) (caudal)	39	aP5, P5, P3
inferoparietal cortex (IPC) (rostral)	40	aP5, aP3, C5
sup. parietal cortex (SPC) (caudal)	7	Pz, P1, P3, aP1, aP3
sup. parietal cortex (SPC) (rostral)	5	aPz, aP1,
premotor cortex	6	aCz, aC1, aC3, aC5, C1
pre-central gyrus	4	Cz, C1, C3
post-central gyrus	1,2	C3, aPz
primary somatosensory	3	same as for 1 and 2
frontal eye field	8	Fz, F1, aC3

* Using the data of Tallalraach and Szikla 1967.

† Left side listed for convenience; add 1 to odd numbered electrodes for homologous right-sided placements. Electrode nomenclature modified from Picton et al. (1976) for consistency. Starting from the frontal pole, the coronal plane arrays are designated Fp, aF (anterior frontal), F, aC, C, aP, P, aO, O. See Fig. 3a: Expanded 10-20 System.



49 CHANNEL RECORDING MONTAGE

Figure 3b. 49 electrode recording montage used in the bimodal (auditory/visual) study.

FIGURE 3b.



Figure 3c. Research volunteer wearing 64 channel recording cap.

November 13, 1984 (56)

well-practiced participant using the paradigm and recording procedure described above. The cue-to-stimulus interval was 1 sec, the visual stimuli were thickened and increased in size to just under a 2 degree visual angle, and the proportion of miscued (no-go) trials was increased to 22%. Current Source Density (CSD) derivations were computed off-line (see Section V.D.1).

III. Pilot Analysis of Data from Final Paradigm

A. Formation of Data Sets

The data of one person (AV07) was used to refine the signal processing and analytic methods to be used in the formal analysis (see Section V). After inspection of polygraphs and behavioral records to eliminate artifacted and incorrectly performed trials, an edited data set of 510 trials remained. These trials were submitted to the ADISORT program (see Section IV.B) to form 6 pairs of data sets: stimulus-registered auditory vs. visual move, auditory move vs. no-move, visual move vs. no-move, and auditory vs. visual no-move; response-registered auditory vs. visual move; and cue-registered auditory vs. visual trials. These 6 pairs of data sets were each examined for the following differences in stimulus, response and performance-related variables: magnitude of stimulus number, response onset time, response movement force, velocity, acceleration and accuracy, adaptive error tolerance measure, "arousal" indices, and vertical and horizontal EOG indices. There was no significant difference within any of the pairs of data sets, except for the prestimulus arousal index ($p(.05)$) in the auditory vs. visual move pair, which may reflect a differential modality-specific expectancy, and the response time, which was 73 msec shorter for visual than for auditory move trials. Only a slight amount of pruning was required to balance the EOG indices so that the pairs of data sets did not differ at a conservative alpha of .2. Response times were pruned at ± 2.5 standard deviations, resulting in response times of 892 ± 127 msec for auditory and 817 ± 145 msec for visual move trials. The final sorted data sets were balanced for all variables (except RT) at an alpha of .2, and consisted of 149 auditory and 215 visual move trials, and 65 auditory and 74 visual no-move trials for the stimulus-registered sets. The cue-registered sets consisted of 119 auditory-cued and 180 visual-cued trials.

B. Examination of Averaged Waveforms

Averaged ERP and Current Source Density (CSD; see Section V.D.1) waveforms were computed from the balanced data sets for all channels and tasks (Figures 4 and 5, and 20a, 21a, 22a and 23a). The major event-related peaks were first determined from the ERP waveforms, and then compared with the CSD waveforms. The CSD waveforms exhibited peaks at the same latencies as the ERPs, but their amplitude distributions differed greatly. (CSD distributions in "head format" are shown in Figures 14 - 16.) CSD peaks were typically more spatially localized than corresponding ERP peaks. Since a computed common average reference was used in computing the ERPs for this participant (AV07), the topographies of ERP peaks differed from those usually found in "off-the-head" referential recordings, and thus will not be discussed here. CSD peaks are labeled according to the latency and

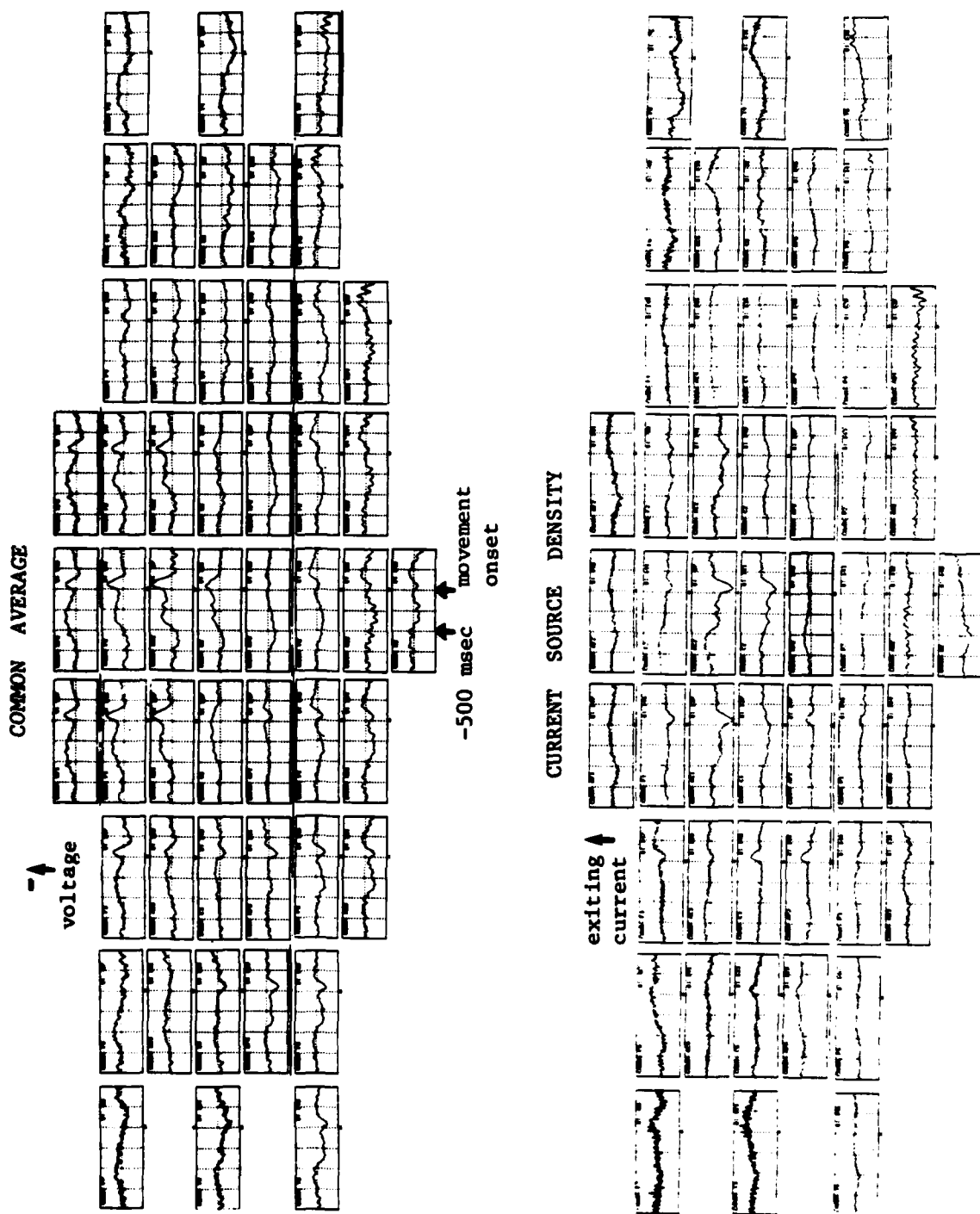


Figure 6. Movement-registered averaged waveforms for auditory trials: common average reference (top) and CSD (bottom).

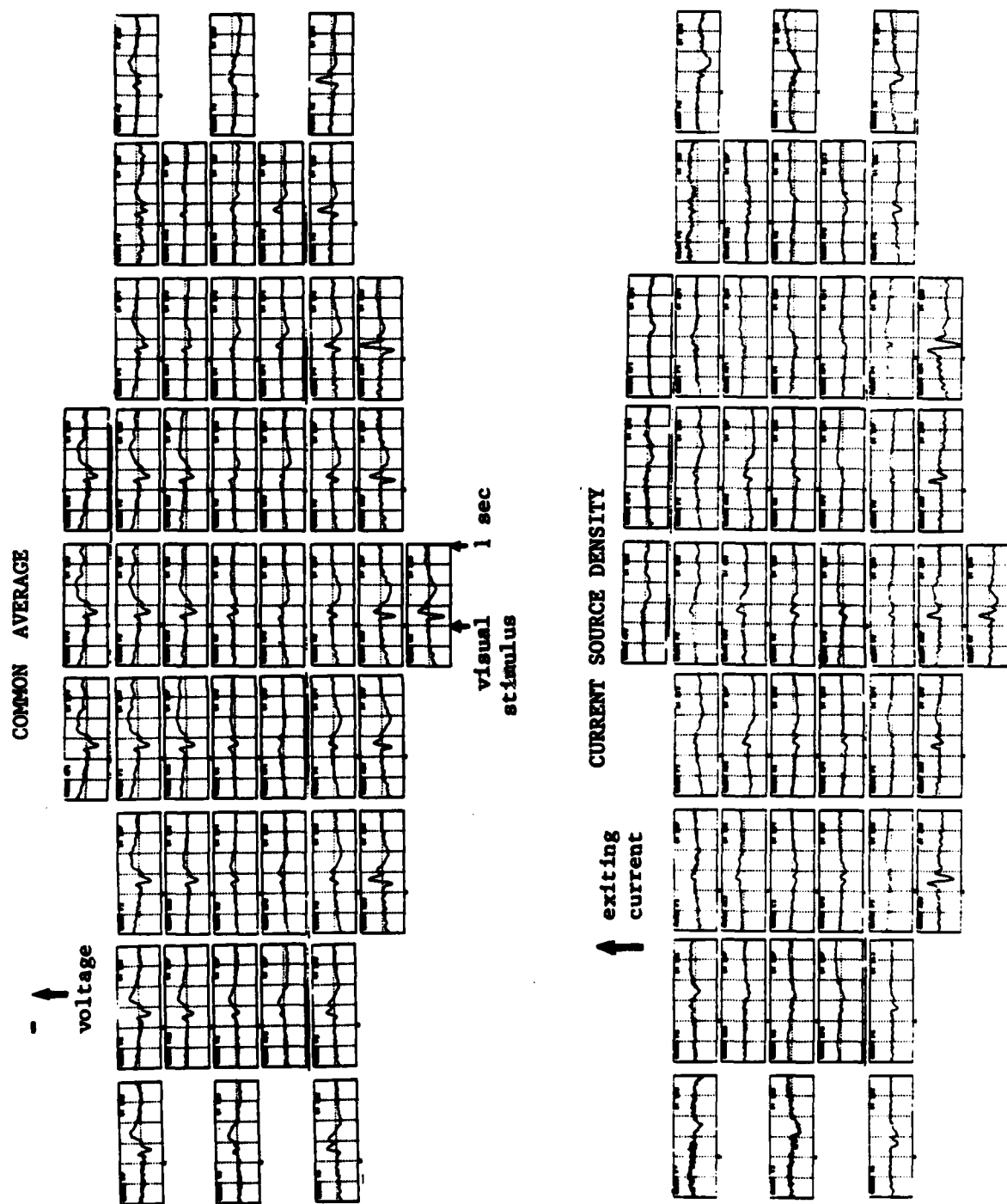


Figure 4. Averaged event-related waveforms for visual move trials from participant AV07. 49 channels. Common average reference (top) and current source density (CSD) (bottom).

November 13, 1984 (56)

polarity at the channel of maximum amplitude (eg. "P117"). Positive amplitude in the CSD derivation indicates exiting current ("source") and negative values entering current ("sink"). Peripheral electrodes will not be considered (see Section V.D). In considering the topographies of CSD peaks, it should be remembered that since the CSD is a measure of the curvature (second derivative) of electrical potential at the scalp, the maximum amplitudes of CSD peaks occur at regions where the curvature of potential is greatest. For example, maximum CSD amplitude for the CNV occurs at anterior parietal sites, where the change in the gradient of potential is greatest.

1. Exogenous Peaks

N100: Visual stimuli elicited a sharp peak (P117; Figure 4), positive ("current out") at posterior parietal and occipital sites (maximum at aOz), and negative ("current in") at anterior locations (maximum at Cz and aP1). A slight lateralization was present, the positive peak being larger at right posterior sites and the negative peak at the left anterior parietal (aP1) electrode. The negative peak was smaller and less localized at the scalp. Auditory stimuli elicited an N109 peak with negative amplitudes at most frontal, central and anterior parietal sites (Figure 5). Maximum negativity was at C2 and aP4, resulting in a right-sided lateralization. A corresponding positive peak was evident only at F5 and aOz.

P200: A second peak occurred at 172 msec for both visual and auditory stimuli. The anterior-posterior polarity was approximately opposite to the preceding peaks in each modality. The visual P172 was positive at most frontal and anterior central sites, with maximal amplitudes at aCz and aC3 (Figure 4). A distinct negative peak was seen only at the anterior occipital (aOz) and right parietal (P4 and P6) electrodes. The distribution of the auditory P172 was similar to the visual peak, but its amplitudes were slightly larger (Figure 5). The resolution of the prestimulus CNV also occurs within this latency range, and probably affects the amplitudes and topography of this peak.

2. Endogenous Peaks

The averaged CSD waveforms for no-move trials exhibited a series of peaks corresponding to the "late positive complex" in the ERPs. The most robust peak occurred at 313 msec for visual no-move trials (P313), and at 281 msec for auditory (P281). The positive peak of the visual P313 occurred at all midline sites, extending laterally at precentral sites and to lateral central electrodes immediately adjacent to the midline; it was largest at aCz, aC1 and aC2 (Figures 16a and 21a). A corresponding negative peak was observed only at peripheral electrodes. The auditory P281 was similar in topography (Figures 16b and 23a), but with amplitudes approximately twice as large at the site of maximum positivity (aCz), and substantially larger at Fz, Cz and aPz. This may have been due to the relative infrequency of the auditory stimuli in a paradigm using visual cues and feedback. Perhaps due to this enhancement of P281, a corresponding negative peak was visible at electrodes situated just within the peripheral ring.

In the visual no-move waveform a late peak occurred between 470 and 525 msec (P500). Its topography was sharply localized with a positive peak

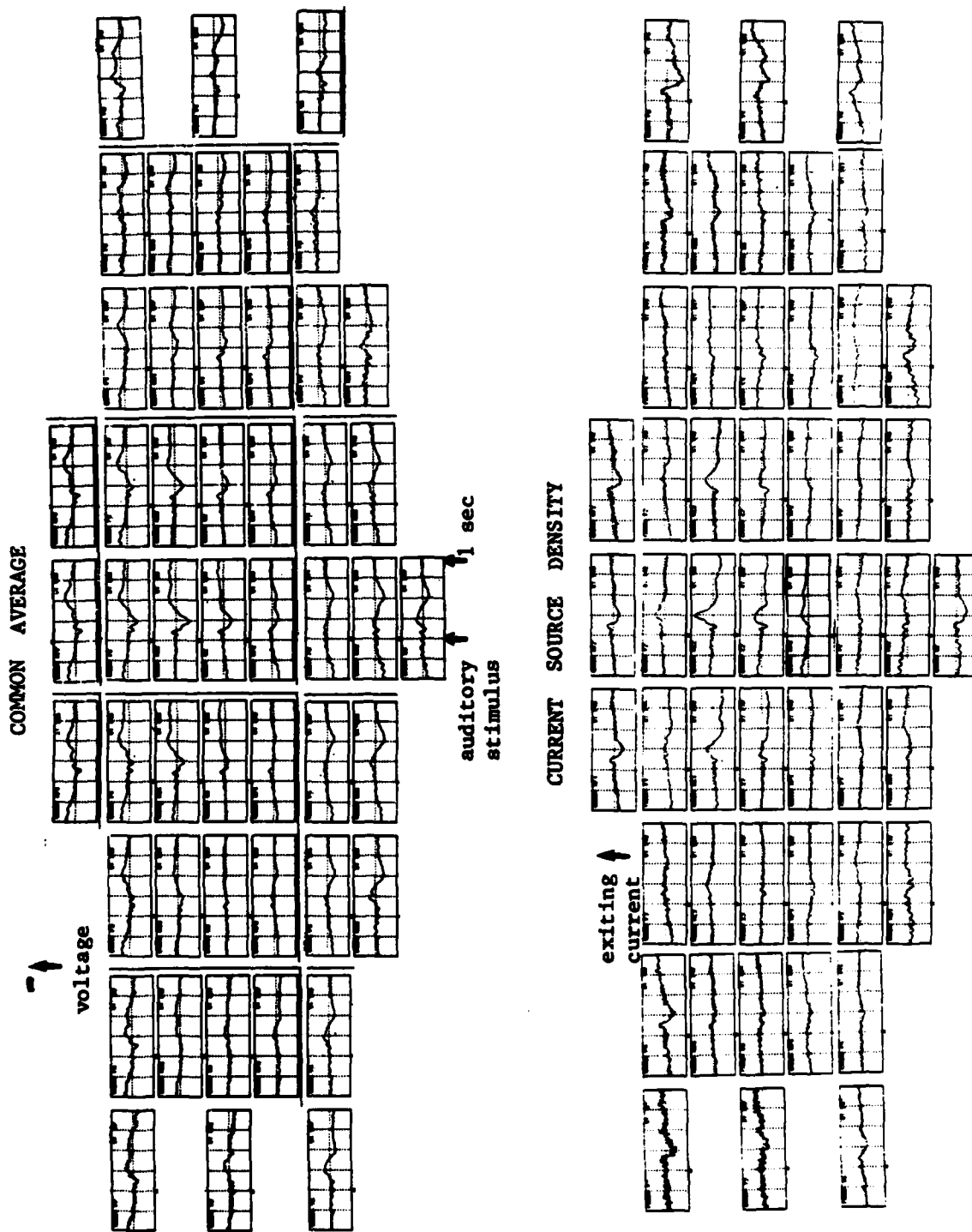


Figure 5. Auditory move waveforms (see Fig. 4).

November 13, 1984 (56)

only at midline sites posterior to Cz (maximal at aPz), and a corresponding negative peak only at midline frontal, precentral, and immediately adjacent lateral sites (Figures 16a and 21a). In the auditory no-move waveform the late wave (P580) peaked between 480 and 600 msec. A distinct positive peak occurred only at midline central and anterior parietal sites (maximum at aPz), while the corresponding negative peak was more widespread, occurring at Fz, F1 and F2, and at aC1 and aC2 (Figure 16b and 23a). At the anterior central midline (aCz) two distinct peaks were visible, a negative peak at 480 msec and a positive peak at 600 msec. The auditory P580 differed from the visual P500 in that its negative component was distinct and large in amplitude at most lateral and peripheral frontal and central sites.

3. Response Potentials

In response-registered averages, mean EMG onset was 65 msec before response movement onset in the visual move trials and 90 msec before response in auditory move trials. Since the auditory and visual waveforms were similar, only the auditory waveforms will be discussed. The topography of movement-related potentials was similar to the right-handed movement potentials of our current bimanual study (see Section V.D.1). The movement-related potentials consisted of a slow ramp-like shift (RP), commencing about 560 msec before response onset, and a peak-like wave (N55), commencing at about the time of average EMG onset and peaking 55 msec after response onset (Figure 6). These two components were localized to a few electrodes, and had slightly different topographies (Figure 15). Also, the morphology of the whole movement-related waveform exhibited distinct differences at various electrodes. The RP consisted of a left-lateralized negative shift, strongest at C1 and aC1, and visible also at Cz, aCz and aC2, and a corresponding positive wave occurring in two distinct regions: one left-sided (aP5, P3 and aO1) and the other right-sided (C4, aP2, aP6 and P4). The N55 peak exhibited a robust negative component similar in topography to the negative RP component, but extending also to midline and left frontal sites and totally absent at C1. The positive component of N55 was present only at left-hemisphere sites (C5, aP3, P1, and C3), and was largest at C3. Unlike the RP, the positive component of N55 was absent from the right hemisphere. The topography of N55 (see Figure 15) may be tentatively interpreted as reflecting the activity of the right-hand region of the motor cortex, which could conceivably produce a current source strongest at aC1 and aCz, and a corresponding current sink strongest at C3. The bifurcated positive topography of the positive RP component is puzzling, as is the lack of any RP shift preceding the positive component of N55 in several electrodes (C3, aP1 and aP3), and the absence of the N55 peak at C1, where the RP negative shift is strong. These findings suggest the activity of multiple generators, an issue which is currently being examined in a study of right and left-handed response movements.

C. Initial Analysis

The results of initial NCP Analysis of this data are discussed in Section V below.

IV. THE ADIEEG III ANALYSIS SYSTEM (Development also sponsored by the

November 13, 1984 (56)

Office of Naval Research, the National Science Foundation, and the USAF School of Aerospace Medicine).

A. Overview of The New System

A third generation system, ADIEEG III, has been developed to perform multi-stepped sequences of analysis on large amounts of data (Figure 7). It has the capacity to handle 64 channels of BP data, plus 6 channels of other physiological information. Over a dozen simultaneous users are handled for data collection, analysis and program development. Over 12 man-years of senior programmer time were expended over the past three years to implement and test this system, which may be one of the most comprehensive systems currently being used for brain potential research. The hardware consists of similarly configured PDP11-60 and PDP11-45 computers, with 800 and 400 MB fixed disks respectively, extended memory busses and 1.25 MB main memory each. Other peripheral devices include 9-track tape drives, terminals and modems, graphics devices and printers, and an 80-channel A/D converter. The RSX multiprogramming operating system is used. The following functions are performed: (1) experiment control, with on-line selection of stimuli and task-difficulty according to the participant's performance, and digitization of up to 70 channels at 256 samples/sec; (2) finite-impulse-response digital filtering for selected passbands; (3) eye-movement contaminant filtering (see Section V.E.1); (4) sorting and pruning of data sets by up to 50 stimulus, response, performance and other variables so that experimental conditions do not differ in irrelevant factors (see Section IV.B); (5) computation of current-source densities (CSDs) from the scalp potential distributions (see Section V.D); (6) computation of averaged ERP and CSD waveforms, and interactive programs for determining the latencies, calibrated amplitudes and integrated energies of visually selected peaks; (7) computation of cross-correlations, power spectra, and Wigner Distributions (combined time-frequency domain) (see Section V.B.2); (8) statistical and heuristic primary feature extraction and within-subject normalization of data (see Section V.A); (9) univariate and linear multivariate statistics using the BMD package; (10) nonlinear, adaptive-layered-network, multivariate pattern recognition which determines invariant features in sets of single-trial data; and (11) time-varying, multichannel linear models of event-related signals. All stages of data management, signal processing and analysis are documented in printed or graphic form. Finally, a menu-oriented "analysis operating system" has been implemented to automate the execution of the many subprograms handling data sets of up to 500 MB, greatly reducing the time required for each complete analysis.

B. The ADISORT Program for Formation and Balancing of Data Sets

Special attention is focused on the preparation of data sets, since we feel that this is a highly neglected aspect of experimental control. In order to form balanced pairs of data sets for each hypothesis, the total set of artifact-free trials from each recording is submitted to the ADISORT program. This is an interactive program which displays the means, t-tests, and histograms of the distributions of about 50 variables for pairs of data sets selected from the total set of edited trials. Pairs of data sets can

ADIEEG III NEUROCOGNITIVE PATTERN RECOGNITION SYSTEM

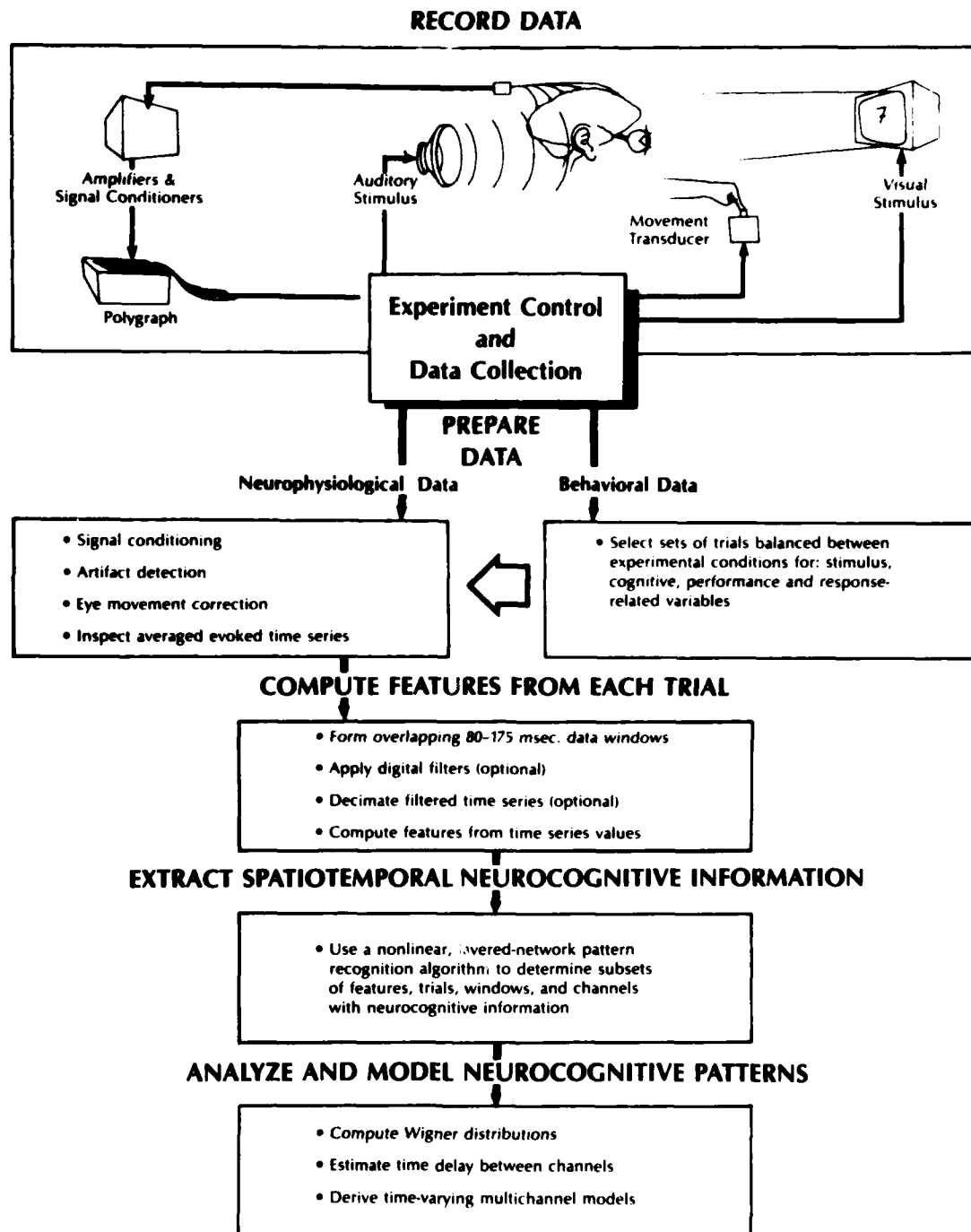
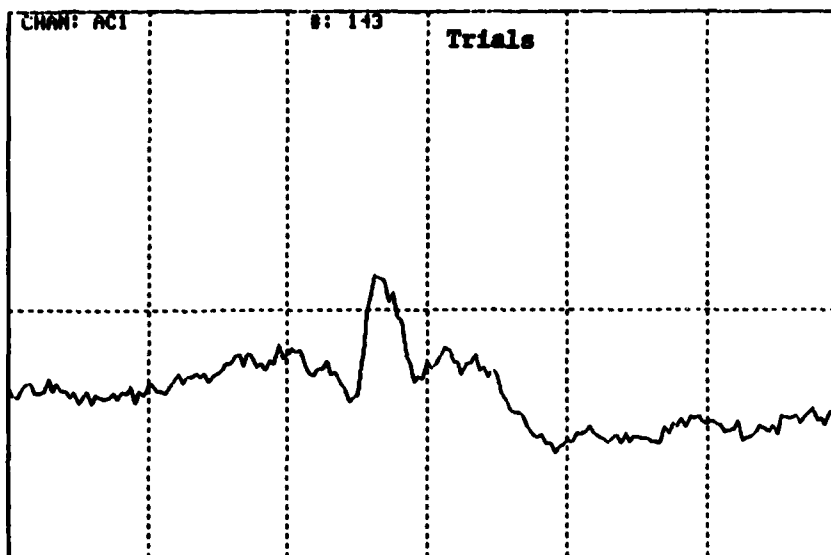


Figure 7. The ADIEEG recording and analysis system for neurocognitive research. Capacity is 64 brain potential channels plus 6 channels for several other physiological signals. Data bases up to 500 megabytes in size can be automatically processed through multi-stage analyses.

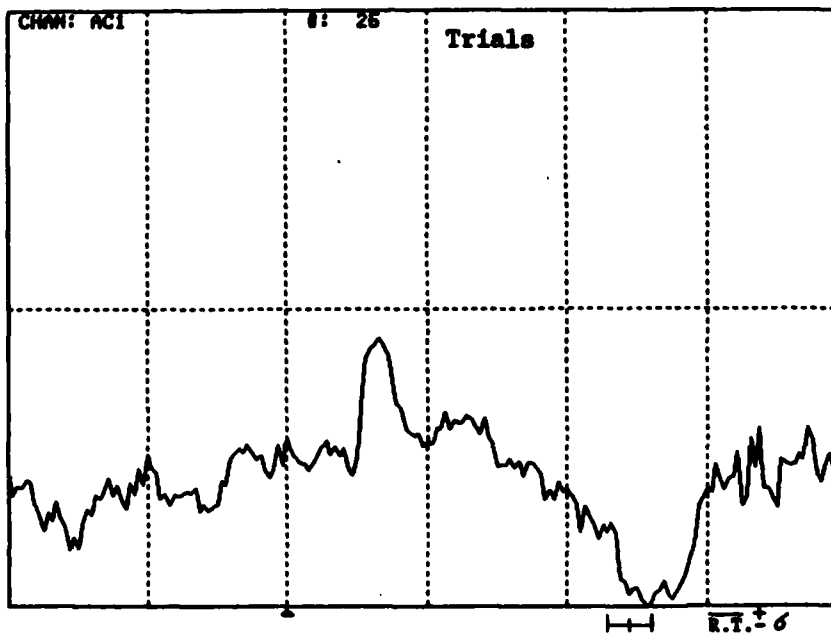
AV07+ S VISUAL MOVE, CORR CLASS IN P2
IFUNCT= 3 RANGE= 141.0

STIM-LOCKED



VMFAST AV07+
IFUNCT= 3 RANGE= 141.0

STIM-LOCKED



Stimulus

+500 msec

Figure 8. Effect of limiting the range of response times on the averaged stimulus-registered waveform for a visuomotor task with right-handed response. The original averaged CSD waveform for the aC1 electrode is at the top (143 trials; R.T. = 819 ± 145 msec). The lower waveform was computed from a set of trials selected as having a signal in the P2 interval by the method described in Section V.A.1, and further reduced to only 25 trials based on a narrow range of response times (R.T. = 509 ± 40 msec). The movement related potentials are clearer in this "purified" stimulus-registered ERP.

November 13, 1984 (56)

be quickly inspected for significant differences in these variables, and pruned of outlier trials until they are balanced, usually to an alpha of .2. The ADISORT program facilitates the handling of large amounts of data, and permits a high degree of control of variables unrelated to the particular hypothesis, including the effects of eye movements. It outputs labeled lists of trials which are then submitted to the signal processing and analysis programs of the ADIEEG system.

For our current bimodal and bimanual studies, the available variables include modality and magnitude of stimulus number, responding hand, response onset time, response movement force, velocity, acceleration and duration, response outcome ("win" or "lose"), error from target pressure, adaptive error tolerance measure (current performance level), and order of the trial within the recording session. Also included are indices of eye movement, EMG activity and arousal, which are measures of integrated energy in the vertical and horizontal EOG channels, the EMG channel and the Pz electrode, respectively, computed in separate 500-msec intervals before and after the onset of cue, stimulus, response and feedback.

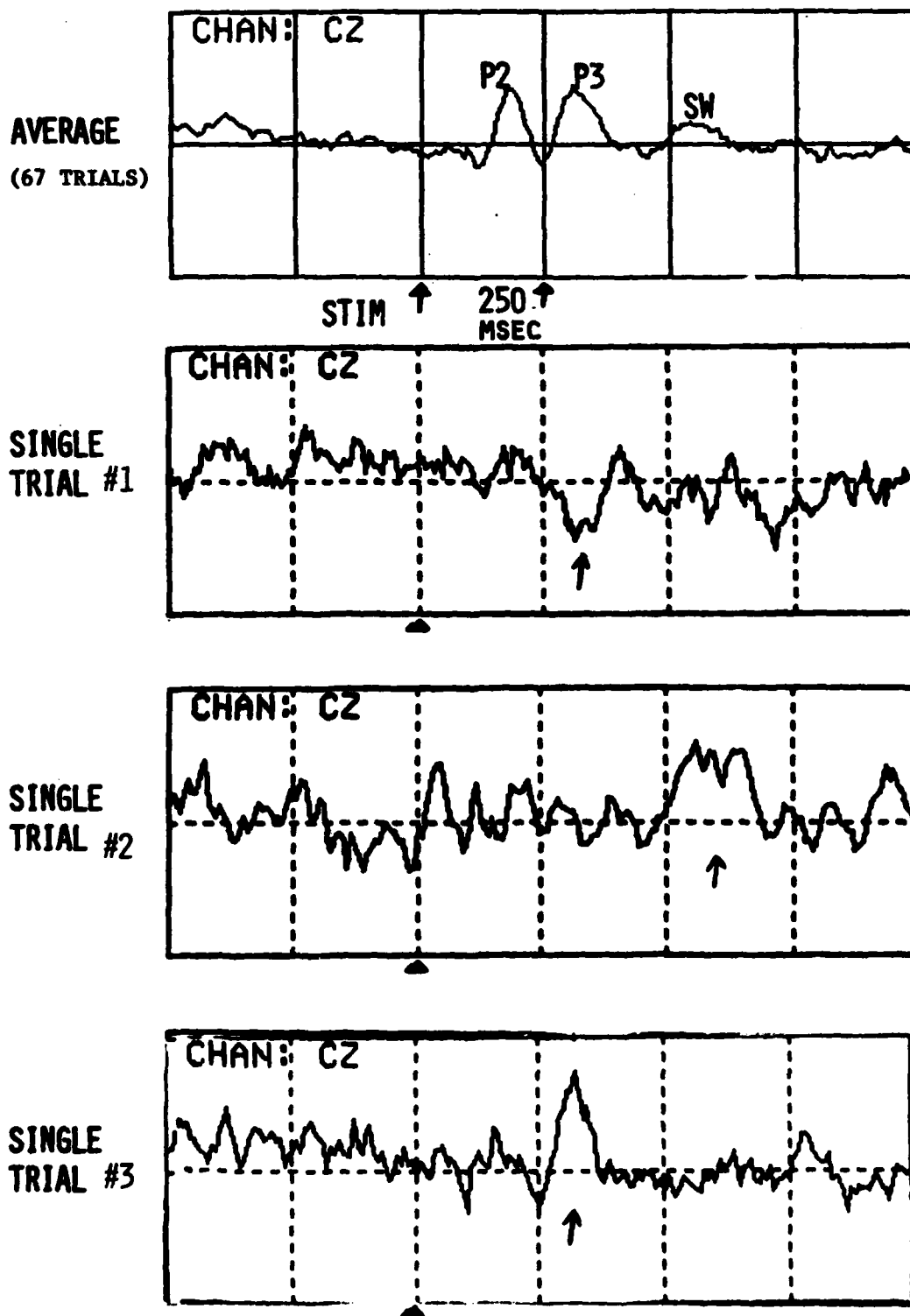
In addition to inspection of experimental variables and formation of balanced data sets, the ADISORT program can be used to form data sets according to a posteriori hypotheses, such as low vs. high error, or short vs. long response times. It allows selection of sets of trials according to a particular criterion, such as a narrow range of reaction times. Figure 8 illustrates the improved definition of movement-related potentials in a stimulus-registered averaged waveform computed from a data set that was pruned to a narrow range of reaction times.

V. DEVELOPMENT AND TRIAL APPLICATION OF NEW ANALYSES (Development also sponsored by the Office of Naval Research, the National Science Foundation, and the USAF School of Aerospace Medicine)

A. Analysis of Sets of Single Trials

1. Rapid Scanning Measure

Expansion of the number of channels recorded greatly improves spatial resolution. However, the increased volume of data (up to 100 megabytes per person) necessitates a means of selecting important channels, intervals and trials to reduce the amount of data prior to final single-trial analysis of spatial interdependencies. Analysis of single-trial data sets suggests that some trials lack clear task-related signals (Gevins, et al, 1984), an observation consistent with visual observations (Figure 9). A means for determining trials, channels and intervals with significant signals was needed. Multichannel features such as correlation are useful tools for measuring relations between signals, but the combinatorial explosion of channel combinations makes such measures cumbersome for scanning large data sets. Single channel measures are preferable because of their low computational requirements. This led to the development of a "scanning" method to select optimal subsets of signal-bearing trials, channels and intervals, and to improve SNR for correlation-based measures. This method uses a single-channel measure of filtered amplitude as a feature for pattern recognition. Trials without consistent task-related signals are



AV07

Figure 9. Comparison of three individual trials with averaged CSD waveform. (Visual no-move stimuli; Cz electrode.) In trial #1 there is a peak at the P3 latency but opposite in polarity to the P3 in the average. In trial #2 there is a peak at the slow wave (SW) latency, but no clear P2 or P3 peaks. In trial #3 only the P3 peak is evident.

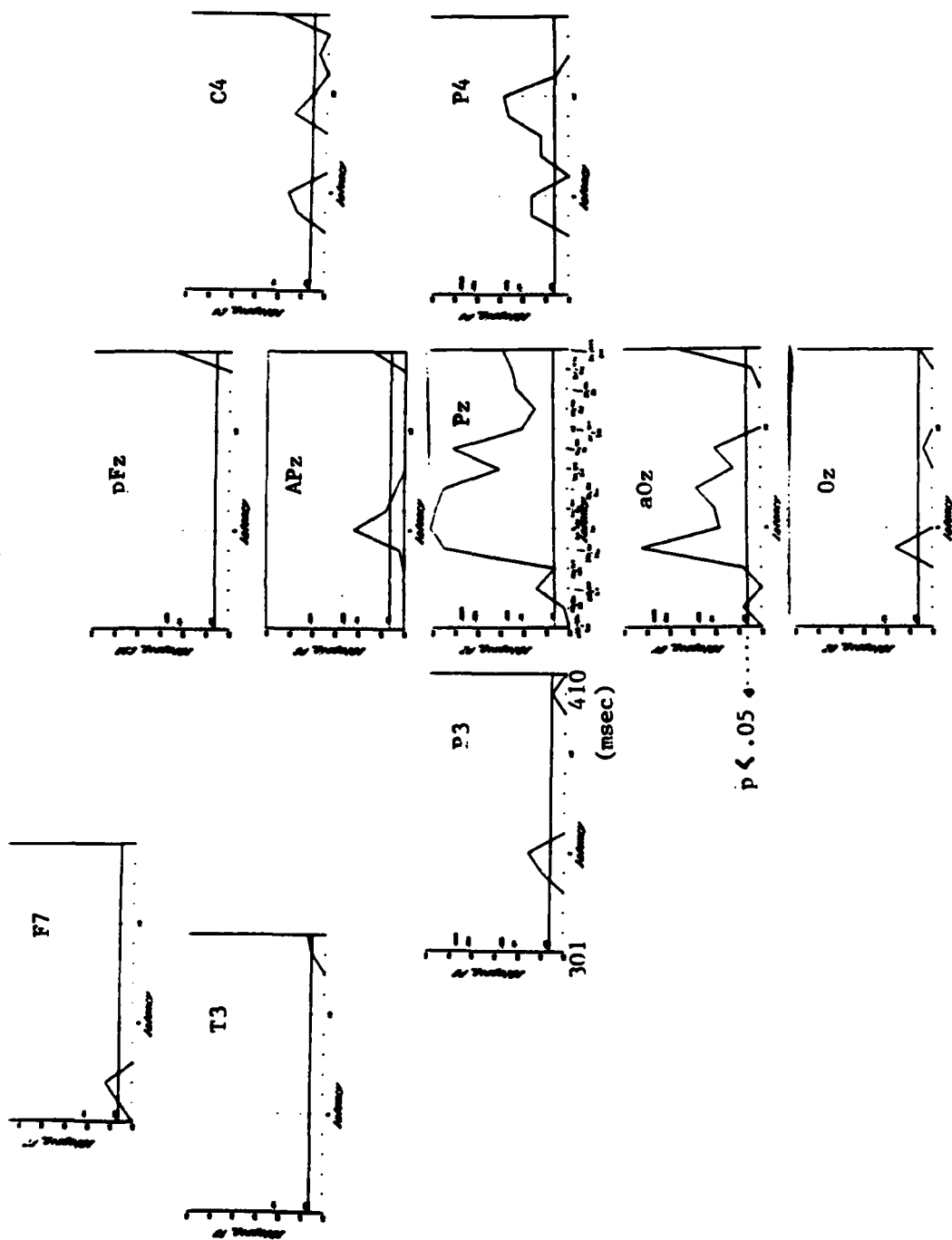


Figure 10. Single-channel scanning measures: significance of between-task pattern recognition classification (y axis) as a function of time (x axis) is shown for the ten "best" electrodes (move vs. no-move visuospatial task; subject S802). The pattern recognition analysis was performed in fifteen overlapping 80-msec wide windows in the latency range from 266 to 445 msec, which spanned the P368 peak that had a strong between-task difference in ERP amplitude. The Pz channel shows very significant discriminations in the intervals from 324 to 379 msec; other channels have weaker or non-significant effects.

November 13, 1984 (56)

rejected if the pattern recognition algorithm is unable to discriminate them from sets of "baseline" data known to have a low event-related signal (see Section V.A.2.b).

A reasonable criterion for a scanning method for single trials is that it yield high classification scores in channels and intervals which have significant peaks in the average waveforms. The obvious candidate for a single-channel measure is the time series values themselves. An initial study was performed using visuospatial task data from a single person (SS02). Segments of the time series 80, 120 and 180 msec in length (128 Hz sampling rate) were used as analysis windows. Using the negative log of the significance of between-task (move vs. no-move visuospatial task) discrimination as the output variable, the progression of discriminability over time was observed for each channel by advancing the analysis window one data-point at a time. In the P3a interval (266 to 445 msec), the PZ channel had a robust result, consistent with the average ERP (Fig. 10). The same measure was applied to the data from participant AV07 performing the auditory/visual numeric judgment task over a wider range of latencies. The results are shown in Figure 12 in topographic "head" format. (See Figure 11 for explanation of the topographic head displays used for the figures in this section.) Significant but weak between-task differences occurred primarily in the intervals centered at 250, 313, and 375 msec, reflecting activity related to the N242 and P313 peaks elicited by the infrequent no-move stimuli.

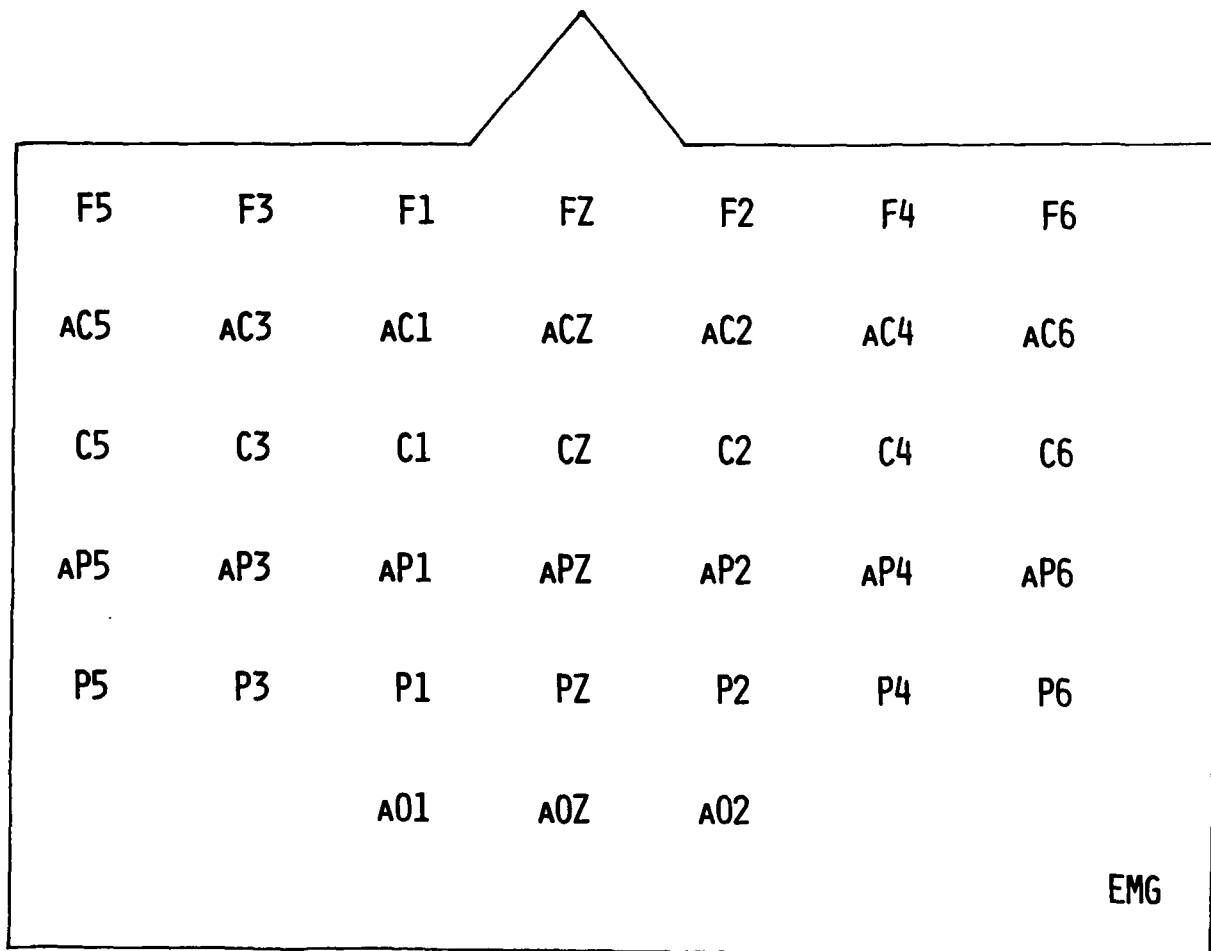
The time series was then lowpass filtered at 7 Hz to remove alpha and beta components. The filter was a 17 point linear-phase FIR design with 20 dB attenuation (.01 power gain) at 16 Hz, so that decimation by 4 produced only minor aliasing error. This produced results with better between-task discrimination (up to about 80%) (Figure 13).

2. Application of Scanning Measure to Within-Task Analysis

a. Precue Interval Baseline

1) Stimulus-Registered A/V Move Tasks

The purpose of the scanning measure was to choose trials with a clearer task-related signal. The "reference" ensemble of features should ideally be derived from intervals with no task-related signal so that signal-bearing trials can be optimally discriminated. In the bimodal experiment, the averaged CSDs show a relatively small amount of energy in most channels prior to the cue. A series of NCP Analyses was performed on the visual and auditory move (correctly cued) trials, using a time interval centered 375 msec before the cue as reference. For visual stimuli (Figure 14a), the analysis interval centered at 117 msec shows a pattern of significant signals related to the N117 peak at posterior sites. Some activity can also be seen at occipital sites in the adjacent intervals due to overlap in the 125-msec wide analysis intervals centered on these closely spaced peaks. The anatomic distribution of significant signals in the P2, N2 and P3 intervals corresponds only approximately with the averaged CSD topographies. This may be due to the use of the pre-cue EEG as reference, which is certainly not free of task-related activity. In the slow wave (SW) interval, the pattern of significant signal sites is separated into anterior and posterior regions, as might be expected for the



CENTERPOINT OF INTERVAL
(MSEC)

Figure 11. Topographic "head" displays for NCP Analysis results and CSD amplitude distributions. Thirty-eight channels are shown; the 11 peripheral CSD channels were not analyzed. In these diagrams, the front of the head is up, the analysis interval centerpoint (in milliseconds) is given underneath, and the NCP results are indicated as dot-densities corresponding to the negative log of the significance level of pattern recognition classification at the individual electrode sites (darker density = higher significance level). The NCP significance scale is at the top of Figures 12-16, while the CSD scale is given below in Figures 14-16.

STIMULUS EVENT

AV07

TASK CODE 1

RAWVMN

SCALE:

140.0 127.5 115.0 102.5 90.0 77.5 65.0 52.5 40.0

VISUAL MOVE VS. NO-MOVE, UNFILTERED

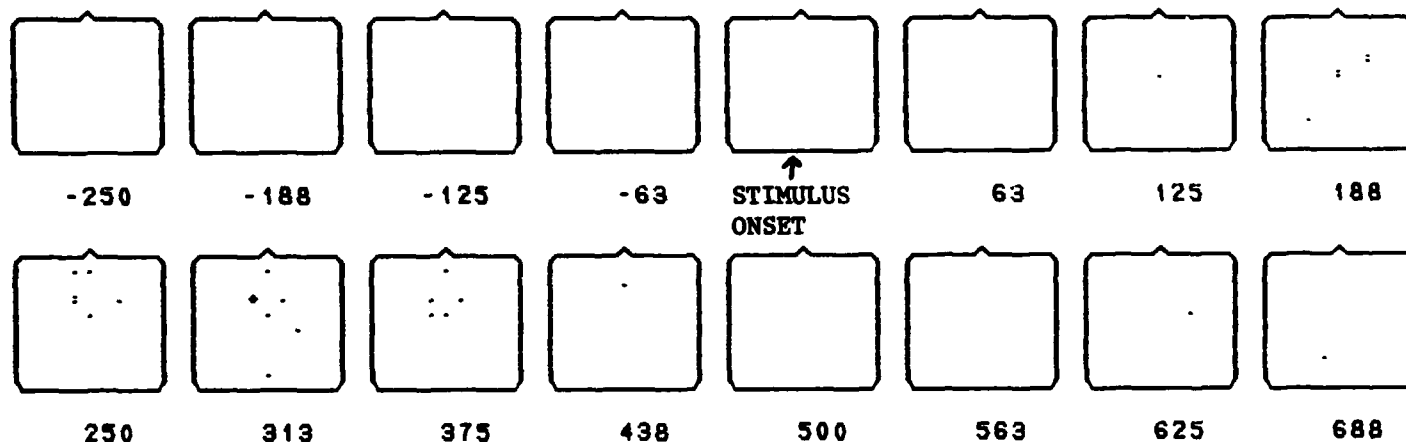


Figure 12. Single channel scanning measure using data-points from unfiltered single-trial time series as features for pattern recognition. Discrimination of correctly cued (move) vs. mis-cued (no-move) AV07 visual trials. Analysis windows 120-msec wide were centered at 16 latencies from 250 msec before to 688 msec after stimulus onset. Electrode sites with higher significance levels are indicated by higher density of dots. (See Figure 11 for explanation of "head" diagrams).

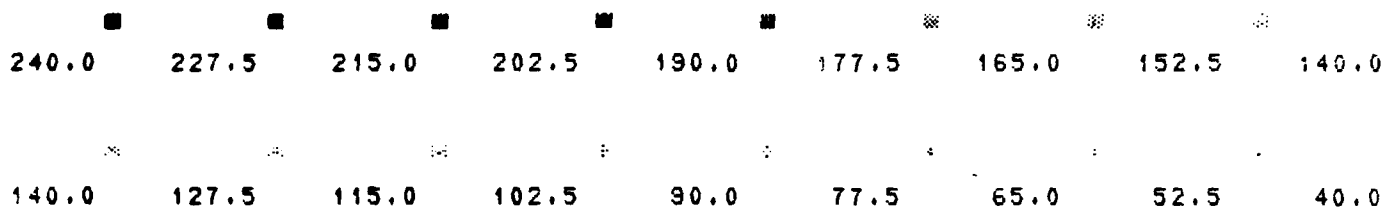
STIMULUS EVENT

AV07

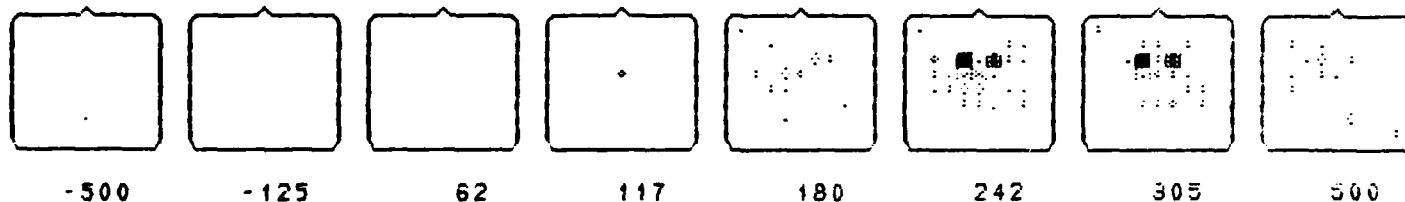
TASK CODE 1

VISMNM

SCALE:



VISUAL MOVE VS. NO-MOVE, FILTERED



AUDITORY MOVE VS. NO-MOVE, FILTERED

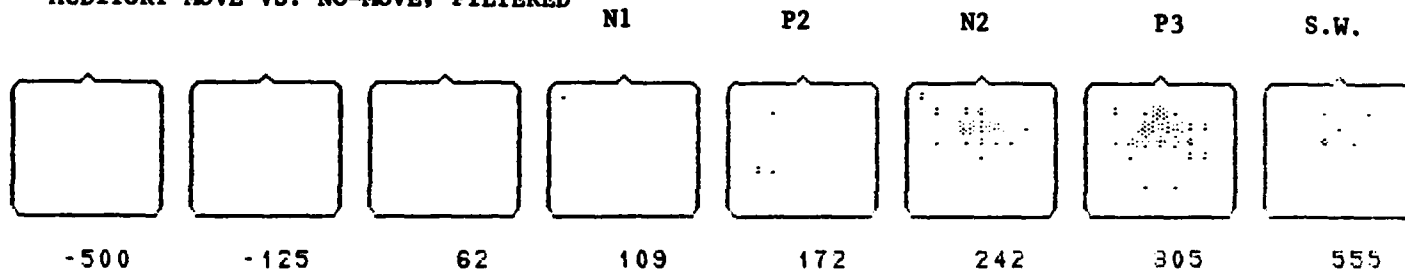


Figure 13. Single-channel scanning measure using filtered data. Three data points from single-trial time series lowpass filtered at 7 Hz were used as features for between-task pattern recognition. Discrimination of correctly cued (move) vs. mis-cued (no-move) trials, in separate analyses of visual (top) and auditory (bottom) conditions. Significance levels of discrimination are higher and more anatomically distinct, especially in the N2-P3 range, than those achieved using unfiltered data (Figure 12). Filtered time series are used in the single-channel scanning analyses in Figures 14-16. (See Figure 11 for explanation of "head" diagrams.)

November 13, 1984 (56)

visual slow wave, which is negative frontally, positive posteriorly, and weak at central locations. In comparison, the auditory slow wave (SW) pattern is distributed over a single centro-parietal area (Figure 14b). For auditory stimuli (Figure 14b), the pattern of significant-signal sites related to the auditory N109 peak is anterior, strongest at lateral central sites (C1, C2, and C3), with weaker activity at some far lateral frontal, precentral and parietal sites. The auditory P171 pattern is also mostly anterior, but is strongly focused at right-sided lateral central and precentral sites adjacent to the midline. The P242 pattern shows some correspondence to the CSD distribution, but with a right-sided preponderance of significant signal sites.

2) Response Registered A/V Tasks

The results of the response-registered analyses were similar for visual and auditory trials (Figure 15). In the 3 intervals leading to movement onset, corresponding to the slow readiness potential (RP) shift, the significant sites were predominantly left-sided, strongest at central sites next to the midline, and increasing in strength with the EMG onset. In the interval centered on the maximum post-response peak of the movement-related waveforms (N62 in visual, N55 in auditory), there was a large increase in the number of sites and strength of the significant signals, corresponding well in anatomic distribution to the positive and negative components of these peaks in the CSD waveforms. Note that discrimination of activity in the EMG channel persists into the last interval, centered about 300 msec after response onset, while significant cerebral signals are almost absent.

b. "Random Data" Baseline

1) Method

Although the energy in the pre-cue averaged waveform was low, it was not zero, perhaps due to task-related preparatory processes. No fixed time interval in an experiment is really representative of a "neutral" baseline state. A statistical technique was therefore developed to generate an ensemble of reference data which would approximate a "neutral" baseline having minimal stimulus-registered activity and average statistical properties similar to each channel of recorded data. Simply put, this technique averages task-related signal statistics over the whole trial by synthesizing a locally stationary process for each channel from randomly chosen epochs of recorded EEG. This process has first and second order statistics which should differ from those of the underlying baseline EEG only by small time-independent constants. To compile the set of pseudo-baseline data, registration points are chosen at random within the recording epoch. For each channel, the features are the filtered and decimated time series values in the intervals immediately following the registration points. The ensemble of such intervals over all task conditions serves as the reference class. The data set representing the task-related signals is composed of intervals centered on the latency of a particular peak of the averaged waveform. Implicit to this idea of a randomized data reference is an assumed model,

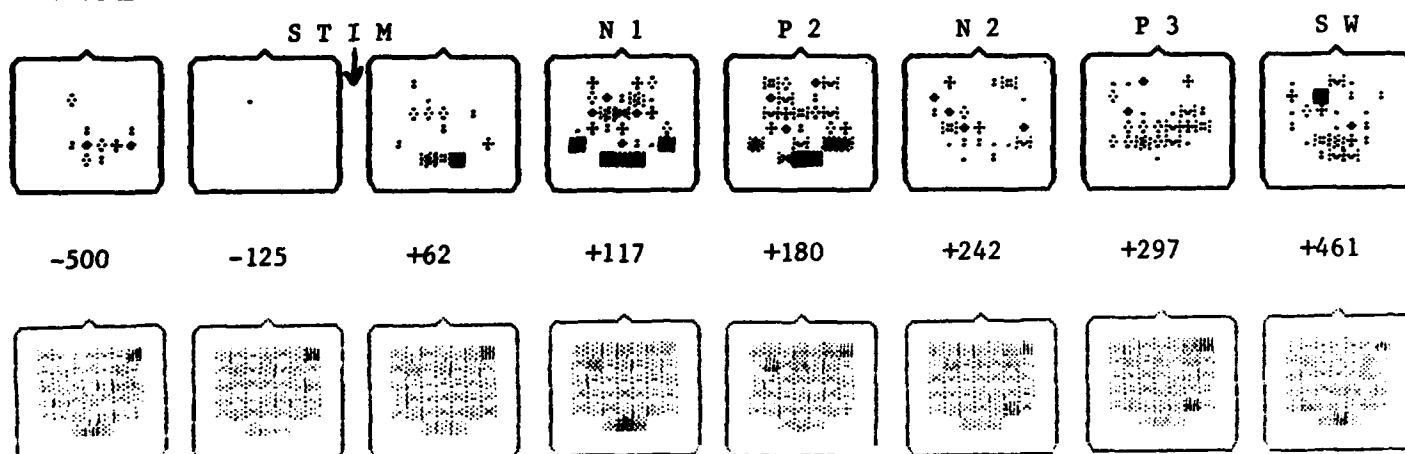
$$x(t) = n(t) + s(t)$$

STIMULUS EVENT
AV07
TASK CODE 1
VISMOV

SCALE:



VISUAL MOVE VS. PRECUE INTERVAL



CSD

SCALE:



Figure 14a. Within-task single-channel scanning measure of visual move trials using pre-cue time series as reference data (top), compared with the averaged current source density (CSD) distributions, at the centerpoint latency of each NCP Analysis interval (bottom). NCP Analysis intervals were 125 msec wide, except for the prestimulus and SW epochs which were 250 msec wide. Channels without significant task-related signals do not appear in the NCP results. (See Section V.A.2.a.1 of text for discussion, and Figure 11 for explanation of "head" diagrams.)

STIMULUS EVENT
AV07
TASK CODE 1
AUDMOV

SCALE:

240.0 227.5 215.0 202.5 190.0 177.5 165.0 152.5 140.0

140.0 127.5 115.0 102.5 90.0 77.5 65.0 52.5 40.0

AUDITORY MOVE VS. PRECUE INTERVAL

S T I M

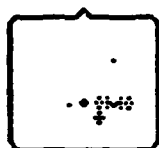
N 1

P 2

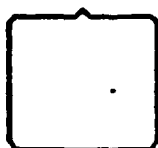
N 2

P 3

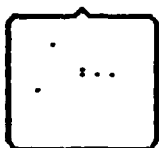
S W



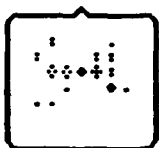
-500



-125



+62



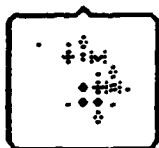
+109



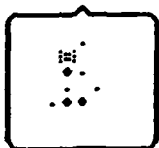
+171



+210



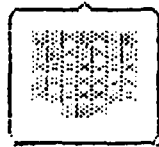
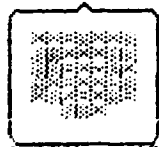
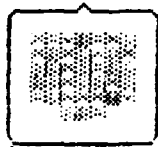
+242



+555



CSD



SCALE:

718.0 629.3 540.6 451.9 363.3 274.6 185.9 97.2 8.5

8.5 -80.2 -168.9 -257.6 -346.3 -434.9 -523.6 -612.3 -701.0

Figure 14b. Within-task single-channel scanning measure of auditory move trials using pre-que time series as reference data (top), and CSD distributions at corresponding latencies (bottom).

SCALE:

240.0 227.5 215.0 202.5 190.0 177.5 165.0 152.5 140.0

140.0 127.5 115.0 102.5 90.0 77.5 65.0 52.5 40.0

VISUAL: NCP

M O V E M E N T



R.T. = 817 ± 145 msec

-375 -250 -125 +62 +313 msec



CSD

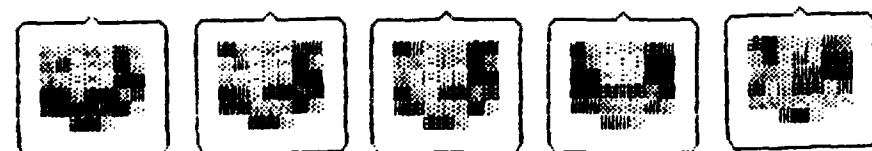
AUDITORY: NCP

M O V E M E N T



R.T. = 892 ± 127 msec

-375 -250 -125 +55 +305 msec



CSD

SCALE:

358.0 292.5 227.0 161.5 96.0 30.5 -35.0 -100.5 -166.0

-166.0 -231.5 -297.0 -362.5 -428.0 -493.5 -559.0 -624.5 -690.0

Figure 15. Within-task single-channel scanning measure of response-registered move trials using pre-que time series as reference data (top), with averaged CSD distributions at corresponding latencies (bottom). Visual trials are shown in upper half, and auditory in lower half. The significance level of discrimination of the right-hand EMG channel is shown at the bottom right corner of the NCP heads. NCP Analysis intervals were 250 msec wide.

November 13, 1984 (56)

where $x(t)$ is the observed process, $n(t)$ is a wide-sense stationary colored noise process, and $s(t)$ is a non-stationary signal process. For simplicity, we assume an additive linear model. However, very little is assumed about the characteristics of $n(t)$ and $s(t)$, and non-stationarity is permitted. In practice, these two processes may be very similar and in fact may well have nearly identical power spectra below 8 Hz. The fundamental difference between them is the non-stationarity of the signal, which is time-locked to experimental events. The influence of this non-stationarity on the sum can be greatly reduced by the introduction of a random variable which is uniformly distributed between 0 and $T-w$, where T is the trial length and w is the analysis window length:

$$\theta \sim U[0, T-w]$$

Then the first order statistics of $x(t+\theta)$ are (for $0 \leq t \leq w$):

$$E(x(t+\theta)) = E(n(t+\theta)) + E(s(t+\theta))$$

The noise term is clearly constant over t , since n is stationary. The second term is the expected value of the local time average of the signal, and is also a constant. Thus, the sum is constant, and not a function of time. The second order statistics are

$$E(x(t_1 + \theta) x(t_2 + \theta)) = E\{n(t_1 + \theta) n(t_2 + \theta)\} + E\{s(t_1 + \theta) s(t_2 + \theta)\} \\ + E\{n(t_1 + \theta) s(t_2 + \theta)\} + E\{s(t_1 + \theta) n(t_2 + \theta)\}$$

For each of these terms, the expectations are nearly identical for any choices of t_1 and t_2 such that $(t_1 - t_2)$ is constant, since nearly all of the possible times will be equally likely (the time points considered may differ for as many as w points out of $T-w$ possible points). For $w \ll T$, the individual time dependencies can be dropped, yielding

$$E(x(t_1 + \theta) x(t_2 + \theta)) = R_{nn}(t_1 - t_2) + R_{ss}(t_1 - t_2) + R_{ns}(t_1 - t_2) + R_{sn}(t_1 - t_2)$$

Therefore, $x(t + \theta)$ is locally (for $0 \leq t \leq w$) stationary. Also, if

$$R_{ss}(0) \ll R_{nn}(0)$$

and

$$R_{ns}(0), R_{sn}(0) \ll R_{nn}(0)$$

(small task-related signal power, small correlation between signal and noise), then

$$R_{xx} \approx R_{nn}$$

Thus, a locally stationary process has been manufactured with small constant time-independent differences in first and second order statistics

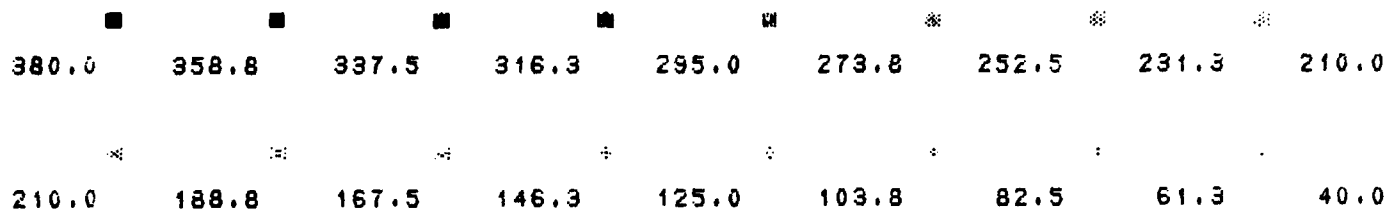
STIMULUS EVENT

AV07

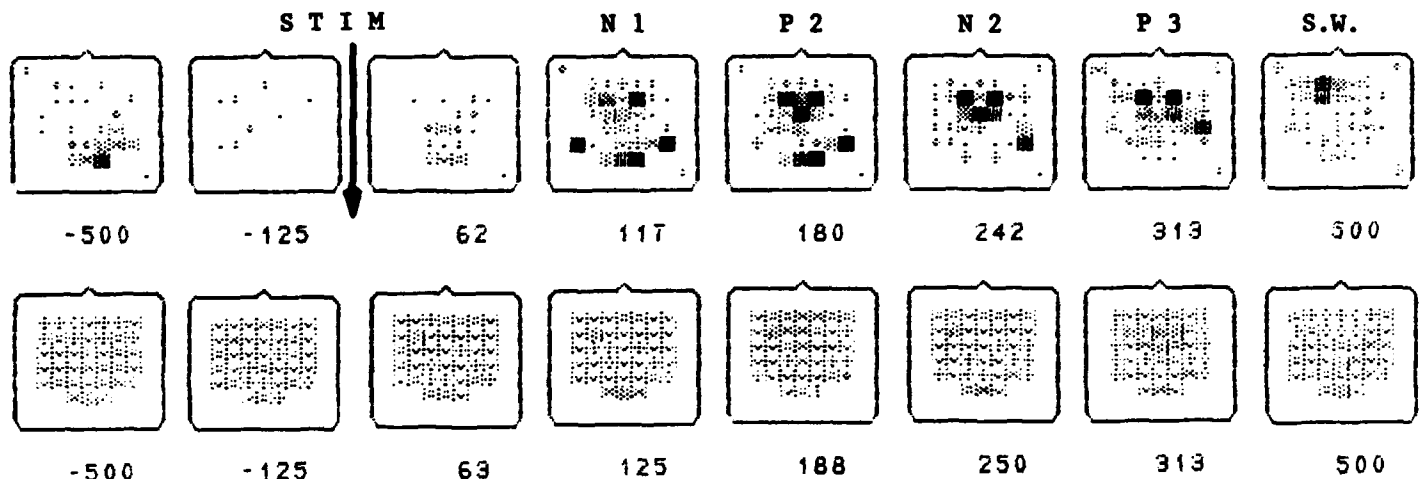
TASK CODE 1

VISUAL NO-MOVE REF TO TRIAL ENSEMBLE WITH RANDOM TIMING

SCALE:



VISUAL NO-MOVE VS. RANDOM



CSD

SCALE:

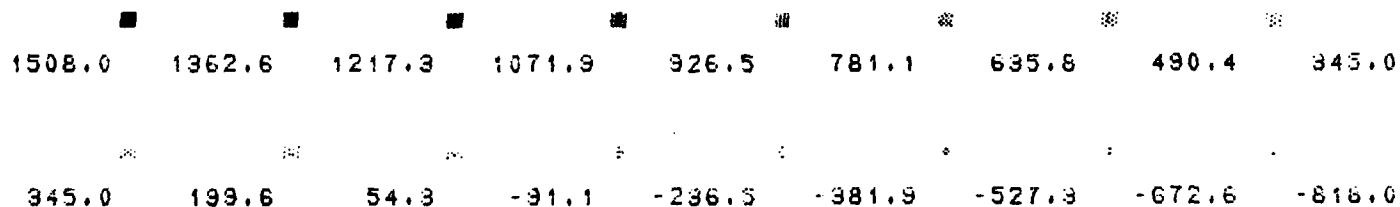


Figure 16a. Within-task single channel scanning analysis of visual no-move (misued) trials (average of trials per channel; range 18-74 per channel) using randomized time series as reference data (top), with CSD distributions at corresponding latencies (bottom). (See Section V.A.2.b.2 of text for discussion.)

STIMULUS EVENT

AV07

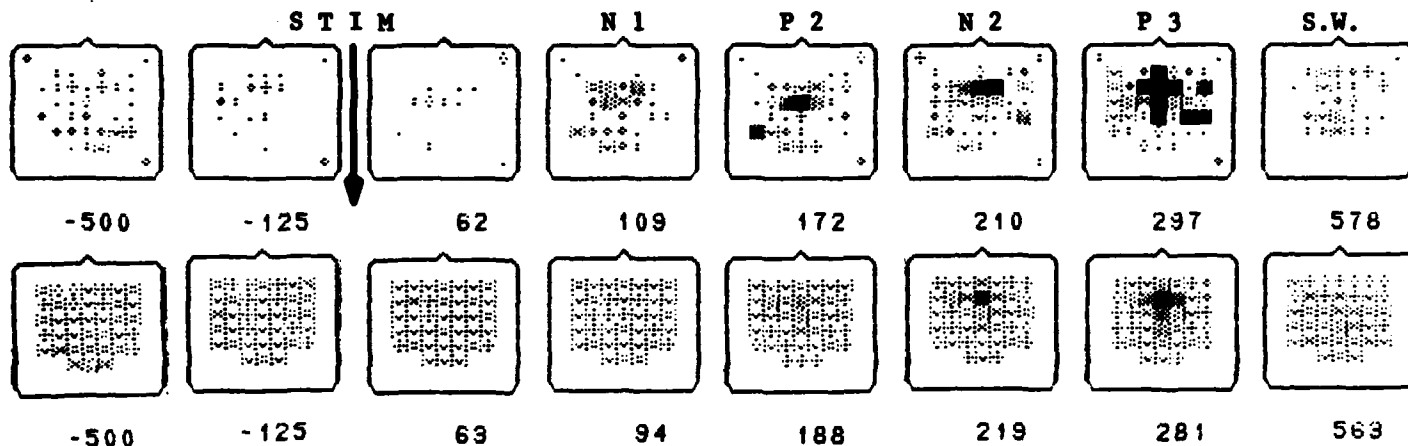
TASK CODE 1

AUDITORY NO-MOVE REF TO TRIAL ENSEMBLE WITH RANDOM TIMING

SCALE:



AUDITORY NO-MOVE VS. RANDOM



CSD

SCALE:

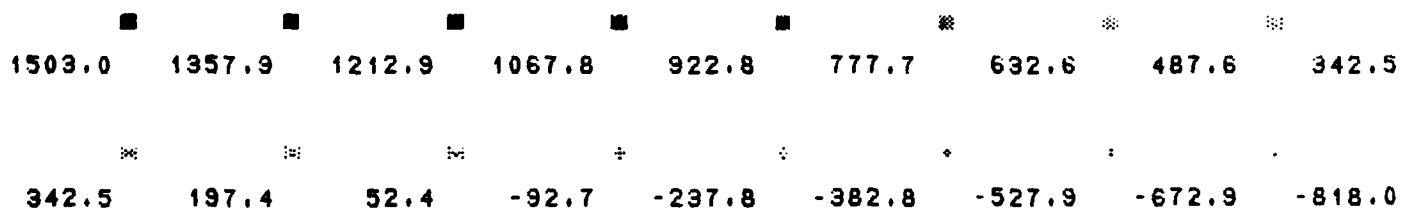
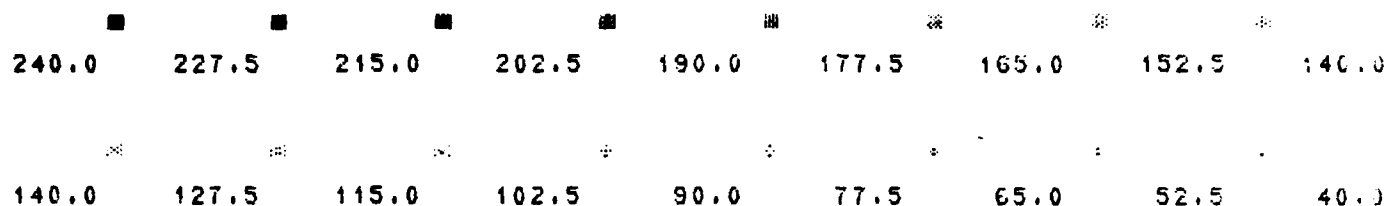
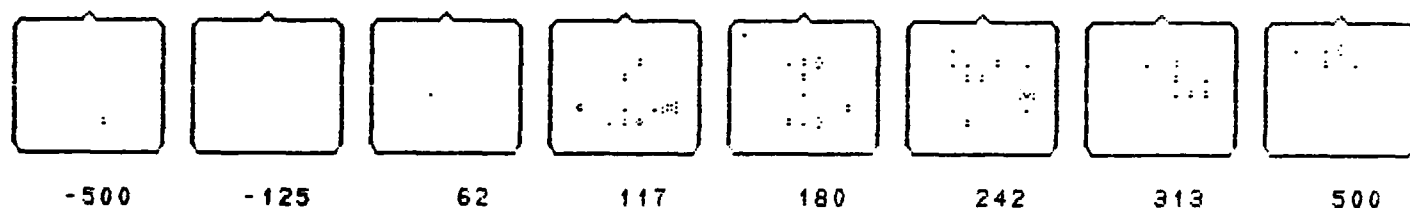


Figure 18b. Within-task single-channel scanning analysis of auditory no-move (miscued) trials (average of 45 trials per channel; range 37-55 trials per channel) using randomized time series as reference data (top), with CSD distributions at corresponding latencies (bottom).

SCALE:



VISUAL NO-MOVE VS. PRECUE INTERVAL



AUDITORY NO-MOVE VS. PRECUE INTERVAL

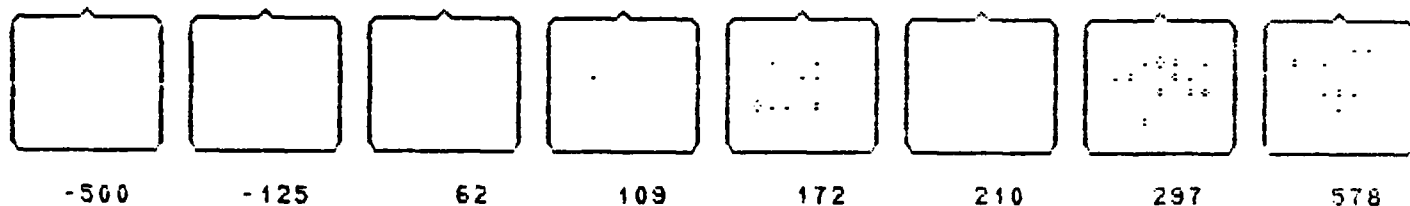


Figure 16c. Within-task single-channel scanning analysis of auditory (top) and visual (bottom) no-move trials using pre-cue time series as reference data. Compare with Figures 14a. and 14b. The use of randomized data as a "baseline" produced much stronger results, and because of this a higher significance scale was used in Figures 14a. and 14b.

November 13, 1984 (56)

from the theoretical underlying baseline EEG process.

2) Application to Miscued (No-Move) A/V Data

NCP Analyses using randomized-data reference sets produced stronger, more anatomically distinct results than analyses using pre-cue data as reference (compare top of Figures 16a and 16b with 16c). Analyses of the no-move trials of participant AV07 for the infrequent miscued visual (Figure 16a) and auditory (Figure 16b) stimuli produced sequences of patterns consisting of electrode sites with task-related signals strong enough to allow 65-75% of the single trials of the task to be discriminated from the random baseline data. The intervals centered on the N1, P2, N2, P3 and slow wave (SW) peaks show a progression of task-related patterns which overlap in time. For miscued visual stimuli (Figure 16a), a right-lateralized pattern at occipital and posterior parietal sites is evident in the N117 interval, and also in the overlapping P180 interval. The auditory P109 interval (Figure 16b) lacks this posterior pattern; the significant signals occurred at midline and lateral central and precentral locations. In the prestimulus interval centered 500 msec before stimulus onset (500 msec after cue), there is a posterior, right-lateralized pattern resembling the posterior pattern of the visual N117 interval. This is especially evident in the visual condition (Figure 16a), but is also visible in the auditory condition (Figure 16b). This interval spans the early CNV ("O") wave, which is known to depend on the modality (in this case visual) in which a cue is presented. The anterior patterns in the visual N117, P180, N242 and P313 intervals may reflect the overlapping activity of these components, as well as the CNV resolution. This is due in part to the overlap of the 125-msec wide analysis intervals centered on these closely spaced peaks. The visual P180 and auditory P172 both have strong anterior patterns focused at Cz, and in the visual P180 interval strong also at anterior central sites (aC1, aCz and aC2). In the N210 interval for auditory stimuli the anterior pattern moves forward to precentral sites, where it is right-lateralized and strongest at aC2, whereas in the visual N242 interval there is not much change. In the auditory P297 interval, there is a strong pattern consisting of midline sites from Fz to aPz, and lateral precentral sites (aC1 and aC2), with strong signals also at right anterior parietal locations (aP4 and aP6). In contrast, the visual P313 pattern lacks the midline sites, and resembles the auditory P297 pattern only at the lateral precentral (aC1 and aC2) and anterior parietal (aP4 and aP6) sites. This relative modality dependence of the P3 amplitude distribution may be due to the much greater amplitude of the rarer auditory no-move peak, and to overlapping effects from the modality-dependent N2 peak. The slow wave (SW) interval does not overlap adjacent analysis intervals, and a clear difference between visual and auditory conditions can be seen. The visual SW pattern is divided into separate anterior and posterior regions, as might be predicted from the slow wave distribution for visual stimuli. The auditory slow wave pattern is more evenly distributed.

3. Conclusion

From these results, it seems that the single-channel scanning measure achieved its aim of reducing the data set by isolating intervals and channels with task-related signals prior to measurement of between-channel timing relations. The poor temporal resolution of the scanning measure

CLASSIFIER-DIRECTED TRIAL SELECTION

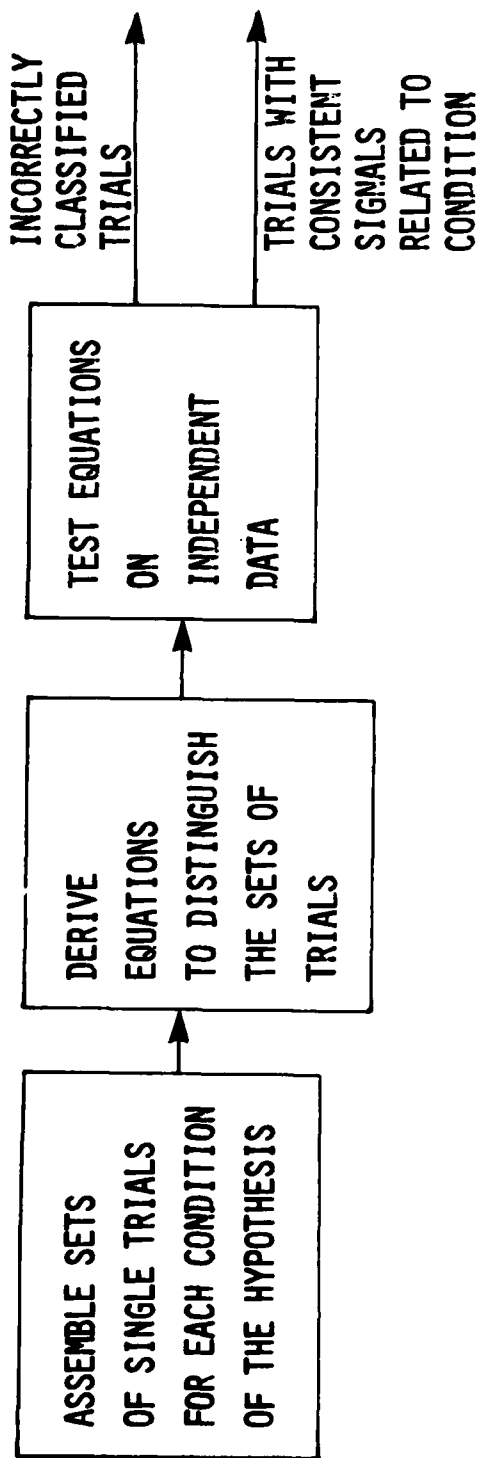


Figure 17. Block diagram of procedure for selecting trials with consistent task-related signals.

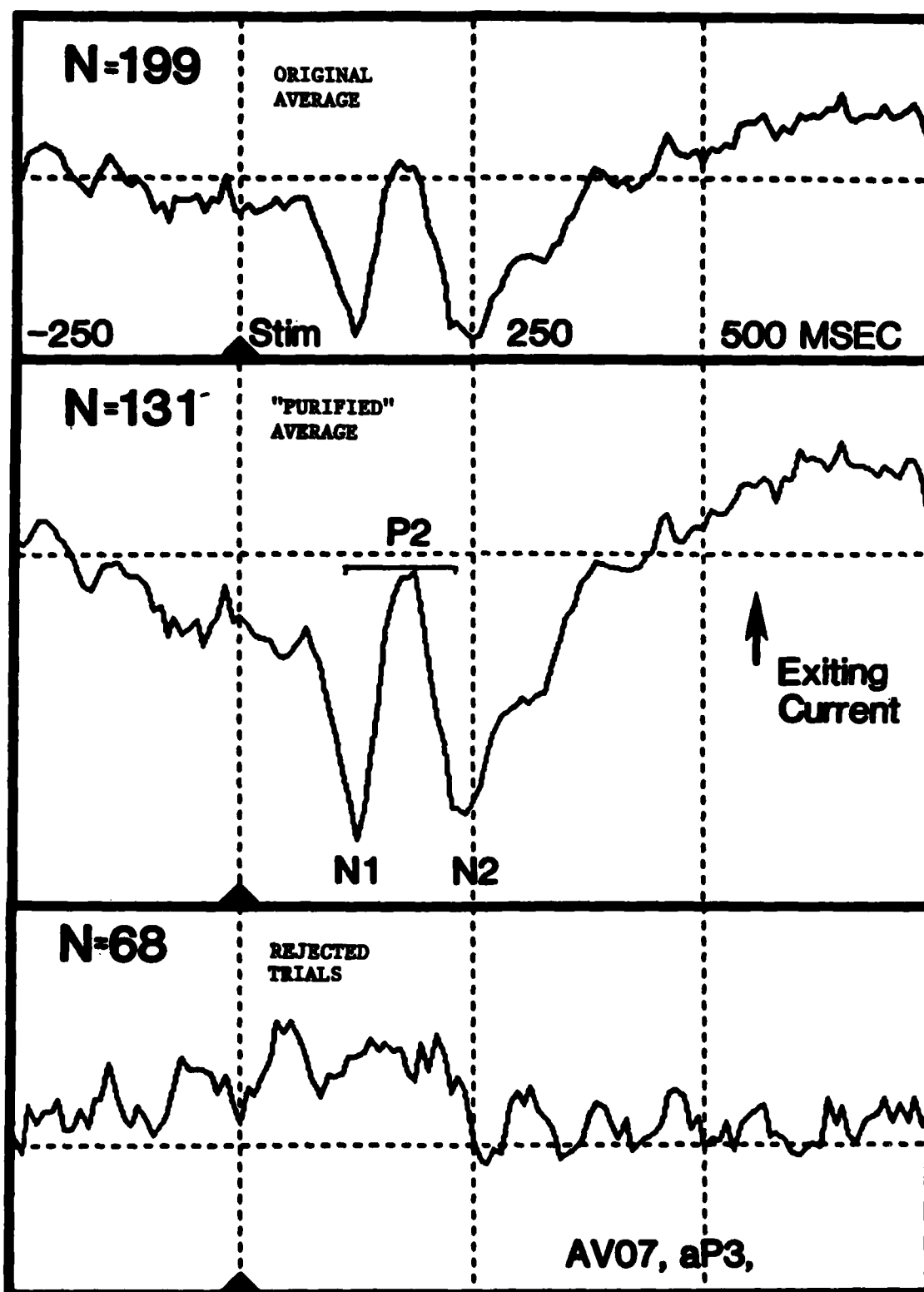


Figure 18. Use of pattern recognition to select sets of individual trials with consistent task-related signals. The averaged waveform of the original 199 trials is at top. The middle "purified" waveform is the average of 131 trials which were correctly discriminated from pre-cue data by the pattern-recognition algorithm using data points from a 125 msec interval centered on the P2 peak. There is an enhancement of the N1, P2 and N2 peaks, as well as the pre-stimulus and pre-movement slow potentials, even with 34% fewer trials than the original average. The 68 incorrectly classified trials produce an average waveform (bottom) which lacks resemblance to the original average and is dominated by ongoing EEG activity.

November 13, 1984 (56)

results from its application to lowpass-filtered data. This will not affect results of the second pass of NCP Analysis which will achieve good temporal resolution by measuring interchannel timing relations on unfiltered data.

B. Averaged Evoked Time Series Analysis

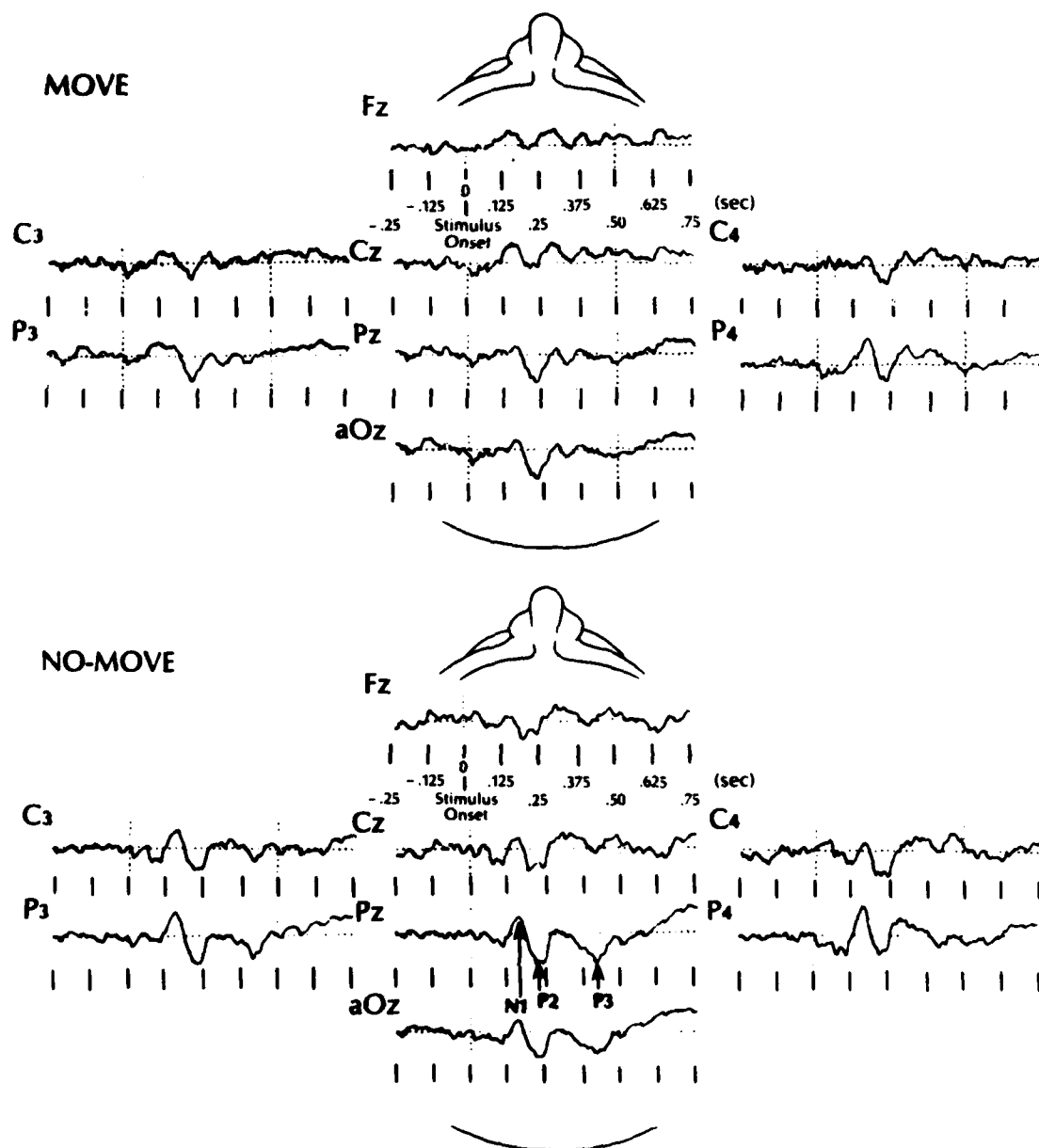
1. "Purified" ERPs

A great deal of effort has been expended in attempts to form improved estimates of the averaged ERP (see reviews in McGillem, et al., 1981; de Weerd 1981; and Gevins, 1984). Most methods assume that task-related signals are present in every trial and also have inherent assumptions about the statistical properties of signal and noise. We have developed a method for ERP estimation without these assumptions. To do this, separate averages are formed from trials which are correctly or incorrectly classified by the single-channel scanning pattern recognition procedure described above (Figure 17). In the averages of correctly classified trials, the ERP peaks are enhanced in comparison with the original averages (Figure 18). The averages of incorrectly classified trials resemble the background EEG. Several dozen applications of this technique suggest that it is successful in identifying trials with poor SNR, and provides a simple method of ERP estimation without the a priori assumptions about the characteristics of an unknown signal made in techniques such as Wiener or minimum mean-square error filtering. While the classifier we use is a nonlinear, layered network algorithm, similar "purified ERPs" were also obtained with simpler discriminant functions such as those produced by the widely available BMDP7M program.

The simplified procedure may be summarized as follows: 1) Filter the single trials to remove alpha and beta components; 2) Decimate the resulting time series to produce features for a simple (Fisher) linear discriminant function. Choose points from a time region of interest as one class, for example the P3 peak. The other class can be timepoints from an interval with low average energy (such as the pre-stimulus). Preferably, the reference class may be obtained by the "random data" baseline technique described in the previous section; 3) Compute the Fisher discriminant function from these classes and attempt to classify the feature sets; 4) Compute the average of the unfiltered trials corresponding to the filtered trials which were correctly classified in (2). This is the enhanced ERP estimate.

2. Wigner (Time-Frequency) Distributions

The ERP waveform is a function of time and does not provide explicit frequency information. Power spectra of ERP waveforms provide frequency information but obscure time-dependent phenomena. A view of the spectrum as it changed over time would give a new view of the evolution of different frequency components of the ERP. A simple approach would be to compute the spectrum over highly overlapped windows of the average ERP. However, such a "spectrogram" would smear together events within each analysis window. While there is an unavoidable trade-off between frequency and time resolution (known as the Heisenberg Uncertainty Principle), the spectrogram is an inflexible way of determining this choice. The octave-band filters



Figures 19 a & b. Two representations of 8 average ERP channels for "move" and "no-move" visuospatial tasks. Looking down onto the top of the head, the nose is at the top of each set of 8 channels. Figure 19a shows the average time series of 40 no-move and 37 move trials. These trials were selected by a statistical pattern recognition algorithm as having consistent task-related signals which differed between the move and no-move tasks. Three of the most commonly studied ERP peaks are indicated on the Pz channel of the no-move task. Of these, the P3 peak is larger in the infrequently occurring no-move task. Figure 19b shows the pseudo-Wigner Distribution of the analytic signal of the same data. This representation shows that the event-related processes are changing rapidly in both time and frequency. The first moment along the time axis for each frequency is the group delay, while the first moment along the frequency axis at each time is the instantaneous frequency. There is a build-up in energy after the stimulus,

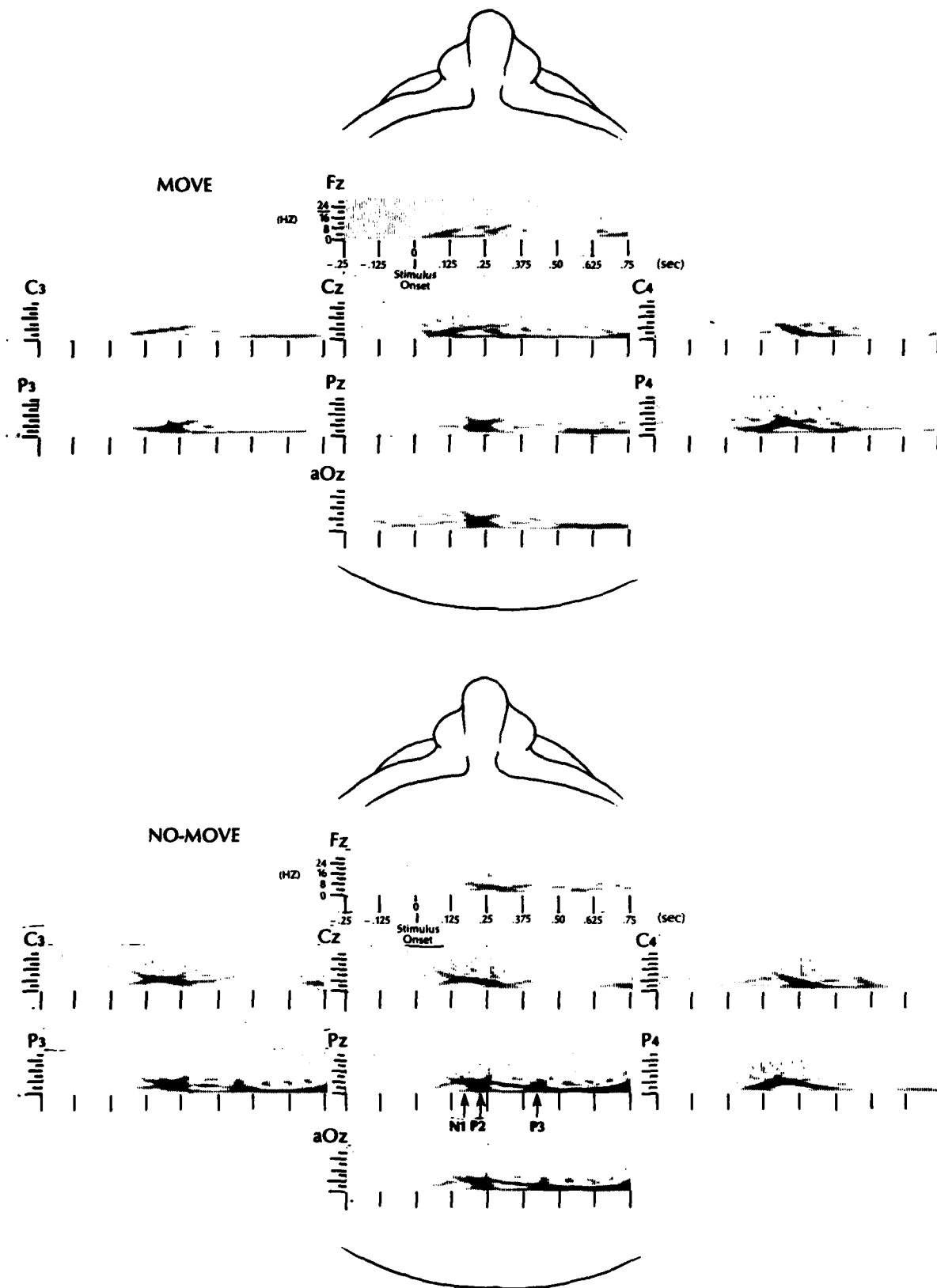


FIGURE 19b.

November 13, 1984 (56)

of de Weerd (1981) at least optimally trade off time resolution for frequency resolution in different observed bands, but the choices are still pre-determined and inflexible. A preferred method is to compute a function of time and frequency called the Wigner Distribution (Claassen and Mecklenbrauker, 1980; Janze and Kaizer, 1983) which approximates the instantaneous energy for a given time and frequency. Its correspondence to such a function is only approximate, because it can have negative values, and because the Uncertainty Principle still requires us to give up some frequency resolution for a narrowing of time resolution. However, the Wigner transformation gives a raw "distribution" which can be averaged over many different time and frequency regions to give valid energy estimates. Thus, the Wigner Distribution is a basic time-frequency function without fixed resolution trade-offs. In fact, all other time-frequency distributions of the general type called the Cohen class (Cohen, 1966), including the spectrogram, can be derived as time-smear versions of the Wigner Distribution. In practice, the "purified" ERPs show strong enough energy "peaks" in the Wigner Distribution that very simple interpretations of the time and frequency locations of signal energy are valid. This is true because local averages will all show the predominance of energy in the observed peak regions.

The Wigner Distribution is defined as

$$W_x(t, \omega) = \int_{-\infty}^{\infty} e^{-j\omega\tau} x(t + \tau/2) x^*(t - \tau/2) d\tau$$

with $x(t)$ the average ERP, ω the frequency variable, and τ the dummy integration variable. (Note: in practice, finite intervals are analyzed, giving rise to the windowed or "Pseudo" Wigner Distribution. For properly windowed signals, this causes a minor blurring in the frequency direction, but no blur in the time direction). Integration over time or frequency yields the power spectral density and the instantaneous power functions respectively, i.e.,

$$\int_{-\infty}^{\infty} W_x(t, \omega) d\omega = |X(\omega)|^2, \quad \frac{1}{2\pi} \int_{-\infty}^{\infty} W_x(t, \omega) d\omega = |x(t)|^2$$

Further,

$$T_x(\omega) = \frac{1}{|X(\omega)|^2} \int_{-\infty}^{\infty} t W_x(t, \omega) dt$$

the expected value of the time variable is the average time, which may be viewed as the group delay, and

$$\Omega_x(t) = \frac{1}{|x(t)|^2} \int_{-\infty}^{\infty} \omega W_x(t, \omega) d\omega$$

the average frequency value for each time point is the instantaneous frequency.

The Wigner Distribution is actually best calculated from the analytic signal of the "purified" average, which is the complex-valued signal whose real part is the original time series, and whose imaginary part is the Hilbert Transform of the real part. The magnitude of this complex time series is the temporal envelope of the real time series.

November 13, 1984 (56)

Figure 19 shows the (Pseudo) Wigner Distributions for several channels of the average of correctly classified trials for participant SS02 in a previous visuomotor experiment.

Figures 20 through 23 show (Pseudo) Wigner Distributions for several channels of the average of correctly classified trials for AV07.

C. Test of Principal Components Analysis (PCA) for Defining Analysis Windows

Principal Components Analysis (PCA) has become a standard procedure for primary feature extraction in ERP analysis. Recently, this procedure has come under criticism from a variety of quarters (Gevins, 1980; Rosler and Manzey, 1981; Hunt, 1984; Wood and McCarthy, 1984; Gevins, 1984). Questions have been raised concerning its assumptions of normal data distributions, orthogonality of variance from different physiological generators, and invariance of ERPs across trials, as well as the appropriateness of rotating factors. Studies using synthesized waveforms have indicated misallocation of variance among factors and suboptimal feature extraction (Wood and McCarthy, 1984). Nevertheless, we tested the usefulness of PCA for determining the time intervals for single-trial between-channel correlation analysis. Our previous method was to center analysis windows of a standard size on ERP peak latencies for each participant as assessed by an expert from the averaged ERPs. An effective automated method of interval selection could possibly provide greater precision and objectivity, especially in the case of overlapping "components". To this end, a series of PCAs with Varimax rotations were performed on subaverages of "move" and "no move" trials from the data of one to four participants in a previous study (Gevins, et al, 1983, 1984). Averaged digitized values were lowpass filtered (McClellan-Parks filter with cutoff at approx. 30 Hz) and decimated by 2 to reduce the number of variables in the PCA. Analysis windows were then set according to the latencies where the significant factor loadings for "large" factors (i.e. those representing the most variance) were consistently large over a continuous time interval. Ten to thirteen factors were required to account for more than 90% of the variance; of these, some were similar in latency and duration to peaks in the ERP waveforms, while others were not. Further, the amount of variance accounted for by factors corresponding to the peaks which were maximally different between conditions were not always correspondingly large. None of the PCA-determined windows performed as well in between-task pattern recognition analysis using single-trial correlations as the 180-msec wide windows centered on the manually-picked ERP peaks. It is difficult to determine which of the possible problems with PCAs led to its inferior performance as a means of determining intervals for pattern recognition analysis of correlations. The conclusion we draw is that use of windows centered on the manually picked ERP peaks is superior for our purposes.

D. Current Source Density Transform

1. Derivation of Current Source Densities

VISUAL MOVE TASK AV07 Current Density

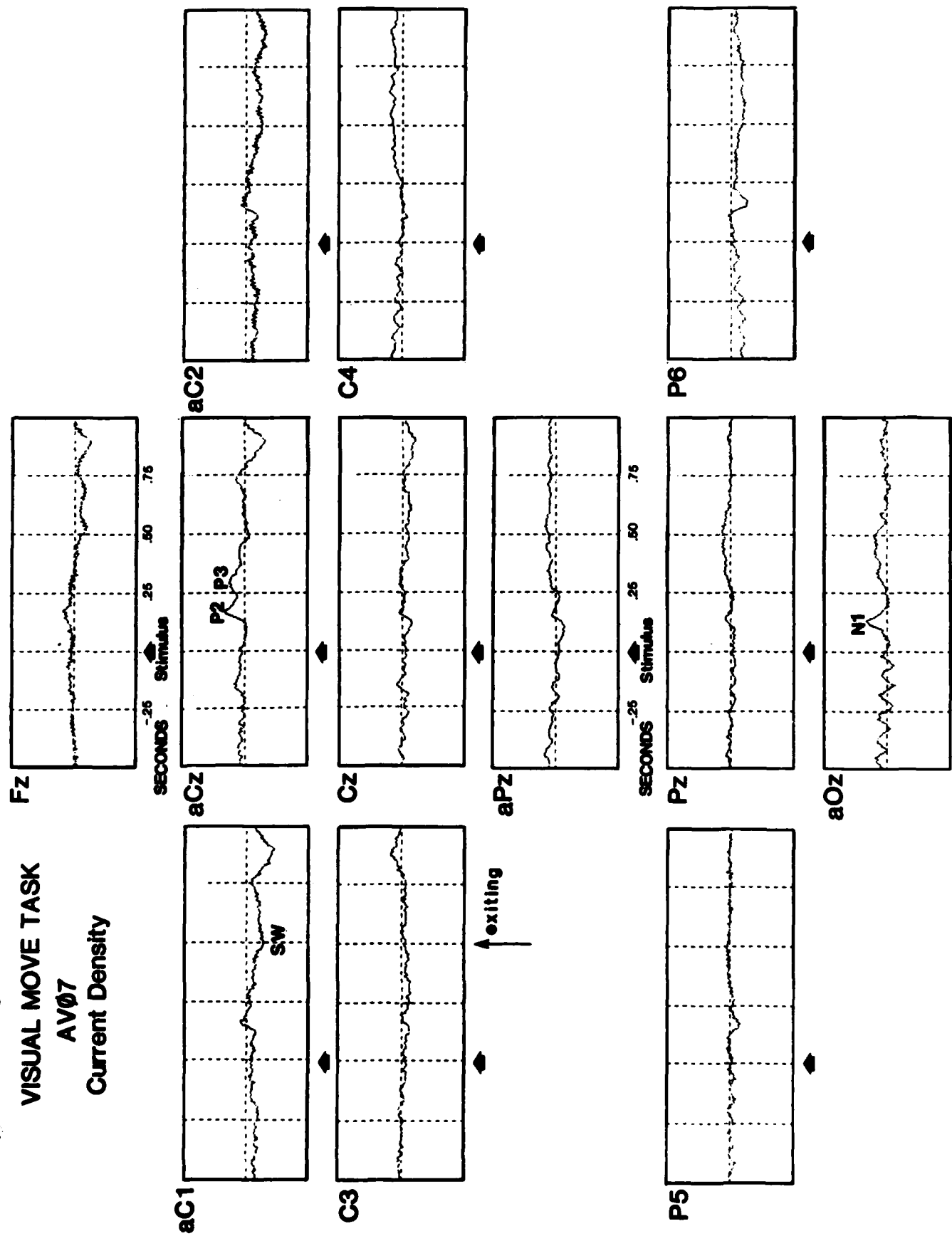


Figure 28a. Twelve representative channels of current source densities for visual move task from participant AV07. Average of trials (22 to 38 depending on the channel) which had task-related signals in the P2 and P3 intervals and which were further restricted to a reaction time of 828 msec \pm 31 msec.

VISUAL MOVE TASK

AV07

Current Density

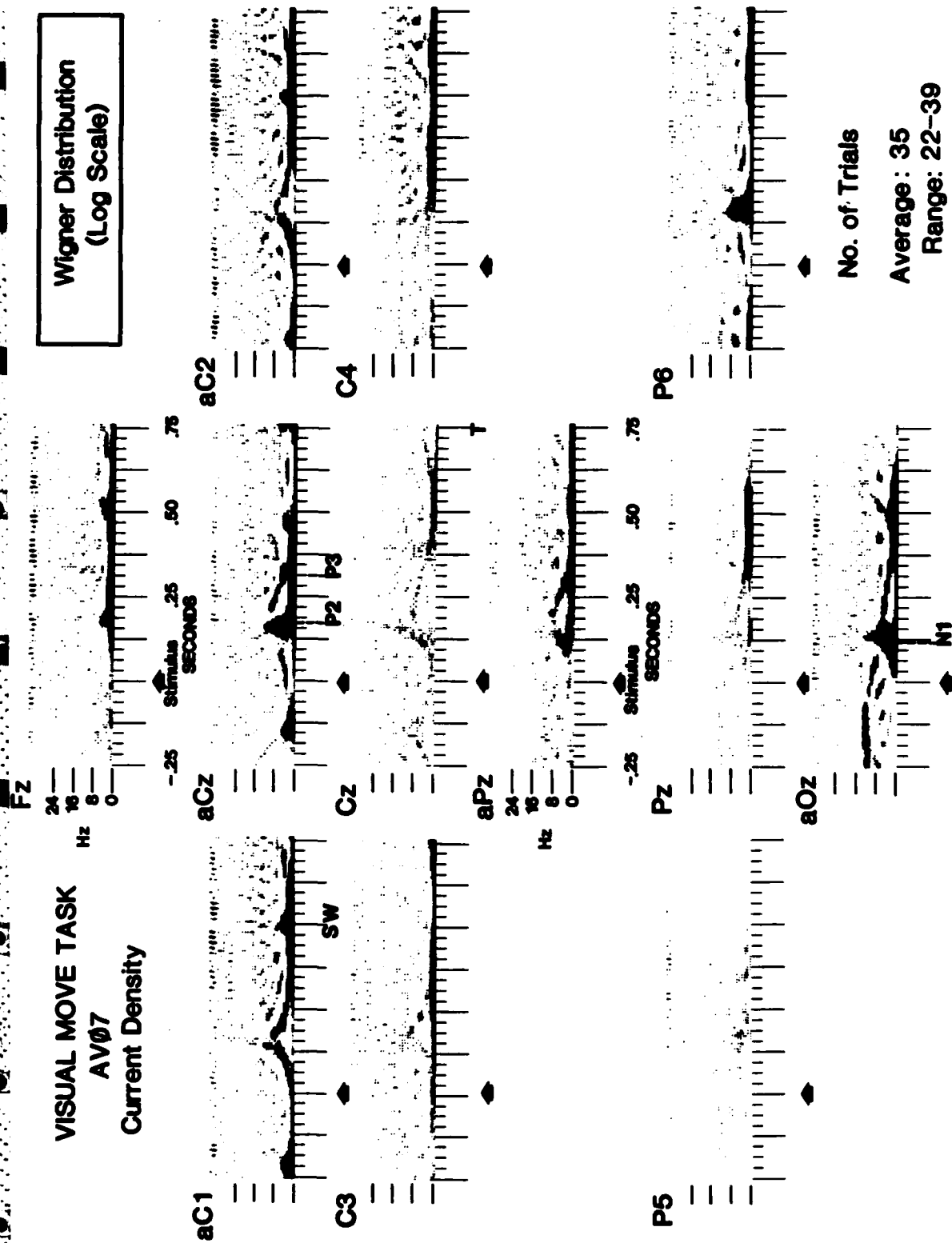


Figure 20b. Log Wigner Distributions of same data as Figure 20a. Note the "N1 hump" at aOz with major energy between 0 and 8 Hz which terminates abruptly before 200 msec and is followed by a slow glide down in frequency. The "p2 hump" at aCz and P6 is similar in spectral distribution, but occurs about 40 msec later. The log transform is used to compress the range, allowing comparison between conditions on the same gray level scale. Since there are too few gray levels, the scale saturates. A color version is being implemented to overcome these limitations.

VISUAL NO-MOVE TASK

AV07

Current Density

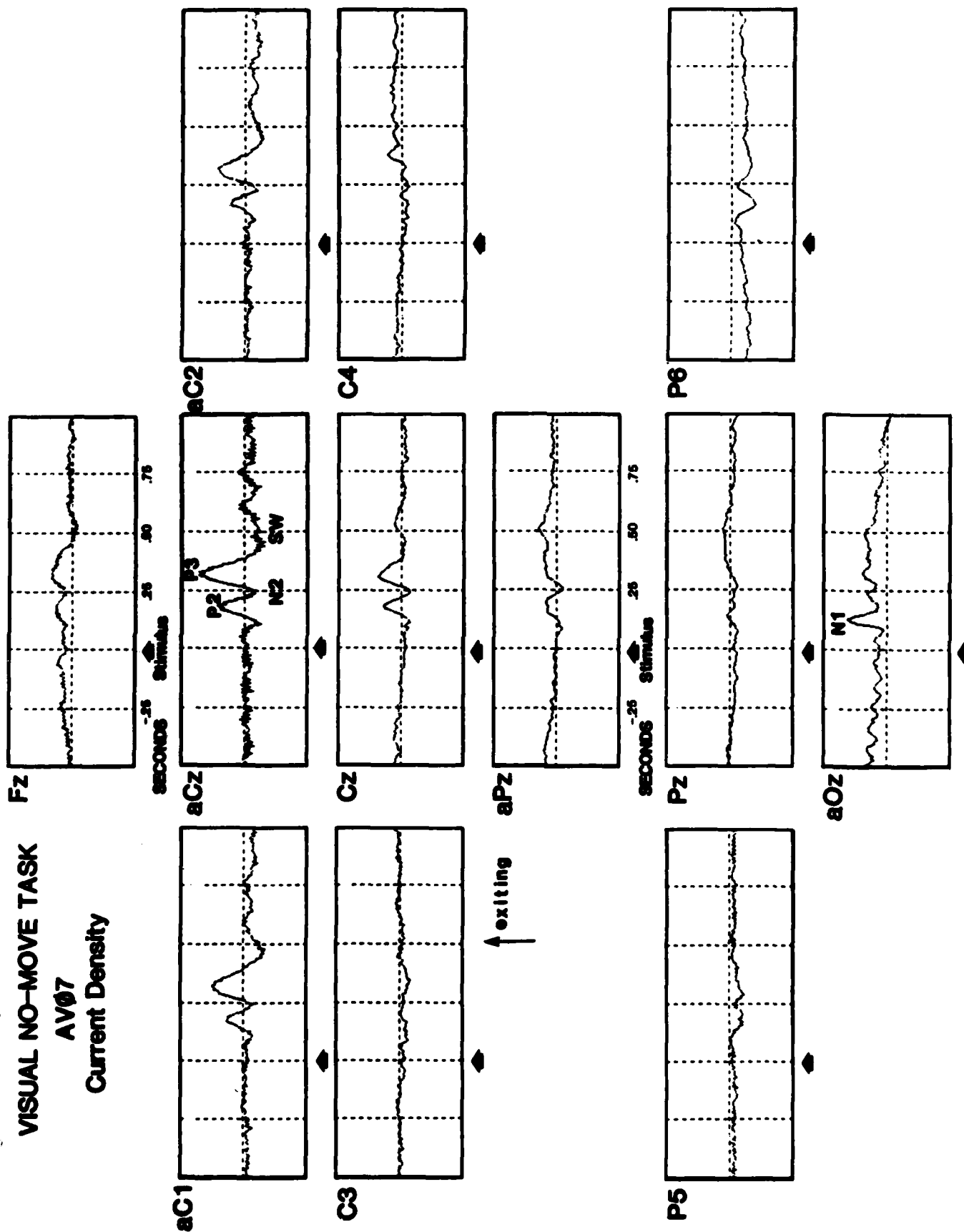


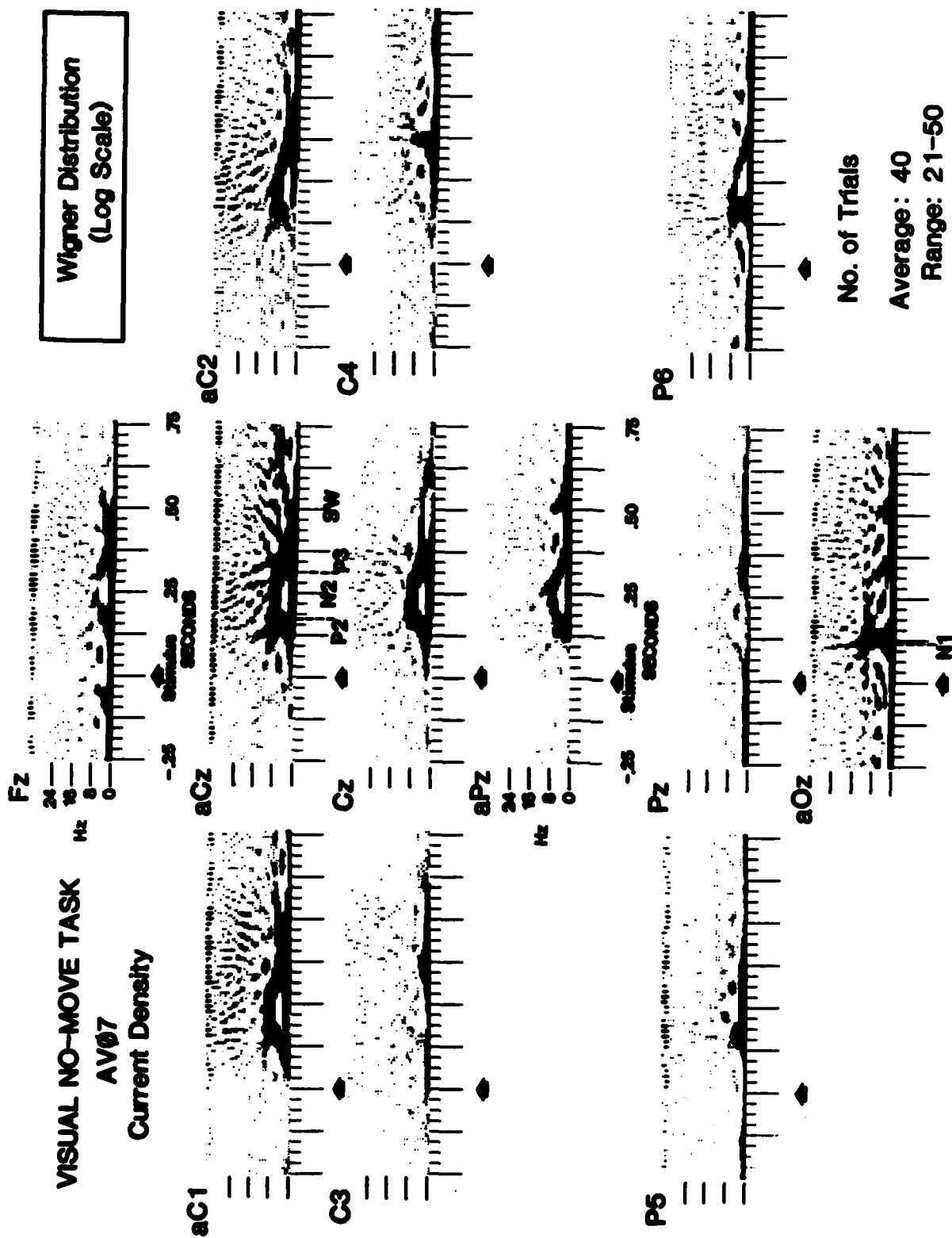
Figure 21a. CSDs for infrequent visual no-move task from participant AV07. Average of trials (21 to 50 depending on the channel) which had task-related signals in the P2 and P3 intervals.

VISUAL NO-MOVE TASK

AV07

Current Density

Wigner Distribution
(Log Scale)



No. of Trials

Average: 40

Range: 21-50

Figure 21b. Log Wigner Distributions of same data as Figure 21a. The "denut hole" after the "P2 hump" at aCz, aC1, aC2, Cz and Pz is a dropout of about 2-5 Hz activity. The "P3 hump", commencing at about 300 msec, begins to lose power above 6 Hz before about 375 msec. By about 300 msec all that remains is some low-frequency power centered at about 2 Hz corresponding with the slow wave.

AUDITORY MOVE TASK

AV07

Current Density

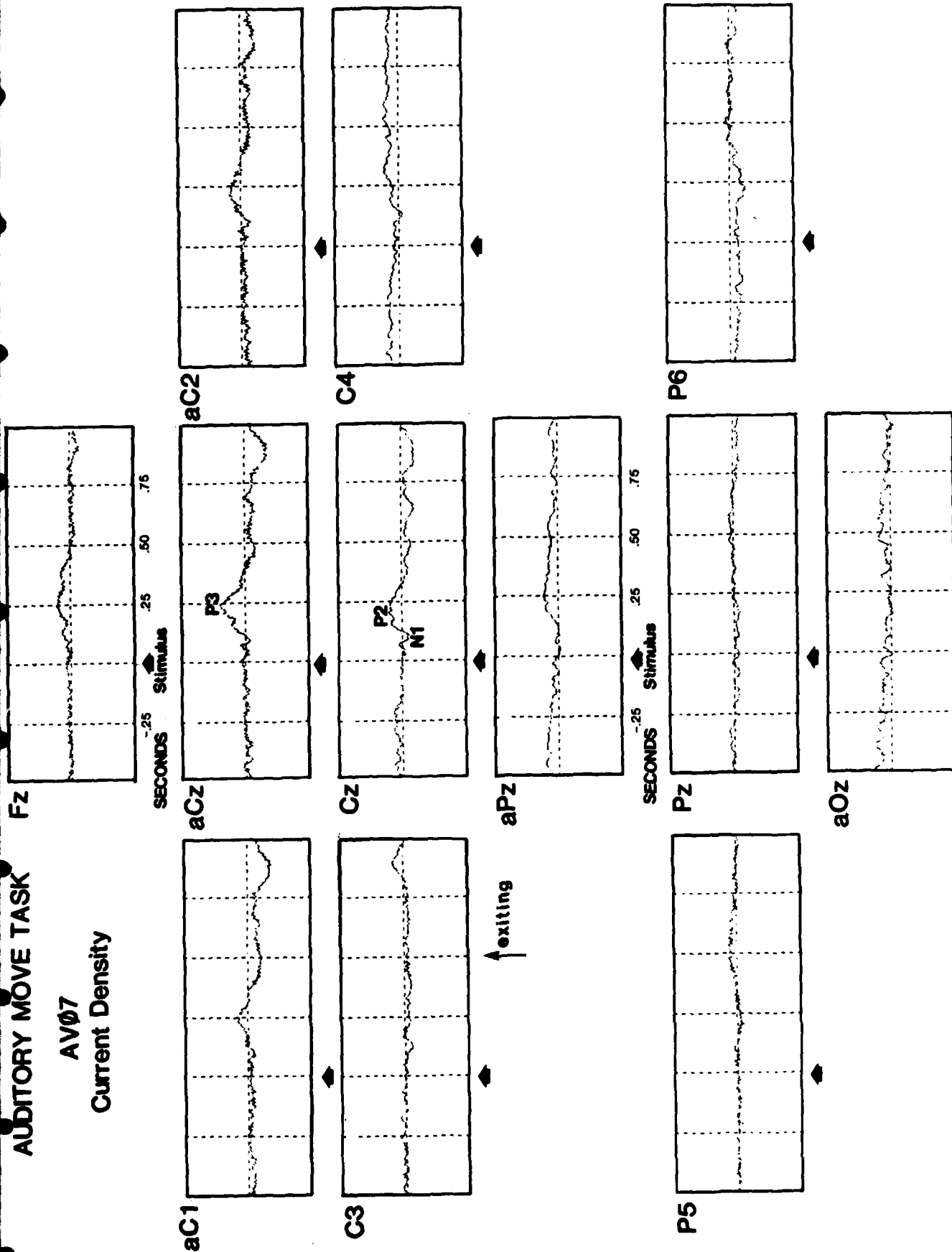


Figure 22a. CSDs for auditory move task from participant AV07. Average of 25 to 35 trials depending on the channel which had task-related signals in the P2 and P3 intervals and which were further restricted to a reaction time of 828 msec \pm 31 msec.

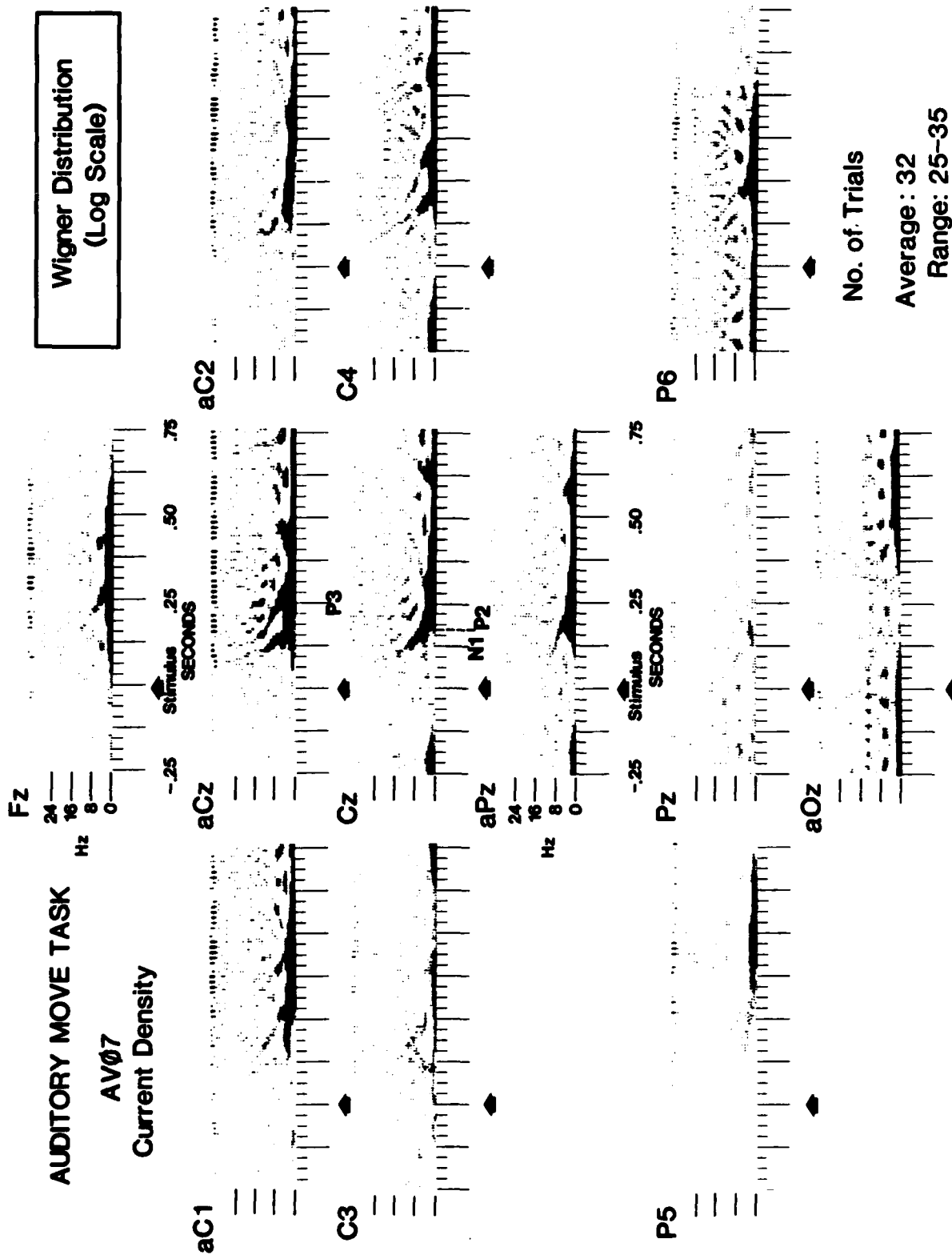


Figure 22b. Log Wigner Distributions of same data as Figure 22a. The "N2-P2 ramp" commences at about 125 msec and declines from about 8 Hz to 4 Hz by about 175 msec.

AUDITORY NO-MOVE TASK

AV07

Current Density

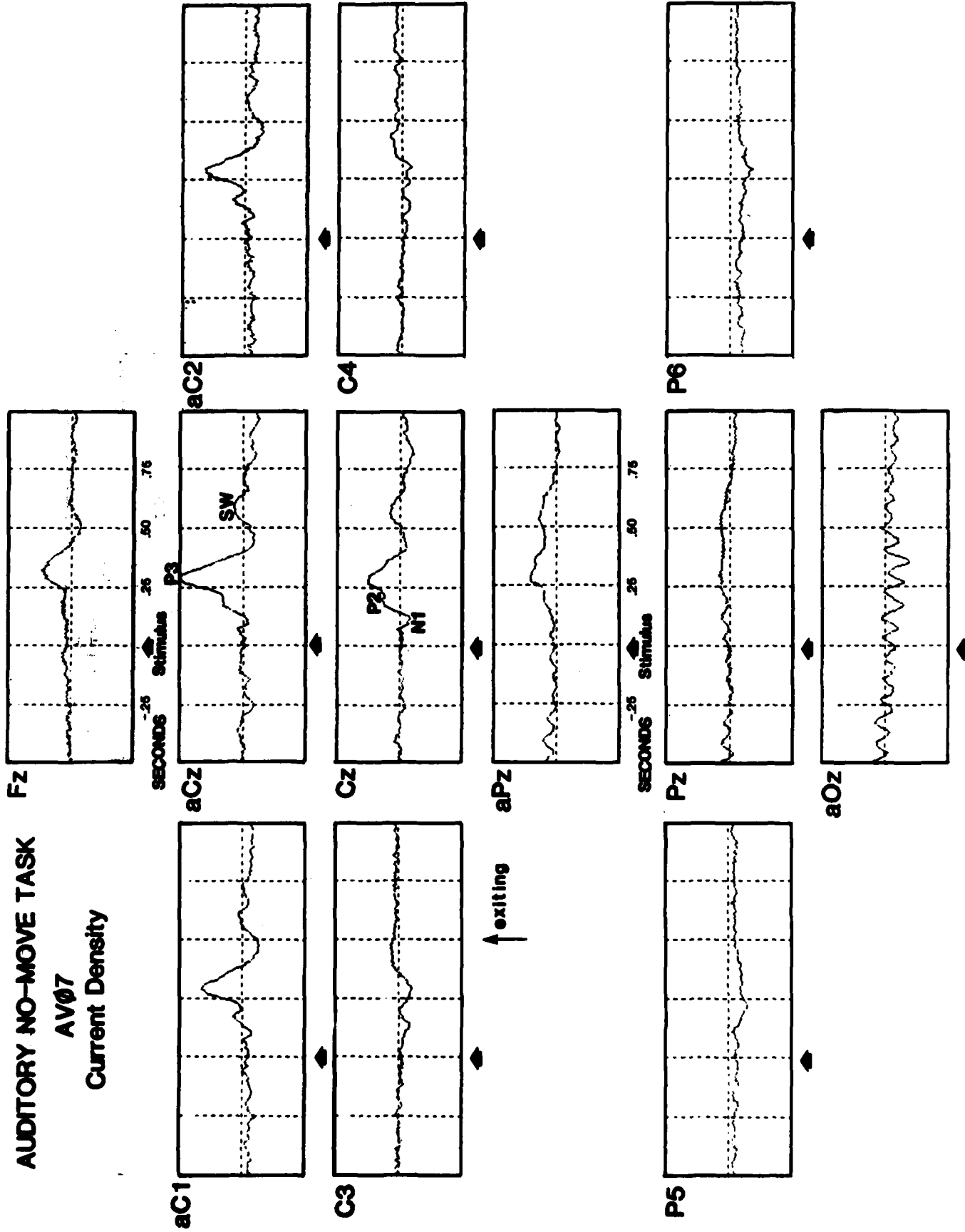


Figure 23a. CSDs for auditory no-move task from participant AV07. Average of trials (29 to 49 depending on the channel) which had task-related signals in the P2 and P3 intervals.

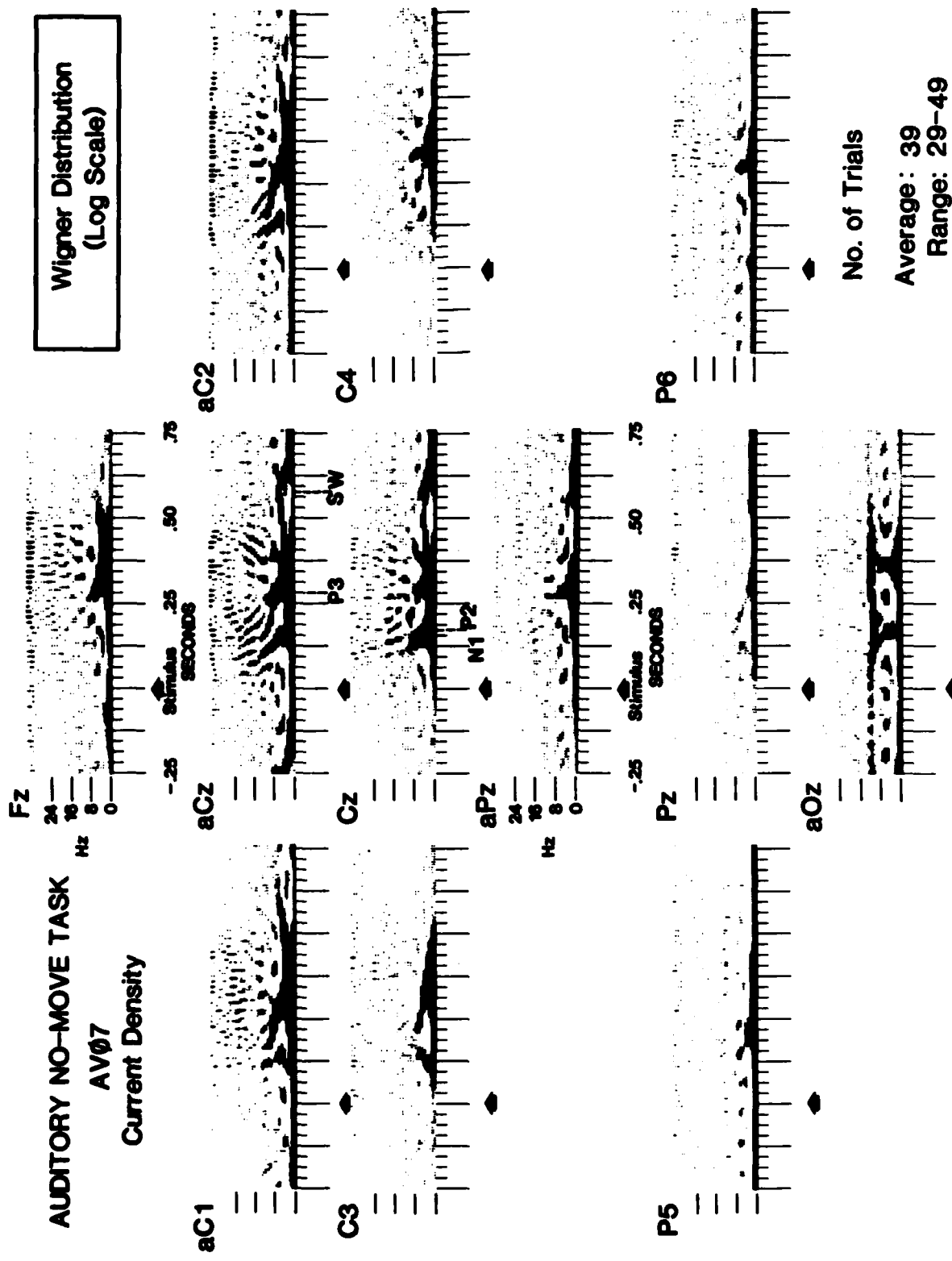


Figure 23b. Log Wigner Distributions of same data as Figure 23a. The "p3 hump", which commences abruptly at about 275 msec and drops off by about 340 msec, spans a DC to about 8 Hz range and then narrows to a lower frequency signal. Note the alpha band activity represented by the dark line at about 11 Hz at aPz. The two "humps" at about 160 msec and about 340 msec.

November 13, 1984 (56)

from Potential Distributions

In order to sharpen the spatial localization of brain activity recorded at the scalp, we convert the event-related potential time series to current source densities (CSD). This method computes the curvature of the potential distribution (the Laplacian transform) at each electrode site. This reflects the sources and sinks in the flow of electrical current at the scalp, which presumably reflects the emergence and re-entry of currents through the skull (Hjorth, 1975, 1982). The advantages are that: 1) the CSD is independent of the choice of reference electrode site; 2) the activity of current sources outside the ring of electrodes immediately adjacent to a particular site are suppressed, and as a result; 3) the crosscorrelation between scalp electrodes due to volume conduction is reduced. When applied to ongoing EEG, it was reported that the interelectrode correlation is reduced by a factor of 2 to 4, depending on the distance between electrodes (Hjorth, 1975). The ability of this type of transform to provide sharper localization of sources of abnormal electrical activity has been demonstrated in several clinical EEG studies (Spehr, 1976; Hjorth, 1982).

We are using CSD derivations in two studies of evoked electrical time series: a visuomotor numerical judgment study comparing right- and left-handed response movements, and the bimodal (auditory/visual) numerical judgment study described in this report. The former was recorded with a 26-electrode montage and the latter with a 49-electrode montage. After applying the CSD transform to each single trial, averaged event-related CSDs were computed, and the latencies of the major peaks determined (Section III). Then the sets of single-trial data were submitted to the first scanning stage of NCP Analysis (as described above) in intervals centered on these peak latencies.

We have implemented the CSD transform in software, using measures of interelectrode distances determined in two ways: reconstruction of the three-dimensional positions of the electrodes using a stereo photogrammetric system (see next section), and direct measurement of interelectrode distances with a flexible ruler.

Since the electrical activity at scalp locations outside the area covered by the electrode montage is not available, CSDs calculated for peripheral electrodes of the montage have fewer "correction" terms, and the validity of their amplitude is questionable. These electrodes are excluded from further analysis.

Averaged event-related CSDs have a higher degree of spatial resolution than corresponding referential ERPs (Thickbroom, et al, 1984). For example, in movement-registered ERPs for finger movements, the readiness potential (RP) and post-movement positivity (PMP) are widespread over frontal and central sites, with larger amplitudes at central sites contralateral to the responding hand (Figs. 24 and 25). In the corresponding averaged CSDs these components are more localized. The RP and PMP exhibit distinct phase reversals between the anterior midline central electrode (aCz) and just one or two lateral electrodes opposite to the responding hand (C3 and aP1 for right hand movements; C4 for left hand movements). This may be an indication of a localized current source midway between these sites, near

RIGHT HAND MOVE

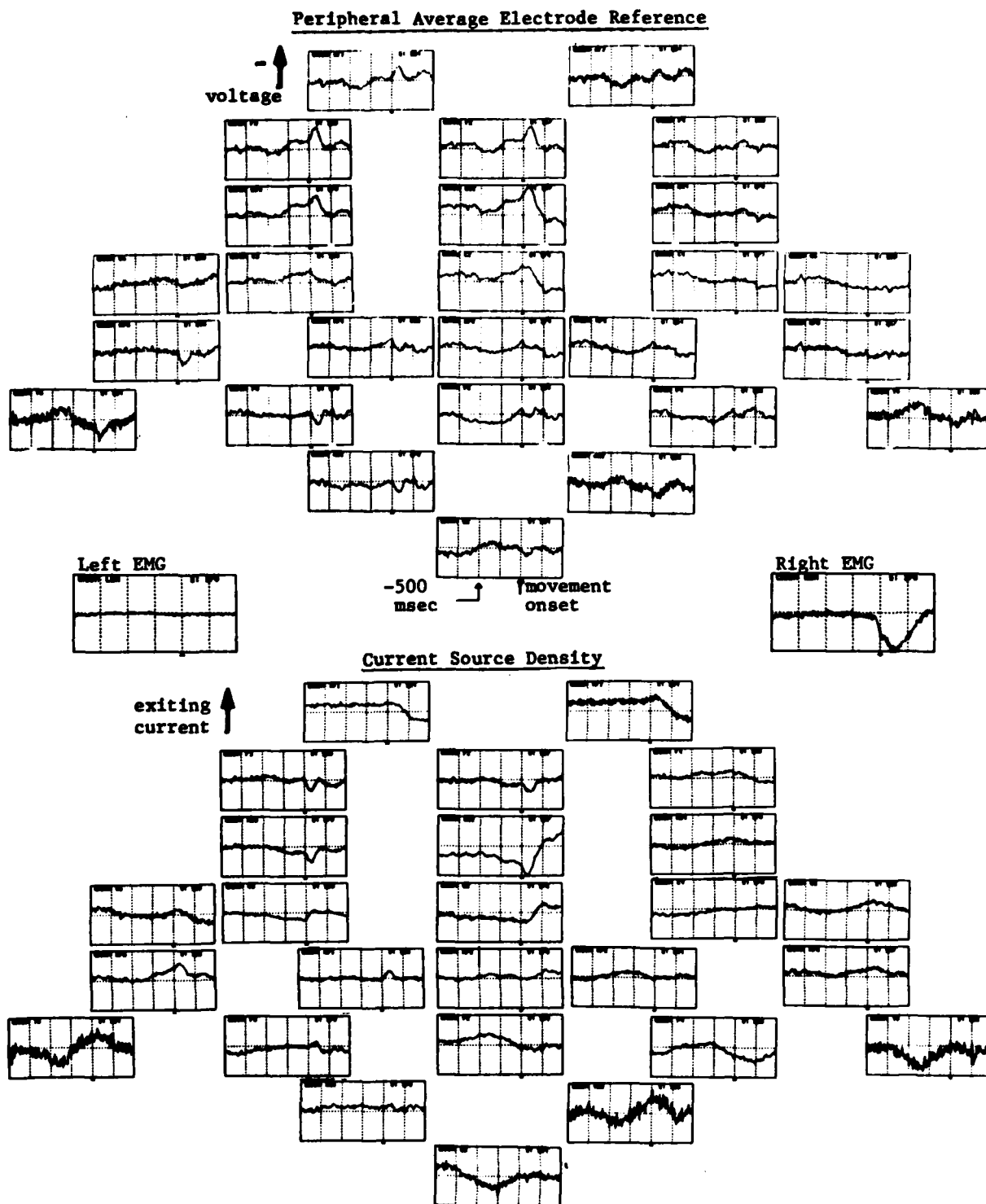


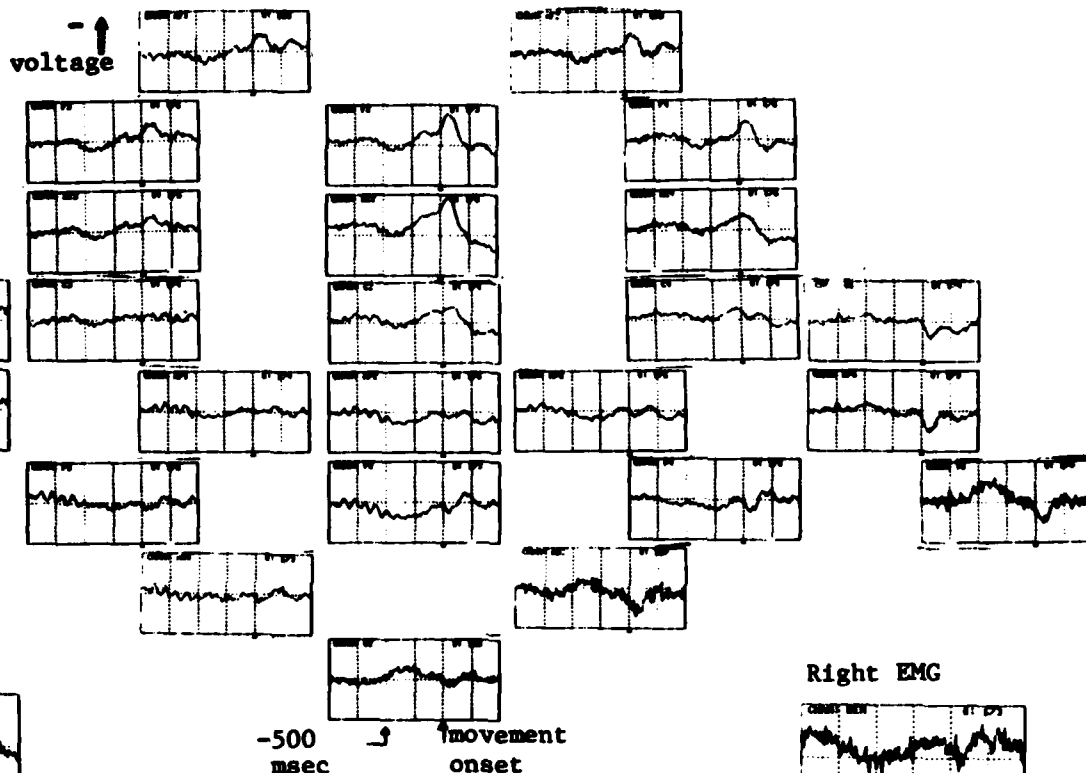
Figure 24. Movement-registered ERPs for an isometric right index finger contractions.

Upper: Average-of-peripheral-electrodes reference. Note relatively widespread anatomical distributions of movement-related components. There is a greater voltage over the electrodes contralateral to the responding hand compared with the ipsilateral electrodes.

Lower: Current source densities. The contralateral effect is greatly enhanced, activity at Cz is greatly reduced, and there is a clearly evident phase reversal of the maximum negative peak of the readiness potential and the post-movement positivity between the sCz and Cz electrodes.

LEFT HAND MOVE

Peripheral Average Electrode Reference



Current Source Density

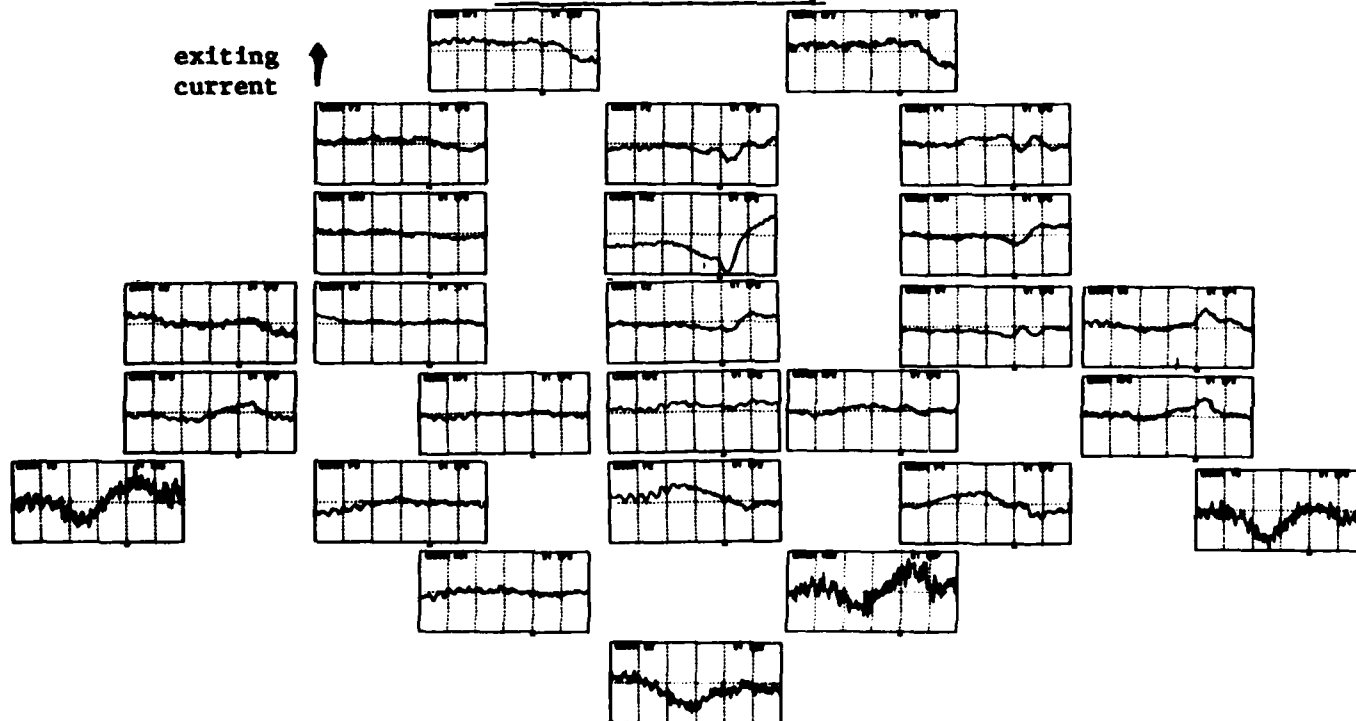


Figure 25. Movement-registered ERPs for an isometric left index finger contraction. Average-of-peripheral-electrodes reference (upper), and current source density (lower). CSD has improved localization of contralateral movement-related activity. Compare with Figure 24.

November 13, 1984 (56)

the cortical motor area for hand and finger movements. The CSD time series for central sites ipsilateral to the responding hand are quite flat in the recordings examined to date. Such an interpretation is in agreement with measurements of event-related magnetic fields. Similarly, for both auditory and visual stimuli, the primary sensory peaks (N100) are more localized in the CSDs than in corresponding ERPs (see Figures 4 and 5).

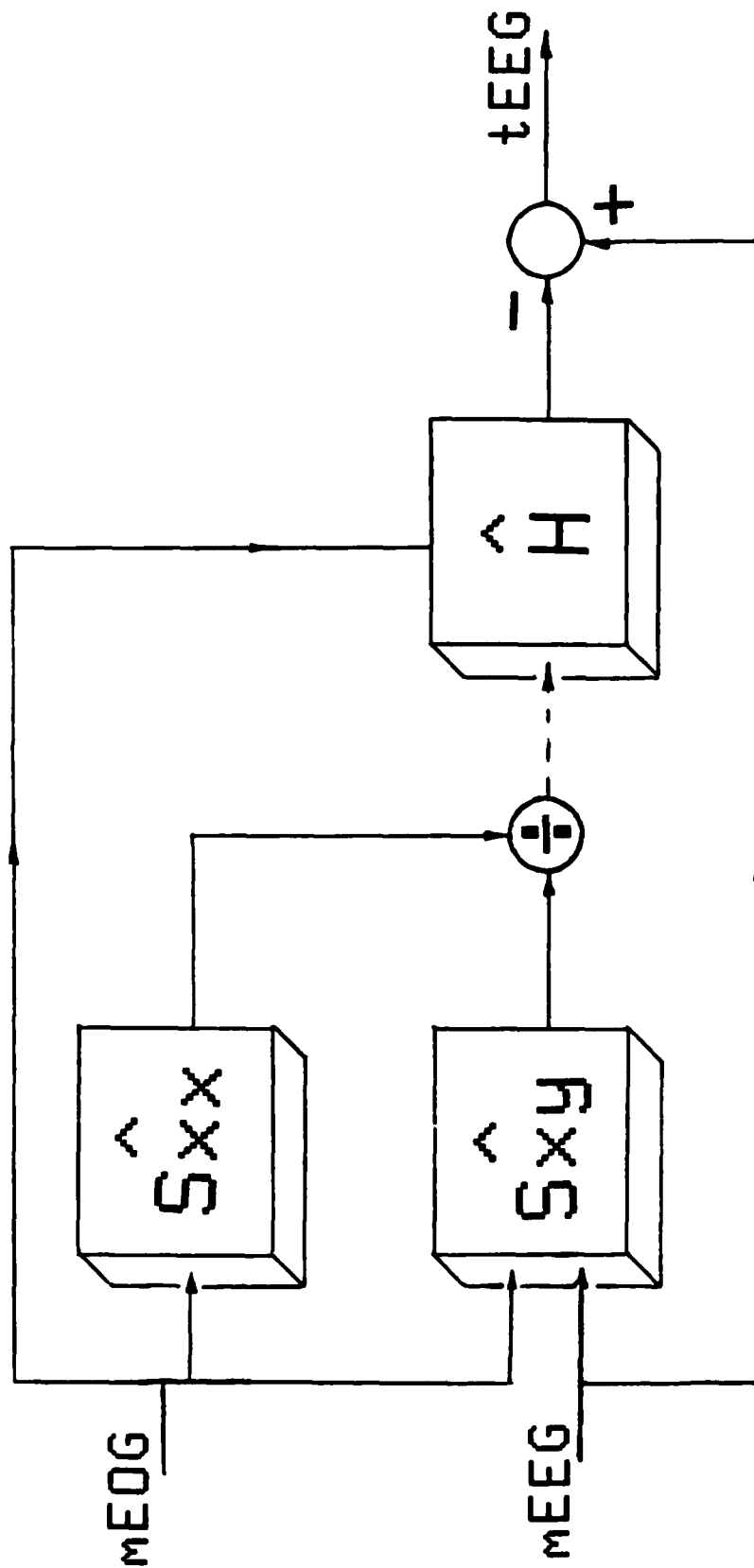
2. Determining Electrode Positions

In order to determine the precise positions of the electrodes for current source density transform and spatial deconvolution, we used a system of stereophotogrammetry developed for orthodontic use. A series of stereo pictures of the participant's head with electrode cap in place was taken. The electrode positions in the photographs were digitized on a digitizing table, along with fiducial marks added by the camera. Computer software then reconstructed the three-dimensional positions of all electrodes. This was done for 2 participants. For one person, before and after measurements were made to investigate the stability of electrode positions across the recording session. The cap was found to be riding up at the back of the head by as much as 17 millimeters. In subsequent recordings we have ameliorated this problem by allowing the cap to settle before applying electrodes. The measures of electrode distances before and after the recording session were used to calculate current source density transforms to assess the dependence of CSDs upon variations in measurements. These CSDs differed only slightly, although individual interelectrode distances differed by as much as 10%. We are currently determining electrode distances for CSD transforms by measuring pairwise interelectrode distances with a flexible plastic ruler. The standard deviations of these distances across persons were under 3 mm, averaging about 2 mm. This consistency suggests that a standard set of interelectrode distances may be used, especially since the sensitivity of the CSD transform to small variations in measurement is slight.

E. Artifact Detection and Filtering

1. Eye Movement Contaminants

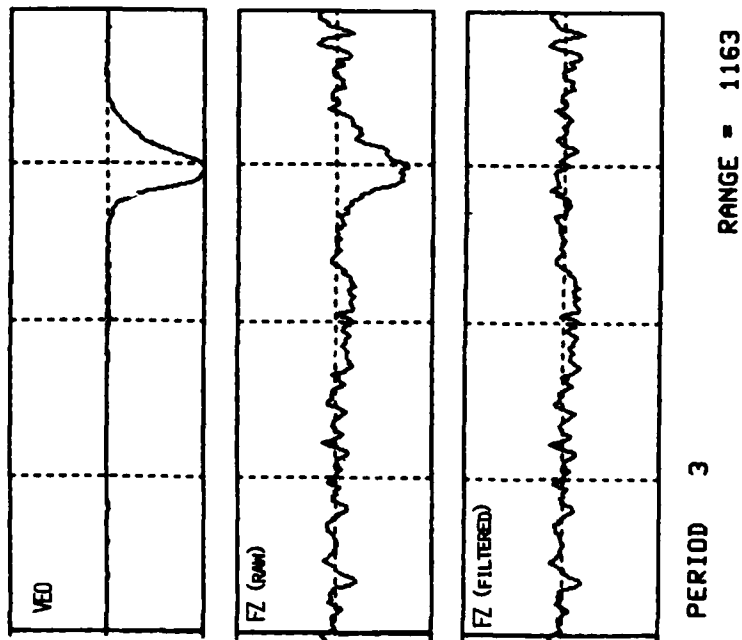
The general problem of artifact filtering is more difficult than that of artifact detection. Filters of various types have been developed to remove artifacts from brain signals, with the most effort directed towards removing eye movement potentials (EOG). Although Johnson and associates (Johnson, *et al.*, 1979) have made a good initial start using optimal digital filters, the removal of muscle potential contaminants (EMG) remains unsolved. Current techniques for removing eye movement artifacts rely on subtraction of a weighted, simultaneously recorded EOG signal from each EEG channel, an idea first put into practice by Gorton and Kamiya (1973), and recently improved by several laboratories. Verleger, *et al.* (1982) present the following method, typical of most current filters: record an EOG channel from electrodes above and below one eye, determine mathematically what an appropriate "scaling factor" should be for each EEG channel, and then subtract the EOG signal multiplied by its corresponding scaling factor from each EEG signal; repeat the procedure using an EOG electrode placed at the outer canthi for horizontal eye movements. The method most commonly used to determine the scaling factor tends to reduce the amplitude of the



EYE-MOVEMENT ARTIFACT FILTERING (SPECTRAL SUBTRACTION METHOD)

Figure 26. Block diagram of spectral subtraction method of eye-movement artifact filtering. See discussion in Section V.E.1.

VM07 SET VAA S2/T4/R6 03-AUG-84



VM07 SET VAA S2/T4/R6 03-AUG-84

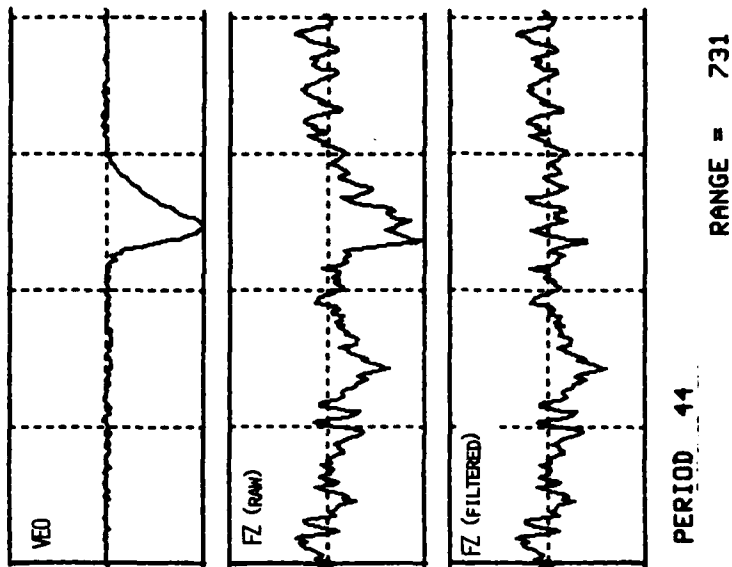


Figure 27. Examples of application of the spectral eye-movement filter to large blink artifacts.

COMPARISON OF EOG FILTERING METHODS ON SMALL BLINK ARTIFACT

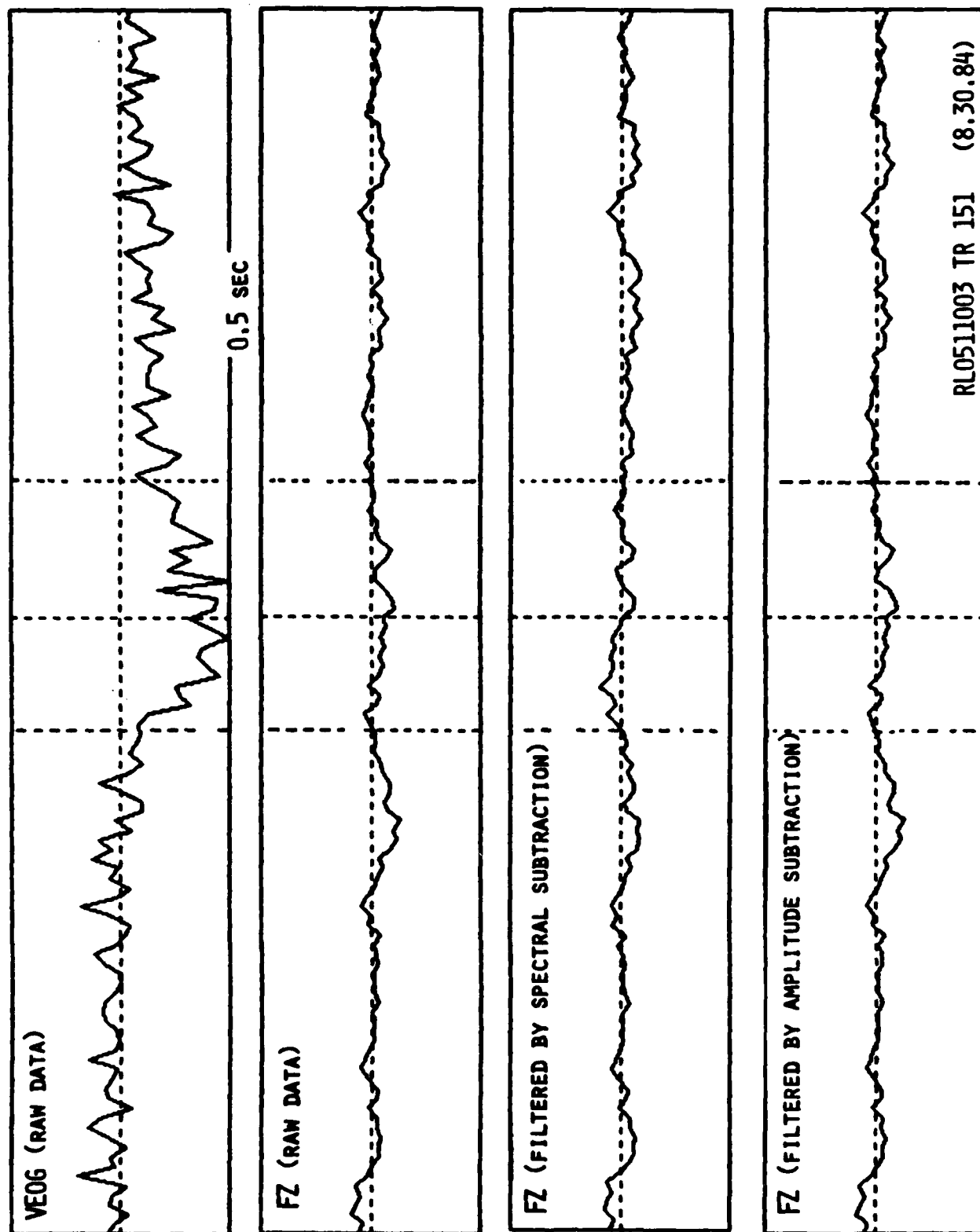


Figure 28. Example of application of spectral and amplitude subtraction eye-movement filters to a small blink artifact. The spectral subtraction methods seems superior in this instance.

November 13, 1984 (56)

EEG signal as well as remove the contaminating eye-movement signals. Gratton et al. (1983) attempt to remedy this problem by removing an estimate of the underlying event-related EEG and EOG activity prior to calculation of the scaling factors. Fortgens and de Bruin (1983) record four (oblique) EOG derivations, and calculate four scale factors to obtain better estimates of vertical and horizontal EOG contaminants. This appears to offer improved results, particularly in frontal and prefrontal channels.

While these algorithms represent good first approximation eye-movement artifact filters, a number of improvements remain to be made. In particular, the transmission of EOG potentials along the scalp and through intervening tissues would seem to be frequency dependent, thus requiring different scaling factors for different frequencies. Although this was first suggested by Whitton, et al. (1978), it was only recently that "short-time" spectral subtraction algorithms were fully applied to this problem (Bonham, et al., In Prep.). In this method, differences in the spectral signatures of eye movement and brain signals are used to create filters which remove eye movement contaminants from each trial (Fig. 26). Estimates are computed for the spectral density of the vertical and horizontal eye movement channels, and the cross-spectral density of the eye movement channels with each of the brain signal channels. Convolving the inverse Fourier transform of the ratio of these two quantities with each trial of eye movement channels results in estimates of the eye movement contamination of the brain signal for that trial. This estimate is subtracted from each trial of each brain signal channel. The system transfer function estimate is updated periodically by computing new values for the spectral and cross-spectral densities from recent trials. In initial evaluations the method appears to work very well (Fig. 27), exceeding the performance of the Gratton et al. (1983) amplitude subtraction method (Fig. 28) as assessed by a decreased ability to distinguish unartifacts from filtered trials using a nonlinear classifier.

2. Artifact Database

a. Overview

The current methods for editing polygraphs rely on the off-line procedure of detecting artifacts by visual inspection. Such a procedure is very labor-intensive. This database is a first step in the generation of algorithms which will eventually replace visual editing by an automated editing process.

A database was assembled of eight types of artifacts identified by visual inspection of the EEG's strip chart for the bimanual study. The study involved scalp recordings made from twenty-six sites, and additional channels for vertical and horizontal eye movements and for muscle potentials from the flexor digitorum. aPz was used as the reference electrode. A Bioelectric Instruments Model AS-64P amplifier with .10 to 50 Hz passband (12 db/octave rolloff) was used with a full-scale gain of 120 uv. EEG's were monitored on two eight-channel Beckman Accutrac and on one sixteen-channel Beckman Accutrace. Paper speed was set at 15 mm/sec.

The eight types of artifacts are: vertical eye movements (VEOG), horizontal eye movements (HEOG), muscle contamination (EMG), electrode sways (SWAY),

	TOTAL	GROSS	MOD	CUE	STIM	MOVE	FDBK
VEOG	1938	840 43%	1098 57%	851 44%	306 16%	375 19%	406 21%
HEOG	752	269 32%	483 68%	186 25%	115 15%	213 28%	238 32%
SWAY	6985	1062 15%	5923 85%	1917 27%	1769 25%	1679 24%	1620 23%
POP	176	34 29%	142 71%	33 19%	18 10%	45 26%	80 45%
GMD	3650	2227 61%	1423 39%	1218 33%	876 24%	769 21%	787 22%
PUL	4910	270 5%	4640 95%	1216 25%	1225 25%	1239 25%	1230 25%
BMG	2123	--	--	593 28%	501 24%	504 24%	525 25%
DUL	3824	--	--	956 25%	956 25%	956 25%	956 25%

TABLE 3: Distribution of Artifacts in Data Base.

November 13, 1984 (56)

gross movements (GMO), electrode pops (POP), electrode drying up, loose or dead (DUL), and pulse and EKG (PUL). The criteria according to which the artifacts were characterized will be discussed below. The goal of this study was to provide a database for the generation of algorithms which will permit the eventual automation of the current visual editing procedure.

One run from each participant was randomly selected for analysis. This provided a total of 9 sample runs, representative of the beginning, middle and end of the 5 to 7 hour recording sessions. Each artifact was characterized according to where it occurred in a given 6 sec trial of the run, i.e., during the cue (CUE), stimulus (STIM), movement (MOVE) or feedback (FDBK) events of each trial. Therefore, in any given trial, a single artifact could have occurred at four places; since there were generally 171 trials per run, there were 684 possible occurrences (4×171) of each type of artifact. More than one artifact could have occurred simultaneously. Artifacts were also characterized according to whether they were gross or moderate (VEOG, HEOG, SWAY, GMO), and regular or irregular in the case of the contamination by pulse (PUL). EMG and DUL were not evaluated according to degree of severity.

Table 3 shows the total number of each type of artifact that occurred over all the runs included in this study, as well as the proportion which were identified as gross or as moderate. In addition, Table 3 shows the distribution of the artifacts across the four types of events in terms of absolute number and in terms of what proportion that number represents of the total number of occurrences.

b. Criteria for Identification of Artifacts.

VEOG: Contamination by an eyeblink was considered to be gross VEOG artifact. Gross VEOG artifacts often contaminated the frontal (aF1, aF2, F3, F4) brain channels and represented forty-three percent of the total number of VEOG artifacts. An example of gross VEOG contamination is found in Figure 29. Moderate contamination generally occurred as a result of movement of the VEOG electrodes and represented fifty-seven percent of the total eye contamination. An example of moderate VEOG contamination is shown in Figure 30.

HEOG: Saccades or shifts due to horizontal gaze were the most common types of HEOG artifact. An HEOG artifact was identified as being gross if it exceeded approximately 400 msec in duration or about 50 uv in amplitude. Overall, 32% of the HEOG artifacts were considered to be gross and 68% moderate. An example of a gross HEOG artifact is shown in Figure 31. An example of moderate a HEOG artifact is shown in Figure 32.

SWAY: Electrode sways appearing on the strip chart write-outs may be largely attributed to movements of the electrode wire or to movement of the quick insert ball in the plastic holder. Movement of the hat itself or small subtle head movements may also be reflected as a sway of an electrode. A sway with a peak-to-peak drift exceeding approximately 100 uv in 2 sec was considered to be a gross artifact. More moderate sways were characterized with a peak-to-peak drift of less than approximately 100 uv in 2 sec, or alternatively with an amplitude drift exceeding approximately

November 13, 1984 (56)

100 uv over a longer period of time. Table 3 shows that the distribution of sways was about constant across all events. Essentially, this means that sways tended to occur throughout trials, and not at brief intervals within a trial. In addition, as shown in Table 3, 95% of the sways were noted to be moderate and 15% to be gross. An example of a gross electrode sway is shown in Figure 33. An example of a moderate sway is shown in Figure 34.

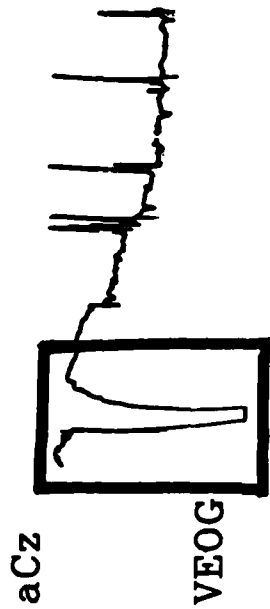
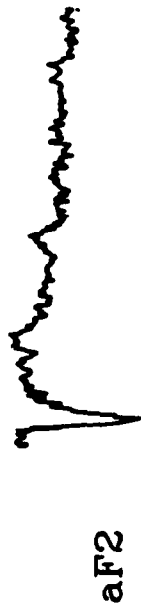
ELECTRODE POPS: The degree of severity of the electrode pop was determined according to its amplitude. Those electrode pops with an amplitude exceeding about 50 uv were considered to be gross, with moderate electrode pops having an amplitude of less than about 50 uv. Table 3 shows that 81% of the electrode pops were considered to be moderate, and 19% gross. An example of a gross electrode pop is shown in Figure 35. A moderate electrode pop is shown in Figure 36.

GROSS MOVEMENT: Large deviations (artifacts) in the EEG tracings are often the result of head movement. In these cases, the resulting artifact was identified as being gross, as distinguished from a more moderate artifact due to movement, when the size of the signal saturated the strip chart for that channel. Sixty-one percent of the movement artifacts were identified as being gross, and 39% were identified as being moderate. Examples of GMD contamination, gross and moderate, are shown in Figures 37 and 38, respectively.

PULSE/EKG: The contamination by pulse or EKG, a transient periodicity in the EEG, was characterized as either regular or irregular. Pulse was characterized as irregular (95%) primarily, and was characterized as being regular only a small proportion of the time (5%). An example of regular pulse is shown in Figures 39. An example of irregular pulse in the EEG is shown in Figure 40.

EMG: Muscle potential (EMG) contamination of the EEG was also identified, and was noted to occur especially in the frontal and temporal channels. It was noted that EMG present during the CUE event tended to remain present throughout the entire trial. Examples of EMG are shown in Figure 41 for frontal channels and Figure 42 for temporal channels.

ELECTRODE DRYING UP/LOOSE/DEAD : This type of artifact was due to poor (if any) conduction between the scalp and the electrode. The contact may be insufficient, (loose: Figure 43) as a result of the conductive gel drying up. A dead electrode (flat EEG traces: Figure 44) tends to indicate that there is no conduction at all. It is not surprising, then, that when the artifact was present in one event of a trial, it was present for the entire trial. These types of artifacts were not considered in terms of degree of severity.



9 FIGURE 29: GROSS VEOG - EYE BLINK
(RL0413: TRIAL 84)

FIGURE 30: MODERATE VEOG
(RL0217: TRIAL 200)



FIGURE 31: GROSS HEOG
(RL0413: TRIAL 77)

FIGURE 32: MODERATE HEOG
(RL0413: TRIAL 64)

50 uV



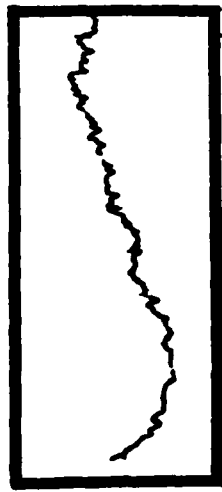
Cz



F4



Pz



C5



Oz



C6



FIGURE 33: GROSS SWAY

(RL0413: TRIAL 141 - PZ)

FIGURE 34: MODERATE SWAY

(RL0413: TRIAL 21 - C5)

aF1



aF2



aCz



FIGURE 35: GROSS ELECTRODE POP

(RL0617: TRIAL 58 - aF2)

FIGURE 36: MODERATE ELECTRODE POP

(RL0617: TRIAL 107 - aF1)

50uv



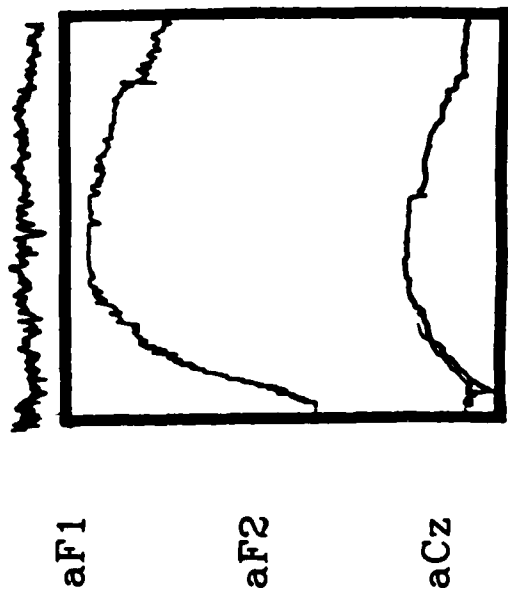


FIGURE 37: GROSS GMO
(RL0511: TRIAL 48 -
aF2, aCz)

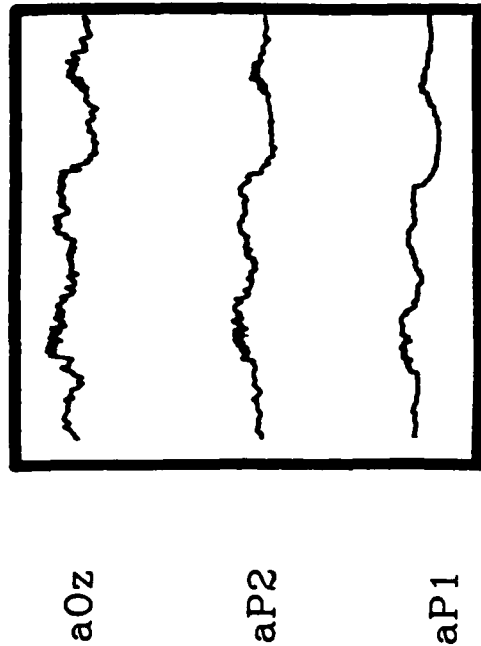


FIGURE 38: MODERATE GMO
(RL0413: TRIAL 53 -
aOz, aP2, aP1)

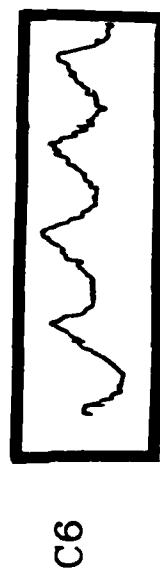


FIGURE 39: PULSE REGULAR
(RL0413: TRIAL 15 - C6)



FIGURE 40: PULSE IRREGULAR
(RL1015: TRIAL 84 - C3)



aO1



aO2

50 uv

aF1

aO1

aF2

T5

aCz

T6

FIGURE 41: EMG

(RL0712: TRIAL 33 - aF2)

FIGURE 42: EMG

(RL0511: TRIAL 107 - T5, T6)

Pz

Oz

Oz

C3

C3

C4

FIGURE 43: DUL (LOOSE ELECTRODE)

(RL0511: TRIAL 42 - Pz)

FIGURE 44: DUL (DEAD ELECTRODE)

(RL0914: TRIAL 44 - Oz)

50 uv L

November 13, 1984 (56)

VI. BIBLIOGRAPHY

Adey, W.R. Tissue interactions with nonionizing electromagnetic fields. Physiological Reviews, 1981, 61:435-514.

Ary, J.P., Klein, S.A., and Fender, D.K., Location of sources of evoked scalp potentials: Corrections for skull and scalp thicknesses. IEEE Trans. Biomed. Eng., BME-28, No. 6:447-452, 1981.

Barth, D.S., Sutherling, W., Engle, J.Jr. and Beatty, J. Neuromagnetic Evidence of spatially distributed sources underlying epileptiform spikes in the human brain, Science, 1984, 223: 293-296.

Baumrind, S., and Curry, S. Merging of data from different records in craniofacial research & treatment. In, Handbook of the 1984 Workshop on Nontopographic Photogrammetry, American Society of Photogrammetry, July 1984.

Bonham, B., Morgan, N., Gevins, A. An improved eye-movement filter for brain electromagnetic signals. In Prep., 1984.

Claassen, T.A.C.M. and Mecklenbrauker, W.F.G. The Wigner distribution - a tool for time-frequency signal analysis. Phillips Journal of Research, 1980, 35(3): 217-250.

Cohen, D. and Cuffin, N. Demonstration of useful differences between magnetoencephalogram and electroencephalogram, Electroenceph. Clin. Neurophysiol., 1983, 56: 38-51.

Cohen, L. Generalized Phase-space distribution functions. J. Math. Phys., 1966, 7:781-786.

Cooper, R., Winter, A., Crow, H. and Walter, W. Comparison of subcortical, cortical and scalp activity using chronically indwelling electrodes in man. Electroenceph. Clin. Neurophysiol., 1965, 18: 217-228.

Curry, S. Moffitt, F., Symes, D. and Baumrind, S. A family of calibrated stereometric cameras for direct intra-oral use. SPIE Proceedings, Vol. 361 (1982), pp. 7-14.

Darcey, T.M., Ary, J.P., and Fender, D.H. Methods for the localization of electrical sources in the human brain, Prog. Brain Res., 1980, 54:128-134.

de Weerd, J.P.C.M. Estimation of evoked potentials: a study of a posteriori "Wiener" filtering and its time-varying generalization, (PhD thesis Katholieke Universiteit te Nijmegen), The Netherlands: Krips Repro Meppel, 1981.

Dismukes, R.K. New Concepts of molecular communication among neurons, The Behavioral and Brain Sciences (1979) 2: 409-448.

Doyle, J. and Gevins, A. Cortical restoration of scalp recorded brain

November 13, 1984 (56)

potentials by spatial deconvolution, In Prep.

Elul, R. Gaussian behavior of the electroencephalogram: Changes during performance of mental task, Science, 1969, 164:328-331.

Elul, R. Randomness and synchrony in the generation of the electroencephalogram. In, Petsche, H. and Brazier, M. (Eds.), Synchronization of EEG activity in epileptics, New York: Springer-Verlag, 1972a: 59-77.

Elul, R. Genesis of the EEG. Int. Rev. Neurobiology, 1972b, 15:227-272.

Fortgens, C. and Bruin, M.P. Removal of eye movement and ECG artifacts from the non-cephalic reference EEG. Electroenceph. Clin. Neurophysiol., 1983, 56: 90-96.

Freeman, W.J. Mass Action in the Nervous System, New York: Academic Press, 1975.

Freeman, W. J. Nonlinear dynamics of paleocortex manifested in the olfactory EEG. Biol. Cybernetics, 1979a, 35: 21-37.

Freeman, W.J. Nonlinear gain mediating cortical stimulus-response relations. Biol. Cybernetics, 1979b, 33: 237-24.

Freeman, W. J. EEG analysis gives model of neuronal template-matching mechanism for sensory search with olfactory bulb. Biol. Cybernetics, 1979c, 35: 221-234.

Freeman, W.J. A physiological hypothesis of perception, Perspectives in Biology and Medicine, 1981, 24:561-592.

Freeman, W.J. The physiological basis of mental images, Biol. Psych., 1983, 18(10):1107-1125.

Gevins, A.S., Zeitlin, G.M., Doyle, J.C., Schaffer, R.E., Yingling, C.D., Yeager, C.L. and Callaway, E. EEG correlates of higher cortical functions. Science, 203: 665-668, 1979.

Gevins, A.S. and Schaffer, R.E. Critical review of research on EEG correlates of higher cortical functions. CRC Reviews in Bioengineering, 1980, 113-164.

Gevins, A.S., Doyle, J.C., Schaffer, R.E., Callaway, E. and Yeager, C. Lateralized cognitive processes and the electroencephalogram. Science, 207: 1005-1008, 1980.

Gevins, A.S., Doyle, J.C., Cutillo, B.A., Schaffer, R.E., Tannehill, R.S., Ghannam, J.H., Gilcrease, V.A. and Yeager, C.L. Electrical potentials in human brain during cognition: new method reveals dynamic patterns of correlation. Science, 213: 918-922, 1981.

Gevins, A.S., Schaffer, R.E., Doyle, J.C., Cutillo, B.A., Tannehill, R.S. and Bressler, S.L. Shadows of thought: Rapidly changing, asymmetric

November 13, 1984 (56)

brain-potential patterns of a brief visuomotor task. Science, 220:97-99, 1983.

Gevins, A.S., Doyle, J.C., Cutillo, B.A., Schaffer, R.E., Tannehill, R.S., Bressler, S.L. and Zeitlin, G. Neurocognitive pattern analysis of a visuomotor task: Low-frequency evoked correlations. Psychophysiology, In Press, 1984.

Gevins, A. Pattern recognition of human brain electrical potentials. IEEE Trans. Patt. Analysis Mach. Intell., 1980, PAMI-2(5): 383-404.

Gevins, A.S. Dynamic brain electrical patterns of cognition. In, Proc. 3rd Annual IEEE Conf. Biomed. Eng., Houston, T-BME8-81, 1981: 586-587.

Gevins, A.S. BEP evidence for lateralization of higher cognitive functions. In Hellige, J.B. (Ed.) Cerebral Hemisphere Asymmetry: Method, Theory and Application, Praeger Press, New York, 1983a: 335-382.

Gevins, A.S. Overview of the human brain as a distributed computing network. Proc. IEEE Int'l. Conf. Computer Design (ICCD '83), Port Chester, N.Y., 1983b.

Gevins, A.S. Analysis of the electromagnetic signals of the human brain: milestones, obstacles and goals. IEEE Trans. Biomed. Eng. BME-31(12), 1984, In Press.

Gevins, A.S. Quantitative Human Neurophysiology. In H.J. Hannay (Ed.), Experimental Techniques in Human Neuropsychology, Oxford Press, 1984a, In Press.

Girton, D.G. and Kamiya, J. A simple on-line technique for removing eye movement artifacts from the EEG. Electroenceph. Clin. Neurophysiol., 1973, 34: 212-216.

Gratton, G., Coles, M.G.H., and Donchin, E. A new method for off-line removal of ocular artifact. Electroenceph. Clin. Neurophysiol., 1983, 55(4): 469-484.

Hjorth, B. An on-line transformation of EEG scalp potentials into orthogonal source derivations, Electroenceph. Clin. Neurophysiol., 1975, 39: 526-530.

Hjorth, B. An adaptive EEG derivation technique, Electroenceph. Clin. Neurophysiol., 1982, 54: 654-661.

Hunt, E. Mathematical models of the event related potential. Air Force Office of Scientific Research, Annual Report, 1984.

Kaufman, L. and Williamson, S. Magnetic location of cortical activity, Annals of the New York Academy of Sciences, 1982: 197-213.

Kavanagh, R. N., Darcey, T. M., Lehmann, D. and Fender, D. Evaluation of methods for three-dimensional localization of electrical sources in the human brain. IEEE Trans. Biomed. Eng., 1978, BME-25 :421-429.

November 13, 1984 (56)

Luria, A. Higher Cortical Functions in Man. New York: Basic Books, 1966.

MacLin, E., Okada, Y.C., Kaufman, L. and Williamson, S.J. Retinotopic map on the visual cortex for eccentrically placed patterns: first noninvasive measurement, Il Nuovo Cimento, 1983, 2:410-419.

Nicholas, P., and Deloche, G. Convolution computer processing of the brain electrical image transmission. Int. J. Bio-Medical Computing, 1976, 7:143-159.

Okada, Y.C. Inferences concerning anatomy and physiology of the human brain based on its magnetic field, Il Nuovo Cimento, 1983, 2: 379-409.

Petsche, H., Pockberger, H. and Rappelsberger, P. On the search for the sources of the electroencephalogram, Neuroscience, 1984, 11(1):1-27.

Picton, T., Woods, D., Stuss, D. and Campbell, K. Methodology and meaning of human evoked potential scalp distributed studies. Proc. 4th Intl. Cong. on Event Related Potentials of the Brain. Hendersonville, N.C., EPA-600/9-77-043, 1978, 515-522.

Posner, M. Chronometric Explorations of Mind. Lawrence Erlbaum Assoc., N.J., 1978.

Richer, F., Barth, D.S., and Beatty, J. Neuromagnetic localization of two components of the transient visual evoked response to patterned stimulation, Il Nuovo Cimento, 1983, 2:420-428.

Ritter, W., Rotkin, L. and Vaughan, H. The modality specificity of the slow negative wave. Psychophys., 1980, 17:3;222-227.

Roland, P. Cortical regulation of selective attention in man. J. Neurophys., 1982, 48:5, 1059-1078.

Romani, G.L., Williamson, S.J., and Kaufman L. Tonotopic organization of the human auditory cortex, Science, 1982, 216: 1339-1340.

Rosler, F. and Manzey, D. Principal components and varimax-rotated components in event-related potential research: some remarks on their interpretation. Biological Psychology, 1981, 13: 3-26.

Sidman, R.D., Giambalvo, V., Allison, T., Bergey, P. A method for localization of sources of human cerebral potentials evoked by sensory stimuli, Sensory Processes, 1978, 2:116-129.

Simpson, R., Vaughan, H. and Ritter, W. The scalp topography of potentials in auditory and visual go/no-go tasks. Electroenceph. Clin. Neurophysiol., 1977, 43:864-875.

Speckman, E. J., Caspers, H. and Elger, C.E. Neuronal mechanisms underlying the generation of field potentials, In, Elbert, T., Rockstroh, B., Lutzenberger, W. and Birbaumer, N. (Eds), Self-regulation of the Brain and Behavior, Springer-Verlag, New York-Tokyo-Berlin-Heidelberg, 1984.

November 13, 1984 (56)

Talairach, J., Szikla, G., Tournoux, A., Prossalenti, A., Bordas-Ferrer, M., Covello, L., Jacob, M. and Mempel, E. Atlas of Stereotaxic Anatomy of the Telencephalon: Anatomico-Radiological Studies, Paris, Masson & Cie, 1967.

Tecce, J. Contingent negative variation (CNV) and psychological processes in man. Psych. Bull., 1972, 77:2;73-108.

Thickbroom, G., Mastaglia, F., Carroll, W. and Davies, H. Source derivation: Application to topographic mapping of visual evoked potentials. Electroenceph. Clin. Neurophysiol., 1984, 59:279-285.

Verleger, R., Gasser, T. and Mocks, J. Correction of EOG artifacts in event-related potentials of the EEG: aspects of reliability and validity, 1982, Psychophysiology, 19(4): 472-480.

Whitton, J.L., Lue, F. and Moldofsky, H. A special method for removing eye movement artifacts from the EEG. Electroenceph. Clin. Neurophysiol., 1978, 44: 735-741.

Williamson, S.J., and Kaufman, L. Biomagnetism, Journal of Magnetism and Magnetic Materials, 1981a, 22(2): 129-202.

Williamson, S.J., and Kaufman, L. Magnetic fields of the cerebral cortex, In S.N. Erne, H.D. Hahlbohm, H. Lubbig (Eds.), Biomagnetism, Walter de Gruyter, New York, 1981b: 353-402.

Williamson, S.J., Romani, G.L., Kaufman, L. and Modena, I. (Eds.), Biomagnetism: an Interdisciplinary Approach, Plenum, New York, 1983.

Wood, C.C. and McCarthy, G. Principal component analysis of event-related potentials: simulation studies demonstrate misallocation of variance across components. Electroenceph. Clin. Neurophysiol., 1984, 59: 249-260.

END